Physical Characteristics of Nitinat Lake, 2003

By

Grant Lamont

B.Eng., University of Victoria, 1999

A THESIS SUBMITTED IN PARTIAL FULFILMENT OF
THE REQUIREMENTS FOR THE DEGREE OF

Master of Applied Science

IN

THE FACULTY OF GRADUATE STUDIES

(CIVIL ENGINEERING)

UNIVERSITY OF BRITISH COLUMBIA

January 2005

© Grant Lamont, 2005

Abstract

Nitinat Lake is a long, narrow, and strongly salt-stratified fjord-lake located on the west coast of Vancouver Island, British Columbia. It is connected to the ocean by a 3km long natural channel, only 2.5m deep at low normal tides that limits exchange between the 203m deep lake and the Pacific Ocean. Lake-water may be grouped into two distinct bodies: a weakly stratified bottom layer containing seawater, and a strongly stratified surface layer containing brackish water. The permanently anoxic bottom layer has high concentrations of hydrogen sulphide and a long residence time. At rest, the interface between these two bodies of water ranges from 5m to 15m in depth depending upon location and season. Surface layer salinity was found to correlated well with precipitation in the watershed.

The lake contains several large salmon runs and is home to the largest salmon hatchery in Canada, rearing over 40 million fry annually. Upwelling events of anoxic water are potentially catastrophic for fish hatchery operations such as fish harvesting and juvenile releases, highlighting the need to better understand the physical mechanisms that lead to upwelling. Meteorological, CTD, and thermistor chain data were used to study wind forcing of the interface. If was found that predictions of interface deflections based upon linear theory of surface stress response for a two-body lake were in reasonable agreement with observed data. However, spatial variations in lake properties appear to be the result of tidal exchanges between the lake and the ocean, with anoxic water commonly found at shallower depths at the inland end of the lake than the ocean end. This spatial variation of properties adversely affects linear theory predictions, and further understanding of tidal exchanges and internal lake dynamics are required in order to better predict upwelling of anoxic water at this time.

Keywords: Nitinat Lake, anoxia, seiching, upwelling, BC fjord

Table of Contents

Abstract ii

Table of Contents iii

List of Tables v

List of Figures vi

Acknowledgements x

1.0 Introduction 1

1.1 General Characteristics of Nitinat Lake 2

1.2 Bathymetry 3

1.3 Topography 4

1.4 Major Tributaries 4

1.5 Climate 5

1.6 Winds 6

1.7 Water Properties 6

1.7.1 Temperature 7

1.7.2 Salinity 8

1.7.3 Dissolved Oxygen and Hydrogen Sulphide 9

1.8 History of Anoxic Water Upwelling 9

2.0 Methodology 12

2.1 CTD Casts 12

2.2 Water Samples 16

2.3 Weather Stations 16

2.4 Temperature Sensor Moorings 18

2.5 River Temperature Sensors 19

2.6 Ancillary Weather Data 20

3.0 Data - Physical Properties 22

3.1 Lake Temperatures 22

3.2 River Temperatures 33

3.3 Salinity 36

3.4 Density 47

3.5 Dissolved Oxygen 54

3.6 Relative Chlorophyll Concentrations 58

3.7 Turbidity and Transmittance 59

3.8 Tides 62

3.9 Meteorological Data 67

3.9.1 Temperature, Relative Humidity, and Solar Radiation 67
3.9.2 Wind Data 71

4.0 Discussion 75

4.1 Relationship Between Precipitation and Stratification 75
4.1.1 Estimated of Surface Layer Residence Time 77
4.1.2 Density and Precipitation in 2003 79

4.2 Lake Response to Wind Forcing 81
4.2.1 Wind Forcing On Nitinat Lake 82
4.2.1.1 – Wind Direction, Fetch, and Topography 83
4.2.1.2 – Observations of Wind on Nitinat Lake, 2003 83
4.2.2 Linear Analysis 85
4.2.2.1 Wedderburn Number 85
4.2.2.2 Methodology for Determining h_1 and ρ_1 86
4.2.3 Observed interface Deflections – July 2003 90
4.2.3.1 July Data 91
4.2.3.2 November Data 95
4.2.4 Observed complications 99
4.2.4.1 Beyond Linear Theory 99
4.2.4.2 Comparison of Density and Temperature contours 101

5.0 Conclusions 104

5.1 Lake Characteristics 104

5.2 Relationship between Precipitation and Density 104

5.3 Interface Response to Wind Forcing 105

5.4 Prediction of Anoxic Upwelling 106

5.5 Future Studies 107

References 110

List of Tables

Table 1.8.1 – History of recorded upwelling events at Nitinat Lake. 10

Table 2.1.1 – CTD types and serial numbers used at Nitinat Lake. 12

Table 2.1.2 – Lake Station data for UBC Nitinat Lake study. 14

Table 2.4.1 – Depths of temperature sensors on TC1 and TC2. 19

Table 2.5.1 – Locations of river temperature sensors. 19

Table 4.1.1 – Annual total precipitation at Nitinat Hatchery for years 1994 through 2003. 76

Table 4.1.2 – Quarterly total precipitation at Nitinat Hatchery for years 1994 through 2003. 76

Table 4.1.3 – Monthly precipitation and average discharge rates for 2003, during months when lake properties were measured. 79

Table 4.2.1 – Afternoon winds on July 7 showing spatial variation along length of lake. 84

Table 4.2.2 – 2003 Nitinat Lake density data, base upon CTD casts. 88

Table 4.2.3 – Winds on July 10 at/near S07 recorded with hand held anemometer. 91

List of Figures

Figure 1.1.1 – Map of Nitinat Lake, Vancouver Island, Canada. 3

Figure 1.5.1 – Monthly precipitation data recorded at the Nitinat River Hatchery for 2002 and 2003. 5

Figure 2.1.1 – Sampling stations used on Nitinat Lake during 2003 UBC study..... 14

Figure 2.1.2 – CTD stations used on July 11, 2003. 15

Figure 2.3.1 – Map showing location of meteorological stations M1 and M2, as well as temperature sensor moorings TC1 and TC2. 17

Figure 2.4.1 – Schematic of thermistor chain deployment..... 18

Figure 3.1.1 – Temperature contours for the top 25 m of Nitinat Lake, from February 2003 until February 2004. 25

Figure 3.1.2 – Temperature profiles at stations S02 and S06, showing seasonal variation in surface layer. 26

Figure 3.1.3 – Temperature contours on July 25, 2003. 26

Figure 3.1.4 – Temperature contours in the upper 20m of the lake, taken perpendicular to the thalweg at S06. 27

Figure 3.1.5 – Map showing location of temperature sensor moorings TC1 and TC2, as well as meteorological stations M1 and M2..... 28

Figure 3.1.6 – Temperature data from thermistor mooring 1 from 10:30 PDT July 22 to 18:00 July 24. .29

Figure 3.1.7– Temperature data from thermistor 6775 on mooring 1 from 10:00 PDT July 21 to 18:00 July 24. 29

Figure 3.1.8 – Temperature data from thermistor mooring 2 from 10:30 PDT July 22 to 18:00 July 24. ..30

Figure 3.1.9 – Temperature profiles from CTD data obtained near TC1 and TC2 temperature sensor mooring. The circles represent the depth of the temperature sensors on the thermistor chains. 31

Figure 3.1.10 – Temperature profiles from CTD data obtained at S07 during three different times on July 10, 2003. 32

Figure 3.1.11 – Deep water temperature profiles for stations S02 and S05 during 2003. 33

Figure 3.2.1 – Temperature record from Nitinat River during 2003 study. 34

Figure 3.2.2 – Temperature record from Caycuse River during 2003 study. 35

Figure 3.2.3 – Temperature record from Hobiton River during 2003 study. 36

Figure 3.3.1– Salinity contours on July 10, 2003. 38

Figure 3.3.2 – Salinity contours for the top 20 m of Nitinat Lake, from February 2003 until February 2004. 39

Figure 3.3.3 – Salinity profiles at stations S02 and S06, showing seasonal variation in surface layer. 41

Figure 3.3.4 – Salinity contours on July 25, 2003. 42

Figure 3.3.5 – Salinity contours in the upper 25m of the lake, taken perpendicular to the thalweg at S06. 44

Figure 3.3.6 – Salinity profiles recorded near station S07 between 9:10pm (PDT) on July 23 and 7:40am on July 24, 2003. 45

Figure 3.3.7 – Wind data from the morning of July 22 to the morning of July 23, 2003. 46

Figure 3.3.8 – Salinity profiles recorded at station S04 between 9:30am (PDT) and midnight on July 14, 2003. 47

Figure 3.4.1 – Temperature salinity plot for sea-water with lines (dotted) of constant density. 48

Figure 3.4.2 – Temperature salinity diagram showing water in Nitinat Lake from July (+) and November (o). 49

Figure 3.4.3 – Temperature (solid), salinity (dashed), and density (dash-dot) profiles at S02 in July of 2003 (left plot) and February 2004 (right plot) for the top 30m depth. 50

Figure 3.4.4 – Temperature (solid), salinity (dashed), and density (dash-dot) profiles at S02 (left plot) and S05 (right plot), for water below 40m depth on July 16, 2003. 51

Figure 3.4.5 – Density contours of Nitinat Lake taken on July 16, 2003, using SBE-25 CTD instrument at nine locations in the lake. (Data courtesy Rich Pawlowicz) 52

Figure 3.4.6 – Density contours of Nitinat Lake taken on July 16, 2003, using SBE-25 CTD instrument at nine locations in the lake. 52

Figure 3.4.7 – Temperature contours of Nitinat Lake taken on July 16, 2003, using SBE-25 CTD instrument at nine locations in the lake. 53

Figure 3.4.8 – Salinity contours of Nitinat Lake taken on July 16, 2003, using SBE-25 CTD instrument at nine locations in the lake. (Data courtesy Rich Pawlowicz) 54

Figure 3.5.1 – Dissolved oxygen contours (ml/l) in Nitinat Lake on July 16, 2003. 56

Figure 3.5.3 – Dissolved oxygen contours in Nitinat Lake on November 20, 2003. 57

Figure 3.5.4 – Dissolved oxygen contours in Nitinat Lake on February 17, 2004. (Data courtesy Rich Pawlowicz) 58

Figure 3.6.1 – Contour plots showing the relative concentrations of chlorophyll in volts as recorded during three different seasons on Nitinat Lake, 2003 59

Figure 3.7.1 – Backscatter and transmissivity profiles for stations S06 and S02 on July 10, 2003. 61

Figure 3.8.1 – Map of Nitinat Lake sill. 63

Figure 3.8.2 – Tidal signal from Bamfield Marine Station water level gauge 08545 (dash-dot line) with the water level signal from the pressure sensor on TC1 in Nitinat Lake (solid line). Period is from July 22 to Aug 1, 2003, showing mixed semi-diurnal tides. 65

Figure 3.8.3 – Tidal signal from Bamfield Marine Station water level gauge 08545 (dash-dot line) with the water level signal from the pressure sensor on TC1 in Nitinat Lake (solid line). Period is from September 22 (day 264) to October 2 (day 274), 2003. 65

Figure 3.8.4 – Tidal signal from Bamfield Marine Station water level gauge 08545 (dash-dot line) with the water level signal from the pressure sensor on TC1 in Nitinat Lake (solid line). Period is from October 10 to October 23, 2003. 66

Figure 3.8.5 – Daily precipitation data (mm of rainfall) recorded at the Nitinat River Hatchery, between October 10 (day 282) and October 22 (day 294). 66

Figure 3.9.1 – Air Temperature (°C), Relative Humidity (%) and Solar Radiation (W/m^2) from station M2 during July of 2003 at Nitinat Lake. 69

Figure 3.9.2 – Air Temperature (°C), Relative Humidity (%) and Solar Radiation (W/m^2) from station M2 during October and November of 2003 at Nitinat Lake. 70

Figure 3.9.3 – Compass plots of daily wind data for M2. 72

Figure 3.9.4 – Compass plots of daily wind data for M1. 74

Figure 4.1.1 – Bar graph showing monthly total precipitation from 1994 to 2004, recorded at the Nitinat Hatchery. (Data courtesy Environment Canada and DFO) 76

Figure 4.1.2 – Monthly precipitation for 2002 and 2003, recorded at the Nitinat Hatchery (Data courtesy Environment Canada and DFO). 80

Figure 4.2.1 – Schematic diagram of idealized lake. (a) The state of the lake with no surface stress. (b) The halocline deflection due to surface stress. 82

Figure 4.2.2 – Schematic diagram showing bottom profile of actual lake with bottom profile of the idealized lake (rectangular box) superimposed. 87

Figure 4.2.3 – Theoretical Interface Deflection (m) at end of lake as a function of wind speed, based upon a two-layer box model (H=165m) of lake system using Nitinat Lake data from 2003 as presented in table 4.2.2. 89

Figure 4.2.4 – Wedderburn Number as a function of wind speed, based upon a two-layer box model (H=165m) of lake system using Nitinat Lake data from 2003 as presented in table 4.2.2. 90

Figure 4.2.5 – Change in density as a function of depth. Data from CTD casts at station S06 90

Figure 4.2.6 – Wind velocity recorded at station M2 on July 10. 91

Figure 4.2.7 – Temperature and density profiles from CTD data obtained at S07 during three different times of the day. 93

Figure 4.2.8 – Wind data from MC2 and temperture contours from both TC1 and TC2. 94

Figure 4.2.9 – Wind data, Wedderburn number, and Isotherm movement at TC1. 96

Figure 4.2.10 – Temperature depth profile taken using a CTD on November 19, 2003. 97

Figure 4.2.11 – Temperature plots from sensors at TC1 mooring in 2003 (October 28 – Nov 7). 98

Figure 4.2.12 – Temperature plots from sensors at TC2 mooring in 2003 (October 28 – Nov 7). 98

Figure 4.2.13 – Comparison of temperature and density contours in Nitinat Lake on July 16, 03. 102

Figure 4.2.14 – Comparison of rates of change of temperature and density with depth at two different stations in Nitinat Lake on July 16, 03. 102

Acknowledgements

The author wishes to thank a number of people for their contributions to this work. First and foremost is my thesis supervisor, Bernard Laval, for his many valuable suggestions to this text and encouragement during the writing process. I would also like to thank my second supervisor, Greg Lawrence, for his advice on this study and financial support.

During the field work, a number of people provided assistance and advice. Of note, Rich Pawlowicz and Roger Pieters provided everything from help with calibrations of equipment, to suggestions for improvements in data gathering techniques. Their advice was very much appreciated. Furthermore, all of the maps of Nitinat Lake produced in this document were made using mapping software written by Rich Pawlowicz.

Further thanks are extended to those students who gave of their time to work as field assistants for this study. These people were Averil Lamont, Albert Leung, Joel Atwater, and Daniel Potts. Oxygen and salinity concentrations were obtained using CTD instruments, and these results were verified using bottle samples. Lab assistance in analysing bottle samples was made by A. (Ram) Ramnarine.

The field work for this study would not have been possible without the support of the staff of the *Nitinat River Hatchery* and the *Ditidaht First Nations*. In particular, I would like to thank Phillip Egdar and Fred Sieber for their assistance with on-water data collections, and the entire staff at the Nitinat River Hatchery for their hospitality and sharing their knowledge and experiences on the lake.

1.0 Introduction

Nitinat Lake is a salt stratified fjord-lake located on the west coast of Vancouver Island between Port Renfrew and Bamfield. A shallow sill connects Nitinat Lake to the ocean. This sill, and some of the surrounding shoreline at the south west end of the lake, is located in Pacific Rim National Park while the remainder of the lake is primarily surrounded by crown lands with second growth timber. The Ditidaht First Nation village is located at the northeast end of the lake, and is the only urban development in the Nitinat Lake watershed.

The region surrounding Nitinat Lake is an important part of the Vancouver Island economy. The area is increasingly popular as a tourist destination with close proximity to Pacific Rim National Park and Carmanah Valley, while the lake itself is considered a premier destination in North America for windsurfing and kite-boarding sailors. Traditional resource based industries such as forestry are ongoing in the area, while the lake and surrounding rivers are important breeding grounds for salmon. The Canadian Department of Fisheries and Oceans operates a fish hatchery on Nitinat River that is Canada's largest salmon hatchery with annual take of over 40 million eggs (Nitinat River Fish Hatchery website, DFO).

Despite fish hatchery operations and the increasing use of the lake for tourist activities, few studies have been done on the lake and those that were done occurred in the 1960's and early 1970's. Observations from this early fieldwork indicated that the lake is permanently anoxic and that bottom water conditions have minimal seasonal variations. Nitinat Lake has a history of upwelling of anoxic water that results in disruptions to the local ecology, including significant fish kills on several occasions. Due to the remote nature of the lake, these upwelling events have not been well documented, and are poorly understood. Ozretich (1975) suggested two mechanisms: deep-water renewal by seawater and wind forcing.

The first part of this thesis contributes to the understanding of the limnology of Nitinat Lake. In particular, addressing the following questions: what are the seasonal variations of the physical properties in the lake? The second part of this thesis examines the effect of wind forcing on the interface between the oxygenated surface layer and the anoxic bottom waters. The remaining sections in this chapter provide general information on Nitinat Lake. Chapter 2 describes the data-gathering methodology, while Chapter 3 describes the field data collected on three separate field trips to Nitinat Lake. Chapter 4 describes seasonal variations in lake density stratification and internal response to wind forcing. Chapter 5 summarizes conclusions and makes suggestions for future work. In the remainder of this chapter, sections 1.1 to 1.3 include geographic and bathymetric descriptions of the lake and surrounding area on Vancouver Island, while section 1.4 describes the major tributaries that feed into Nitinat Lake. The characteristics of the local climate are introduced in section 1.5 with specific comment on winds given in section 1.6. Physical water properties in Nitinat Lake, as determined by previous studies, are summarized in section 1.7 focusing on temperature, salinity, dissolved oxygen and hydrogen sulfide levels in the lake. Finally, in section 1.8 a summary of past studies of upwelling events on the lake is given.

1.1 General Characteristics of Nitinat Lake

Nitinat Lake is a long, narrow, and strongly salt-stratified fjord-lake. The lake is approximately 20 km in length, and averages about 1.2 km in width with a surface area of 27.6 km^2 (Figure 1.1.1). It is connected to the ocean by a 3km long natural shallow channel which limits exchange between the 203m deep lake and the Pacific Ocean (Northcote, 1964). Including the sill in the total length, the length to width ratio is approximately 19:1, which is close to the 20:1 average for transverse fjords in British Columbia (Gilmartin, 1962).

The tidal passage that connects the lake to the ocean has depths of 2 to 5 m at lowest normal tide, and varies in width from just 60m at the southern ocean entrance to 520m at the northern end where the sill deepens as it enters the lake. Tidal currents across the sill reach speeds of 3.5 m/s during maximum flood and ebb tides (Broenkow, 1969).

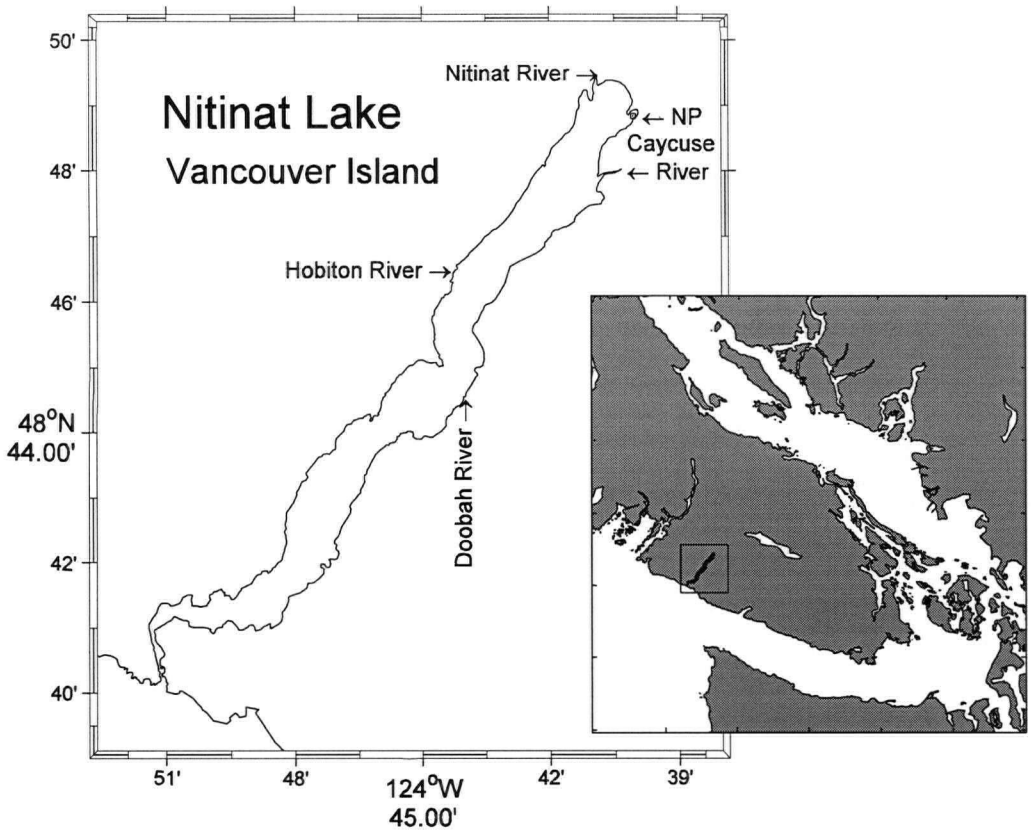

Figure 1.1.1 – Map of Nitinat Lake, Vancouver Island, Canada. The location of major tributaries is indicated by arrows, and the location of the Fish Hatchery net pen is indicated by the dot in the north east bay (NP). Inset shows the southern half of Vancouver Island with the location of Nitinat Lake highlighted in the marked area.

1.2 Bathymetry

In profile the lake is characterized by two distinct regions; the north east basin and the southwest basin. Each basin is U-shaped in cross section, and has a relatively wide and flat bottom of constant depth. The northeast basin has a maximum depth of 203m, which is the deepest in the lake. The southwest basin has a maximum depth of 140m. Between the northeast and southwest basins, near the midpoint of the lake, there is a slight saddle with a maximum depth of 120m. The approximate volume of the lake is 2750 $x10^6$ m^3. (Northcote et. al., 1964)

1.3 Topography

The lake lies in a valley that was deepened by glacial scour and runs perpendicular to the coast of Vancouver Island. As a result, the shorelines of the lake are relatively steep sided and the lake is surrounded by ridges and mountains that run parallel to the major axis of the lake. The highest mountain near the lake, located on the south shore near the lake midpoint, is over 900m in height, while the ridge line along the north side of the lake is generally around 400m above the lake surface.

1.4 Major Tributaries

The major river feeding into Nitinat Lake is the Nitinat River, with a drainage area of about 800 km^2 (Fedorenko et. al. 1979). The Caycuse River is the second largest, followed by the Hobiton and Doobah rivers. The Nitinat, Caycuse, and Hobiton all drain into the northeast basin of the lake while the Doobah drains into the middle of the lake from the south shore (Figure 1.1.1). Runoff patterns are apparently typical of lower level British Columbia coastal rivers with low flows during summer months and high flow rates during winter.

While there are no stream gauge data available for any of the rivers that feed into Nitinat Lake, data are available for the Sarita River which runs near Bamfield to the north of the Nitinat watershed. This river, with a drainage area of 162 km^2, had a mean annual discharge of 19.7 m^3/s for the period between 1949 and 2001. December had the highest monthly mean for this time period at 39 m^3/s while August had the lowest, at just 3.1 m^3/s. The maximum daily average discharge rate was 677 m^3/s (Jan 29, 1960) and the daily average minimum was 0.283 m^3/s (Aug 27, 1951). (Data courtesy of Environment Canada, 2004) Flows in the Nitinat River have been estimated to range from 0.85 to 850 m^3/s (Fedorenko et. al., 1979).

Observed water levels on the lower portion of Nitinat River varied by more than 2m between field trips in July and November. A flood event in October caused river levels to temporarily rise by more than 8m during a three day period as observed at the pump

house for the Nitinat River Hatchery. (Personal correspondence, Hans Galesloot, Nitinat River Hatchery Operations Manager, 2003).

1.5 Climate

The west coast of Vancouver Island is a temperate rain forest. The summer is typically warm and dry, with an average temperature at the coast of 14 °C. Summer winds at the coast are typically light and from the west northwest. Coastal fog is also common during summer months. (Parks Canada, Pacific Rim National Park climate information.)

Winter months are typically wet with an average temperature of 6 °C. Prevailing winter winds are from the southeast bringing frequent storms to the region as the incidence of storms in the North Pacific increases. Snow is infrequent in the coastal region, and there is usually no significant snow pack in coastal watersheds. Total annual rainfall on the west coast is often higher than 300 cm. (Parks Canada, Pacific Rim National Park climate information.) Approximately 75 percent of the total annual rainfall occurs between October and March of each year (Figure 1.5.1, Environment Canada Data, 2003).

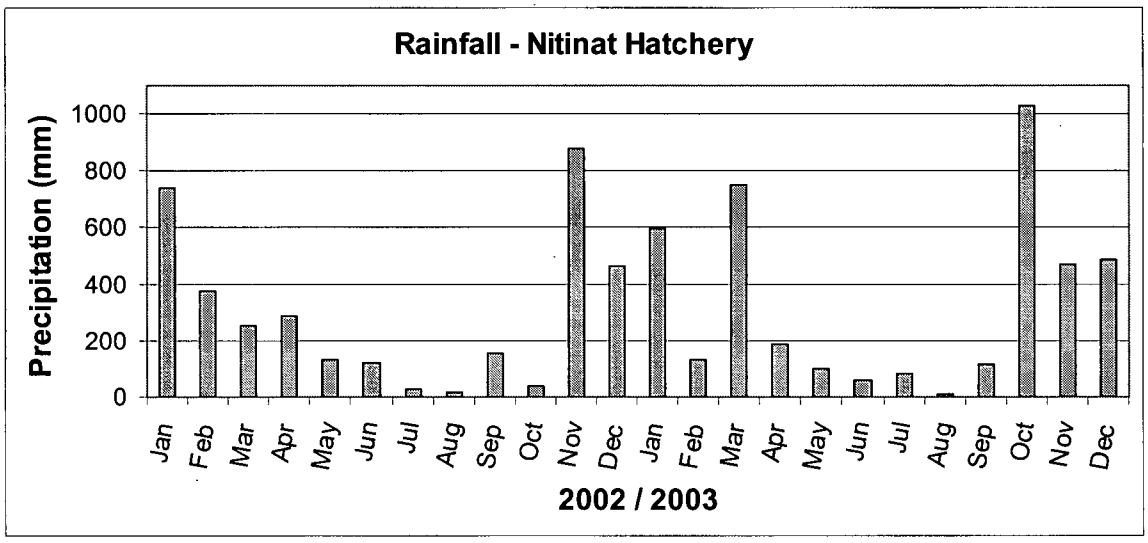

Figure 1.5.1 – Monthly precipitation data recorded at the Nitinat River Hatchery for 2002 and 2003. Annual rainfall was 349 cm and 402 cm respectively. Note low rainfall during summer months. (Data courtesy of DFO and Environment Canada)

By contrast, the interior valleys and east coast of Vancouver Island experience less rainfall and greater seasonal temperature variations. Nanaimo, a city on the east coast of Vancouver Island, has summer average temperatures of 18 °C, winter averages of 3 °C, and total annual precipitation of just 115 cm. (Environment Canada)

1.6 Winds

Due to the local geography, strong surface winds on the lake are most often aligned with the long axis of the valley. In the summer, winds are strongly diurnal due to a thermal gradient between the cool ocean and the warm valleys of central Vancouver Island. Coastal summer fog often magnifies this temperature gradient. In winter months, large scale weather systems are the predominant factors affecting winds on the lake (Ozretich, 1976).

Ditidaht First Nations members, fishermen, and recreational sailors and paddlers have long observed winds to vary spatially along the lake (pers comm. author). However, previous studies did not mention wind variations. Ozretich (1975) who discussed wind forcing, relied upon wind data from the Tofino airport and no historical wind record for Nitinat Lake is available in this regard.

1.7 Water Properties

During the 1960's and 1970's there were a small number of studies done that looked at water properties in Nitinat Lake. Prior to these studies, the lake had only been surveyed by logging companies and government surveyors. Pickard (1961) included Nitinat in a survey of oceanographic features of inlets on the BC coast, which found sea water present in Nitinat Lake in large quantities. In a follow up study Northcote et. al. (1963) sampled water in the lake for temperature, salinity, dissolved oxygen, and hydrogen sulphide which lead to the discovery that deep waters in Nitinat Lake were anoxic. This discovery prompted further interest in the lake, including a study of circulation in the surface layer (Hamilton and Hopkins, 1970) and a more detailed study of the anoxic waters in conjunction with other anoxic water bodies such as the Black Sea, Cariaco Trench and Saanich Inlet (Broenkow, 1969). Further sampling of lake water occurred to

support a study by Fedoranko et. al. (1979) that examined the suitability of Nitinat for a salmon enhancement project by the Federal Government of Canada.

With its extremely shallow sill and deep basin, Nitinat Lake is more similar to shallow sill Norwegian and Scottish fjords than to other British Columbia fjords. The sill plays a major role in determining the characteristics of the lake by restricting tides and isolating the deep waters within the lake from frequent exchange. All surveys of the lake have found sharp thermo- and haloclines in the upper 20m of the lake, as well as some spatial variation in properties between the inland and ocean end of the lake. The remainder of this section reviews specific properties of the lake starting with temperature and salinity characteristics, followed by a brief description of dissolved oxygen and hydrogen sulfide levels in the lake.

1.7.1 Temperature

Surface temperatures in all studies were found to vary depending upon season, while deep water (below 40m) temperatures were found to be seasonally stable near 10 °C. Due to equipment limitations, only the University of Washington oceanography studies measured temperature below depths of 60m, and most studies only sampled in the top 25m.

In all cases a sharp thermocline was observed between 5 and 10m in depth below the surface. Winter studies found surface temperatures between 6 and 8 °C and summer temperatures as high as 18 °C. Near the north end of the lake, Northcote et. al. (1963) observed a slight temperature inversion in summer where the water between 15 and 20m was cooler than the water below 20m. This inversion reversed itself in the winter, resulting in the waters between 15 and 25m being warmer than both the surface layer and the deep waters. This temperature inversion pattern appears to be a common trait, as it is also present in the temperature profiles of Broenkow (1969). (It can not be confirmed in the data of Fedorenko et. al. (1979), as they did not sample below 20m.)

Spatial variations between the south (coastal) and north (in-land) basins of the lake were observed in all studies. The north basin typically has a sharper and shallower thermocline

than the south basin. Also, seasonal temperature variation is slightly greater in the north basin than in the south. These spatial variations are most likely due to tidal mixing near the sill weakening stratification in that area, and the long narrow nature of the lake.

1.7.2 Salinity

Salinity gradients within the lake are similar to temperature gradients. Northcote et al (1963), Broenkow (1969), and Fedorenko (1979) all observed strong gradients in the upper 10m, and generally uniform conditions below 30m. A deep water survey of salinity performed by Broenkow (1969) in June of 1965 in the north basin shows variations between 28 to 30.5 ‰ in the top 10m, increasing to 31 ‰ by 25m in depth, and becoming steady at 31.2 ‰ between a depth of 50 to 200m.

Seasonal and spatial variations in surface salinity are directly tied to precipitation and runoff from tributaries. Pickard (1961) classified Nitinat as a "direct-runoff" inlet, where surface properties are closely governed by precipitation. Broenkow (1969) found that the Nitinat River is dominant in controlling the salinity distribution at the surface. They also determined that the surface layer flows towards the ocean at speeds ranging from 6 to 22 cm/s depending upon the state of runoff, wind, and tides. Surface salinities were always found to increase from the inland end to the ocean, with lowest surface salinities generally in December and January and highest in August or September.

Ocean water entering across the sill during high tides forms a plunging flow, sinking below the surface layer upon entering the lake. It then separates from the bottom becoming an interflow layer at 5-15m depth. The mixing of ocean water with lake water during tidal pumping is the obvious cause of the weaker stratification in the south basin. Other factors, such as bottom water entrainment during estuarine circulation resulting from the net movement of the surface layer towards the ocean may also contribute to the spatial variation within the lake, however the magnitude of entrainment of bottom waters due to this mechanism has not been studied.

1.7.3 Dissolved Oxygen and Hydrogen Sulphide

Northcote (1969) notes that, "one of the most spectacular features of Nitinat Lake is extensive and extreme depletion of oxygen in its deeper water." Every study of Nitinat Lake has found anoxic water below the surface layer, which would strongly suggest that this is a permanent characteristic. Studies noted that zero values were found below 20 m in the north basin, and below 40m in the south basin. This general trend was observed both in winter and in summer observations.

The anoxic conditions arise when oxygen consumption exceeds oxygen renewal. In Nitinat Lake, the weak circulation and limited exchange with ocean water caused by the shallow and long sill is the primary cause of this condition. (Fedorenko, 1979) The weak circulation leads to trapping of nutrients with denitrification and sulfate reduction processes occurring in the deep water. As seawater contains significantly more SO_4^{2-} than NO_3^-, hydrogen sulphide is the major reduced product formed (Broenkow, 1969).

1.8 History of Anoxic Water Upwelling

Localized upwelling events have been observed on the lake by both the Ditidaht First Nations and Nitinat Fish Hatchery employees, and have caused significant fish kills in the lake. Upwelling events are usually localized and are often detected by smell ('rotten egg') or by sight (surface waters turn a 'brown color' - Shortreed, 1987). The record of events is incomplete as there has never been continuous monitoring of the lake, but does provide a starting point for examining conditions that lead to upwelling events (Table 1.8.1). Ozretich (1975) suggests two possible causes leading to upwelling; either strong outflow winds or coastal ocean upwelling coupled with high tides leading to deep water renewal.

Table 1.8.1 – History of recorded upwelling events at Nitinat Lake. Due to the remote location of lake, it is likely that many upwelling events were not recorded, and that this record is incomplete.

Date	*Location*	*Comments*	*Source*
July 2, 1970	Near sill	Very high tides (H=3.27m) Strong westerly winds	Ozretich (1975)
October 13, 1970	Near sill	Very high tides (H=3.21m) Light winds	Ozretich (1975)
October 15, 1972	Near head	Average tides (H=2.77m) Strong outflow (Northerly) winds	Ozretich (1975)
October 22, 1972	Near head (unconfirmed)	Large tides (H=3.56m) No wind data available	Ozretich (1975)
November 5, 1987	Near head	Large tides (H=3.45m) Light winds	Shortreed et al. (1987)
March 21, 2002	Near head (unconfirmed)	Average tides (H=3.03m) No wind data	DFO Nitinat Fish Hatchery
March 8, 2003	Near head	Average tides (H=2.98m) No wind data	DFO Nitinat Fish Hatchery

In the first case, strong winds blowing down the long axis of the lake impart a shear stress onto the surface that 'pushes' the surface layer towards one end of the lake. If sufficient sustained winds are present during times of weak stratification, it is possible that upwelling of anoxic water will occur at the upwind end of the lake. On Nitinat Lake an upwelling event due to wind shear is most likely to occur in the late fall after a dry summer. The upwelling event of October 1972 was most likely caused by the combination of weak stratification and strong NE winds (Ozretich 1975).

In the second case, Ozretich (1975) suggests that Fraser River discharge may play a role in upwelling due to its influence on the intensity of the seasonal halocline in the Stait of Juan de Fuca. A lower than normal discharge will result in a weaker halocline off the south west coast of Vancouver Island. This allows for deeper penetration of the wind stress and results in a greater horizontal Ekman transport of water, enabling more intense upwelling to occur in the event of strong wind forcing. Strong winds may also create higher than predicted water levels through set-up and surge of surface water. If coastal upwelling were to occur during higher than normal incoming tides, it is possible that some of this dense water will enter the lake and, despite mixing across the sill, remain denser than the bottom water, thereby triggering an upwelling event as it sinks into the lake and displaces existing waters. (Ozretich, 1975). The 1970 and 1987 events were likely a result of this deep water renewal mechanism.

Upwelling induced by wind shear has been problematic on Nitinat Lake. First, the density stratification is weakest in the late fall, which coincides with the time that spawning fish are returning to the lake (Ozretich 1975). Second, it is more likely that NE winds will produce upwelling than SW winds since anoxic water is deeper at the south end of the lake than the north (Broenkow, 1969). This is unfortunate due to the fact fish pens used by the Nitinat River Hatchery are located at the north end of the lake.

2.0 Methodology

Three field trips were made to Nitinat Lake during 2003. The first was a single day trip on February 16 to sample along the thalweg using a CTD. As well, Niskin bottles were used to obtain water samples that were analysed for dissolved oxygen. A second trip was made in July to set up meteorological stations, deploy thermistor moorings, and perform numerous CTD transects during a three week period. The final trip to the lake occurred in November to retrieve thermistor moorings and meteorological stations, and to perform more CTD transects of the lake. DFO officers from the Nitinat Hatchery also performed a CTD transect of the lake in September using a pre-configured CTD that was shipped to them from UBC.

The field work was support by the Ditidaht First Nations and the DFO Nitinat River Hatchery, who donated time and boats 'at cost' or at no cost. A majority of the lake work was done from a 6m aluminum fishing boat. This boat was not properly rigged for oceanographic work, but was suitable for hand casting the CTD and gathering Niskin samples.

2.1 CTD Casts

To profile water column properties, probes that recorded conductivity, temperature, and pressure (CTD) were employed. During the 2003 UBC study, several different SeaBird (SBE) CTD probes were used in Nitinat Lake to gather data, and these are listed below in Table 2.1.1.

Table 2.1.1 – CTD model and serial numbers used at Nitinat Lake.

SBE-19	s/n: 2624
SBE-19	s/n: 109
SBE-19	s/n: 2924
SBE-25	s/n: 0258

The bulk of the measurements were recorded using s/n 2624. This instrument had three additional sensors: a transmissometer (WET Labs C-Star), a backscatter sensor (Seapoint Sensors Inc Turbidity Meter), and a Fluoromter (WET Labs WETStar).

Data from CTD casts were processed using SBE data processing software in conjunction with Matlab software to analyze and present data. For the SBE-19-2624 data, the following steps were taken using the SBE data processing software with the raw hex files:

1. Convert – Data files were converted to cnv files with the following outputs:
   Pressure [db]
   Temperature [ITS-90, deg C]
   Conductivity [mS/cm]
   Voltage 1 [backscatter]
   Voltage 2 [Fluoromter]
   Voltage 3 [transmissometer]
   Scan Count
2. Filter – Data were low pass filtered as follows:
   Pressure [time constant = 2 sec]
   Temp [time constant = 0.5 sec]
   Cond [time constant = 0.5 sec]
3. Align – Temperature data were advanced 0.5 seconds.
4. Derive – Salinity [PSU] and Density [sigma-theta] were derived.
5. Bin Average – Downcast data were bin averaged into 0.75m bins, unless otherwise specified in the analysis. Upcast data were discarded.

Unfortunately, there was a problem with SBE-19 s/n 2624 in Nitinat Lake. Near temperatures of 10°C and salinities of 30 PSU strange recordings were observed that manifested themselves as 'ticks' in the temperature data. Readings of conductivity were also noted to be off when compared with an SBE-25 during simultaneous casts (i.e., the SBE25 and SBE19-2624 were tied together and lowered through the water column at the same time) on July 15 and 16 of 2003. No problems with the instrument were noted during calibrations, and technicians from Sea-Bird were not able to determine the cause of the problem. A Matlab® script was written to process the raw hexadecimal files in order to remove the temperature ticks. This was done through a process of deleting the erroneous temperatures (which occurred at regular intervals) and replacing them with a copy of the preceding data line. Once this was done, the hex files were processed as normal.

The bulk of CTD casts were taken at stations along the thalweg of the lake (Figure 2.1.1). Table 2.1.2 lists the coordinates and water depth of each station shown in Figure 2.1.1.

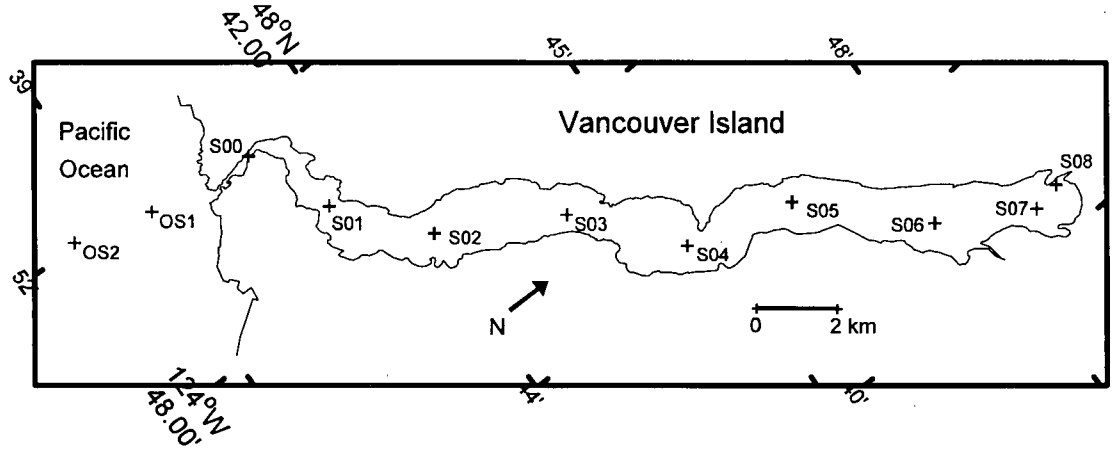

Figure 2.1.1 – Sampling stations used on Nitinat Lake during 2003 UBC study.

Stations one through seven were sampled frequently during each visit to the lake. Ocean stations (OS1 and OS2) were only sampled during July when weather and time permitted. Station zero (located on the sill) and station eight (mouth of Nitinat River) were sampled when time allowed.

Table 2.1.2 – Lake Station data for UBC Nitinat Lake study.

Name	Lat	Long	Water Depth (m)
OS2	N 48° 38.3'	W 124° 52.0'	45
OS1	N 48° 39.3'	W 124° 51.6'	27
S00	N 48° 40.8'	W 124° 51.3'	6
S01	N 48° 41.3'	W 124° 49.5'	68
S02	N 48° 42.2'	W 124° 47.7'	133
S03	N 48° 43.8'	W 124° 46.4'	140
S04	N 48° 44.7'	W 124° 44.5'	121
S05	N 48° 46.3'	W 124° 43.8'	203
S06	N 48° 47.5'	W 124° 41.8'	203
S07	N 48° 48.8'	W 124° 40.8'	190
S08	N 48° 49.2'	W 124° 40.9'	13

CTD casts were done in Nitinat Lake by hand with marked ropes. Each rope was 135 m in length, requiring two ropes to reach the maximum lake depth of 203m. Due to the large stratifications near the surface of the lake, the CTD was lowered at an approximate rate of 0.5m per second for the first 30m of depth, and then at a rate of 1m per second for the remainder of the cast. The sampling rate of the CTD SBE-19 was set to 2 Hz. To sample all nine stations along the thalweg with a CTD required between two and three hours, depending upon the depth of casts and wind conditions on the lake.

During July, mid afternoon winds in the northeast basin of the lake were often higher than 8 m/s, producing 0.5m plus waves. These conditions made it extremely difficult to hand cast the CTD. As a result, the majority of thalweg transects performed in July occurred during the morning hours.

To check for variations in properties across the small axis of the lake, two cross-lake transects were performed on July 11 centered on S06 (Figure 2.1.2). The first transect occurred between 8:30 and 10:00 PDT. The second occurred between 14:00 and 15:30 PDT on the same day.

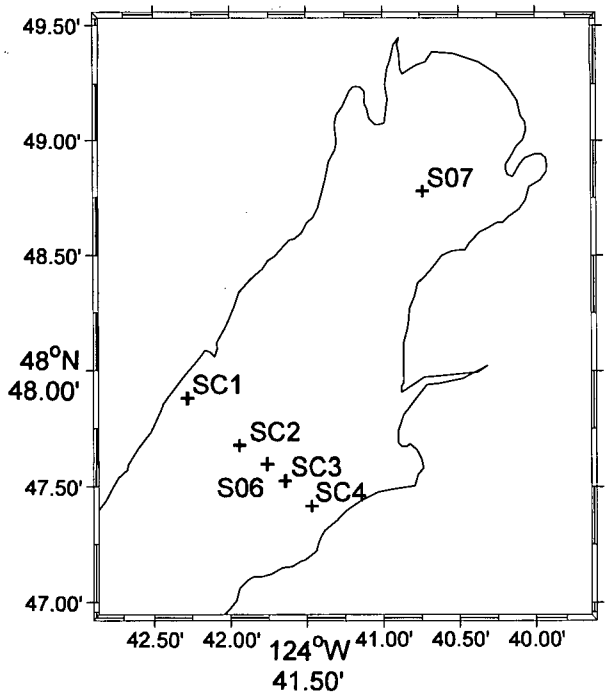

Figure 2.1.2 – CTD stations used on July 11, 2003.

On July 16-17 2003 R. Pawlowicz, B. Laval, and A. Ramnarine from UBC visited the lake and took instrument readings with an SBE-25. Due to the higher resolution and problems that were identified with the SBE-19, temperature, salinity and density data for the deep waters of Nitinat Lake are taken from the SBE-25 data when possible. The SBE-25 also had an oxygen sensor, which was used to obtain contours along the thalweg of oxygen levels. Dissolved oxygen readings obtained with the CTD were calibrated against bottle samples tested using the Winkler method. The February 17, 2004 CTD data were

obtained by Bernard Laval in cooperation with UBC graduate students using instruments loaned by Rich Pawlowicz.

2.2 Water Samples

2.5L Niskin Bottles were used to obtain water samples in conjunction with CTD casts. The purpose of this was to obtain oxygen content data using the Winkler titration method (as the primary CTD did not have an oxygen sensor) and to validate conductivity data given by the CTD.

Water samples were obtained using a marked rope with a single Niskin bottle attached near the bottom end. A weight was fixed to the bottom end of the rope. The line was marked such that the zero point aligned with the bottom opening of the Niskin bottle. It was not possible to obtain Niskin samples below 130m using this method, as this was the maximum length of the rope.

2.3 Weather Stations

Two weather stations were deployed at Nitinat Lake at various times during the 2003 study (Figure 2.3.1). The weather stations were shore based and recorded wind speed and direction, temperature, relative humidity, and solar radiation. Data were recorded in a data logger on site, and downloaded upon recovery of the station. The wind meter was located at the top of a 4.57 m pole that was secured using ropes and large stakes.

Due to the steep shoreline and heavy vegetation, there were a limited number of locations that provided good exposure to wind. Near the sill, a weather station (M2) was deployed on a gravel spit during the month of July. This data logger was removed at the end of the July study period, as the spit was known to be submerged during winter months.

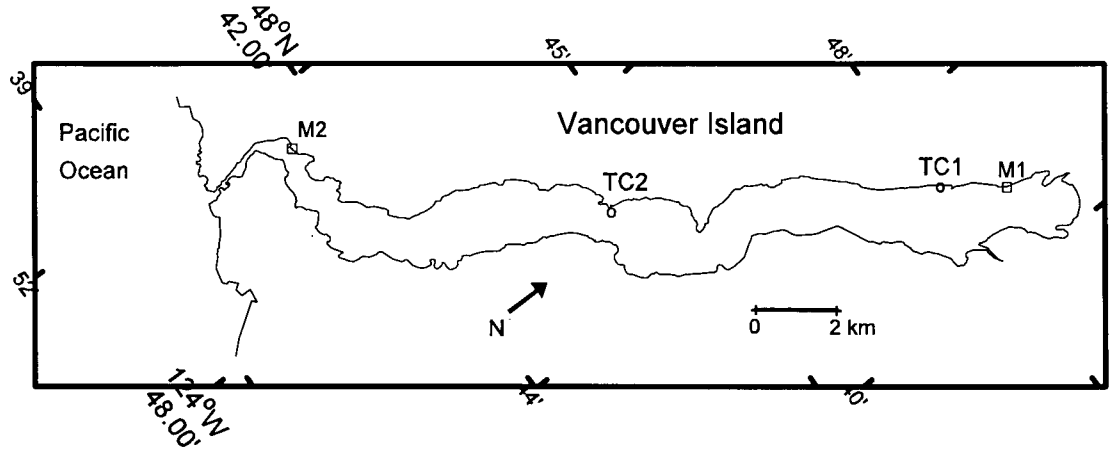

Figure 2.3.1 – Map showing location of meteorological stations M1 and M2, as well as temperature sensor moorings TC1 and TC2.

At the northern end of the lake, a second weather station (M1) was deployed on an abandoned log dump that formed a small prominence into the lake. This provided good exposure to winds blowing along the long axis of the lake, as well as winds from the south. The top of the log dump was roughly 3.5 m above the lake surface, and deemed a safe location to deploy a weather station for the summer and fall. Unfortunately, all of the data recorded at this location between July 7 and October 24 were lost due to a severe flooding event (October 19) that caused the lake level to rise 4 m in just three days. This flood submerged the surface of the log dump and flooded the data logger. The data logger was an older model whose memory was lost the moment the power connection was shorted out by water. An attempt was made at the end of July to download data from the data logger, but problems with the laptop computer batteries in the field prevented this from occurring. The decision to leave the weather station in place at the end of July without returning to download the July data was, in retrospect, a mistake.

It is more difficult to say that choosing the log dump was a mistake that should have been avoided. Various fisheries officers and first nations individuals cautioned that the log dump had been know to flood in the past, but these same individuals also said such instances were extremely rare and that there was usually good warning the lake level was rising. The severity of the October flood event was very unusual in that the lake rose 4m in just three days, and most first nations people agreed that the 2003 flood was the highest that they could remember witnessing.

2.4 Temperature Sensor Moorings

Two moorings with temperature sensors attached were deployed in late July, and removed from the lake in mid November at locations TC1 and TC2 (Figure 2.3.1). Due to the steep shoreline, moorings were run along the bottom of the lake towards the shore (Figure 2.4.1). One end of the mooring line was fixed to a large anchor that was placed at a depth of 40m from the shoreline, and the weighted line with sensors was then played out along the bottom until it reaching the shore, where the other end was fixed to large tree.

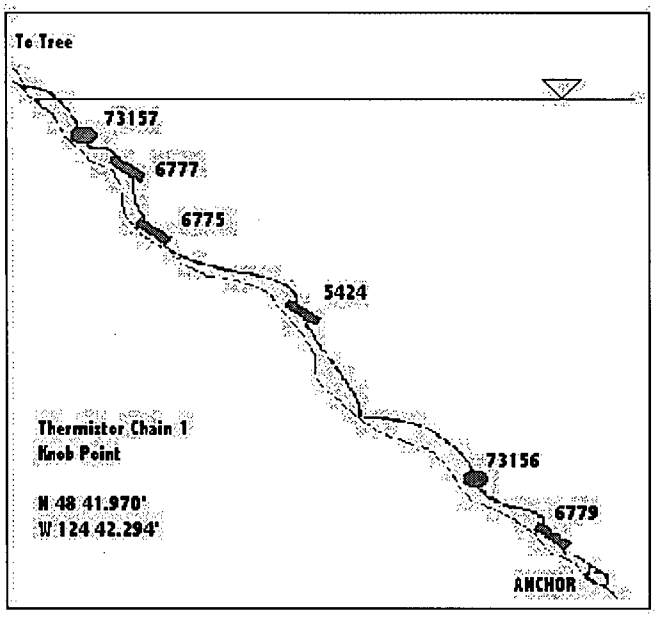

Figure 2.4.1 – Schematic of thermistor chain deployment.

To determine the bathymetry in the desired location, a GPS and depth sounder were used to roughly determine the bottom slope at the mooring location. This information was then used to determine the spacing of sensors during setup of the mooring line.

The advantage of this system was that a smaller anchor could be used as the line was not under tension, no surface or sub-surface floats were required, and sensors would not be subject to movement due to deflections of the mooring line from currents. The disadvantage was uncertainty as to the exact depths of the sensors once deployed, although comparison of CTD casts taken near the moorings at specific times allowed for the approximate depths of each sensor to be determined.

Temperature sensor probes were a combination of Richard Brancker TR1000 sensors and Stowaway (model HTI) instruments (Table 2.4.1). TR1000 temperature sensors recorded data once every minute during the study, while the Stowaway sensors recorded only one every ten minutes due to limited memory. The Stowaway instruments were placed in waterproof plastic containers, and strapped to the mooring line. All instruments were calibrated both before and after deployment in the Oceanography calibration tank at UBC. Time drift of the internal clocks of the instruments was monitored, and found to be less than 10 minutes during the entire study period.

Table 2.4.1 – Depths of temperature sensors on TC1 and TC2. Errors reflect the differences in calculated depth from CTD casts.

TC 1		TC 2	
Sensor s/n	**Depth**	**Sensor s/n**	**Depth**
73157	5.1 m (± 1.0)	73154	4.0 m (± 1.0)
6777	7.6 m (± 1.5)	6782	9.0 m (± 1.0)
6775	15.6 m (± 3.0)	8834	11.5 m (± 3.0)
5424	23.6 m (± 0.4)	73155	18 m (± 4.0)
73156	30 m (± 3.0)	6778	22 m (± 2.0)
6779	36 m (± 3.0)	6776	42 m (± 6.0)

2.5 River Temperature Sensors

Temperature sensors were placed in the primary rivers feeding into Nitinat Lake; Nitinat River, Caycuse River, and Hobiton River. No current or stream flow data was recorded for these rivers as part of this study.

Temperature sensors were set to record data once every 15 minutes. Sensors were Stowaway (model HTI) and placed in waterproof plastic housings with a bag of desiccant. This plastic waterproof container was then placed into a section of aluminum pipe, and bolts were run across with end to secure the sensor inside. The entire aluminum housing was placed in a deep spot in the river, preferably in shade, and attached with chain to a large tree on the riverbank. The location of each sensor is given in Table 2.5.1.

Table 2.5.1 – Locations of river temperature sensors.

MFR	Model	S/N	Lat	Long	Location
Stowaway	HTI	1281	N 48° 47.97'	W 124° 38.44'	Caycuse River
Stowaway	HTI	1284	N 48° 46.47'	W 124° 44.35'	Hobiton River
Stowaway	HTI	3610	N 48° 49.60'	W 124° 40.21'	Nitinat River

On the Nitinat and Caycuse rivers gravel and rock movement were observed during the study period. Significantly, on the Nitinat River the riverbank had eroded several feet, and a number of large trees that had been close to the shoreline had toppled into the river. These events probably occurred during the heavy rainfall period in October. It was not possible to see the locations of the sensors on the river bottom prior to recovery due to sediments in the river, thus it is possible that the sensors were with partially or completely buried in the streambed during the study. The sensors were retrieved using a chain-puller and tackle system.

All temperature sensors were calibrated both before and after deployment. All instrument temperatures were corrected accordingly. Time drift was minimal.

2.6 Ancillary Weather Data

The Nitinat River Hatchery (DFO) records daily air temperature maxima and minima as well as precipitation, and these data were obtained from Environment Canada. In addition, an automated weather station near the mouth of Nitinat Lake (N 48.667, W -124.817) was operated by Environment Canada between December 1992 and December 2001, but was abandoned in place and is no longer functioning. Complete data records that include atmospheric pressure, temperature, precipitation, and wind data from Environment Canada are only available from Vancouver Island airports such as Tofino, Nanaimo, and Victoria.

Until recently, weather data such as mean temperature and precipitation were collected at lighthouse stations along the coast, but Environment Canada stopped archiving these data in 2002 due to budget cuts. Also, some lighthouses have been automated in recent years.

It is possible that satellites have recorded lake surface temperatures in Nitinat Lake, but no attempt has been made to obtain these records for this thesis.

It is not recommended to infer surface winds at Nitinat Lake based upon recorded winds at the Tofino, Nanaimo or Victoria airports. The Victoria and Nanaimo airports are

located on the east side of Vancouver Island, and both are located in wind shadows from westerly and southerly wind patterns. The Tofino airport, while located on the west coast of Vancouver Island, is more than 80km to the northwest and did not necessarily encounter similar weather conditions. During summer months it was not uncommon for the Tofino airport to report no wind and fog, while at Nitinat lake the weather was both sunny and windy.

3.0 Data - Physical Properties

This chapter presents data that were collected at Nitinat Lake between February 2003 and February 2004. These data were obtained using a variety of instruments to measure physical properties of the lake and atmosphere (see Methodology, chapter 2). The chapter first presents physical water properties, followed by water level (tidal) and meteorological data. Sections 3.1 and 3.2 present lake and river temperature data respectively. This includes data from both CTD and sensor moorings. Section 3.3 presents salinity data, as obtained by CTD, while section 3.4 presents the density as derived from temperature and salinity. It is assumed the equation of state for Nitinat Lake is that of seawater in this derivation. Dissolved oxygen levels in the lake are presented in section 3.5, followed by a brief review of Chlorophyll levels (section 3.6) and turbidity and backscatter levels (section 3.7) as observed with the CTD.

Tidal variations and changes in lake surface level elevation were observed using a bottom mounted pressure sensor, and these data are presented in section 3.8. Of note in this section is a review of the interesting flood event that occurred between October 16 and 21, 2003. Section 3.9 presents the air temperature, relative humidity, solar radiation, and wind data that was collected during two separate time periods in 2003 with temporary meteorological stations located on the lake shore.

Subsequent chapters reference and use data which are presented in this chapter; specifically temperature, density and wind data when examining internal lake response to wind forcing. Some of the other data, such as chlorophyll and turbidity levels, are not referenced in later analysis of the lake but were gathered during the course of the lake study and are presented here to give a more complete review of the physical characteristics of Nitinat Lake.

3.1 Lake Temperatures

Temperature is an important property of seawater. Physically, temperature distribution gives clues to the energy flux within a body of water while playing an important role in determining ecological processes. At Nitinat Lake, temperature was measured vertically

within the water column at different locations using a CTD probe (Section 2.1), while a temperature sensor mooring was set in each basin of the lake (Section 2.4). The CTD was used to determine spatial variations within the lake, while the temperature moorings were used to track temporal changes at a specific location.

CTD data were collected at four times during 2003: February, July, September, and November. The February and September data consists of a single transect of the thalweg, while more extensive data were collected during July and November. Temperature transects from different times of the year are shown in Figure 3.1.1 and are representative of the changes in temperature structure in the upper 25 m of the lake during the year. Contours are produced from temperature data obtained at seven stations along the thalweg (Figure 2.1.1), and the locations of these are noted as vertical dashed lines with distances shown in km along the x-axis with S07 as the zero reference.

During the winter months a temperature inversion is observed in the surface layer, suggesting that density is more strongly influenced by salinity than temperature (Figure 3.1.1). There is very little temperature variation observed along the surface of the lake, so long as stations on the sill (S00) and stations at river mouths (S08) are excluded. Surface temperatures in February are near 7°C, increasing to 10°C as depth increases towards 20m. While there is little spatial variation in temperature at the surface, there is a noticeable variation in the 9°C contour near S01, most likely caused by incoming ocean water over the sill.

In early July, surface temperatures are seen to have increased to almost 18°C, while at 20m depth there has been almost no change with water temperatures remaining steady at 10.4 °C. Spatial variations between the two ends of the lake are more evident in July, as temperature contours are seen to deepen slightly and the gradient weaken at stations S01 and S02. In contrast, there is a strong temperature gradient at the north end of the lake between stations S04 and S07 with temperature decreasing rapidly from 17 to 11°C between 2 and 8m in depth.

September data shows the surface waters to be cooling from summer highs (near 20°C at the end of July), but also shows the warmest temperatures at depths of 20 to 25m between stations S01 and S03, with temperatures above 11°C. However, there is almost no change in the depth of the 11°C contour between stations S05 and S07 from July to September.

Between September and November of 2003 the temperature structure in the top 25 m of the lake changed significantly. Surface temperatures became colder than deep water temperatures in the lake creating a temperature inversion, while a pocket of 11°C water formed between the depths of 8 and 13m in the north basin (stations S05 to S07). This 'pocket' of water represents the warmest waters in the lake at this time. However, by February of 2004, the 'pocket' no longer exists, and there is little spatial variation in water temperature contours within the lake (Figure 3.1.1).

Figure 3.1.2 shows individual temperature profiles from four times of the year at two different locations in the lake, S02 and S06. These profiles clearly show the seasonal variation in temperature in the upper layer of the lake, and highlight the spatial differences between the inland and ocean end of the lake. At S02, in the south end of the lake, there is more variation of temperature between seasons to a greater depth, while at S06 there is almost no season variation below 20m. The profiles also clearly show the fall and winter (November and February data) temperature inversion where the surface waters are colder than the deep water below 20m.

Several CTD transects included ocean stations when weather and time permitted, giving a comparison of conditions on both sides of the narrow sill that connects Nitinat Lake with the Pacific Ocean. Figure 3.1.3 shows temperature contours for the upper 25m from stations OS2 to S07. Surface water in the ocean is about 6°C cooler than in the lake. Ocean water below 12m in depth is less than 10°C, which is colder than the deepest water in Nitinat Lake at a depth of 200m. Water on the sill (stations S00 and S00.5) is between 14 and 16°C, which matches with the temperature of water near 5m depth at station S01. Surface waters at the end of July are seen to be above 18°C, almost a degree warmer than on July 10 (Figure 3.1.3), suggesting that the lake had not yet reached its annual peak temperature during the July study period.

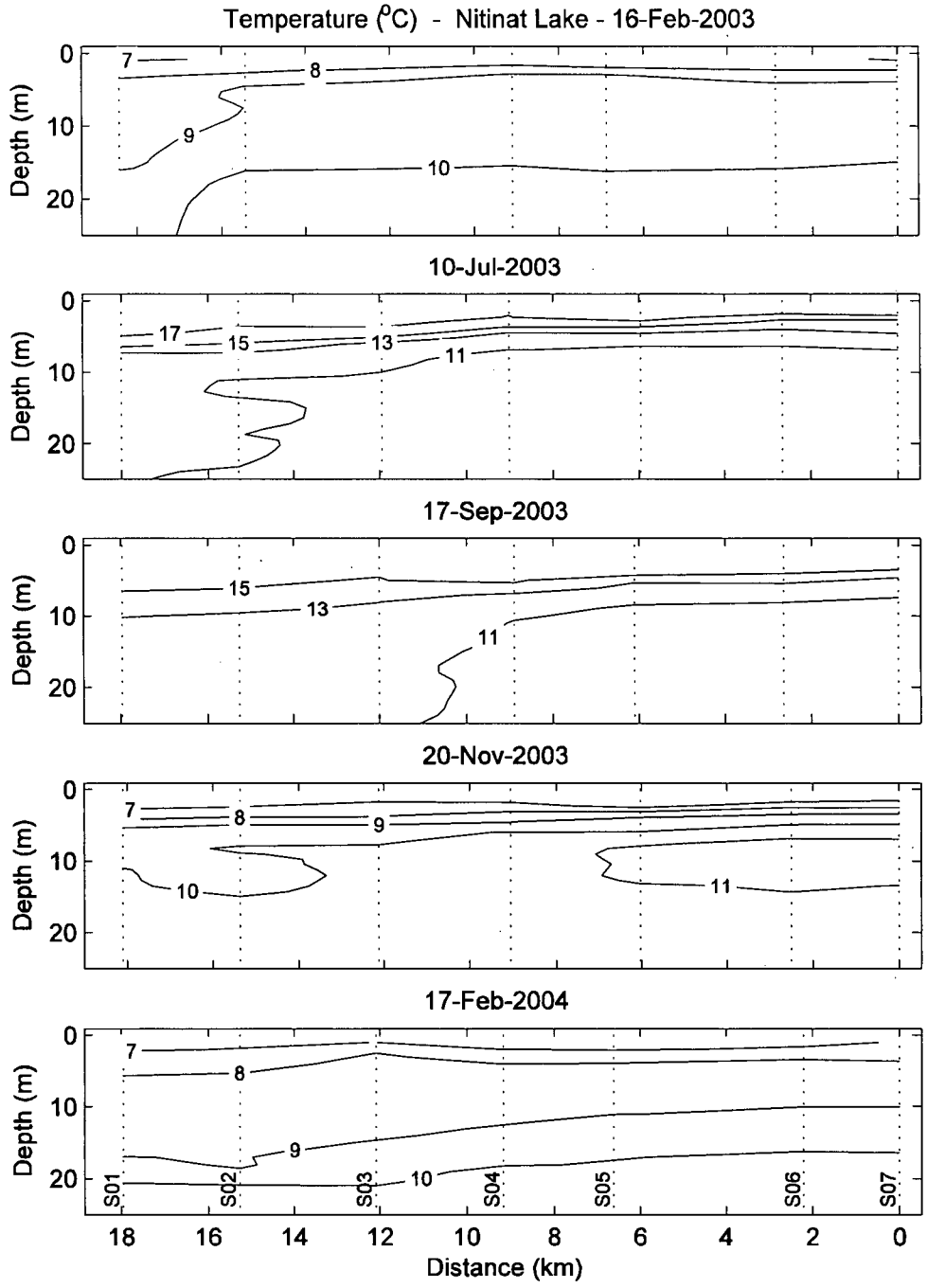

Figure 3.1.1 – Temperature contours for the top 25 m of Nitinat Lake, from February 2003 until February 2004. Temperature inversions are evident during winter months when surface water is cooler than deep water. (February 2004 data courtesy of Rich Pawlowicz)

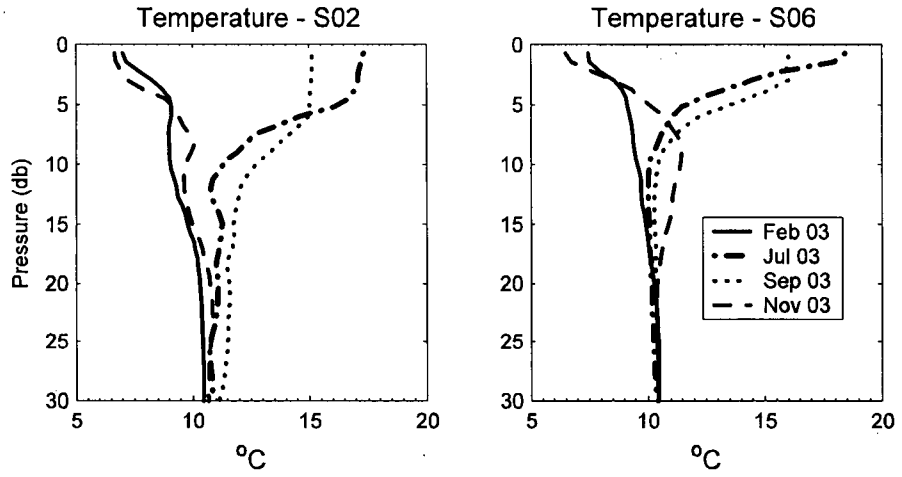

Figure 3.1.2 – Temperature profiles at stations S02 and S06, showing seasonal variation in surface layer.

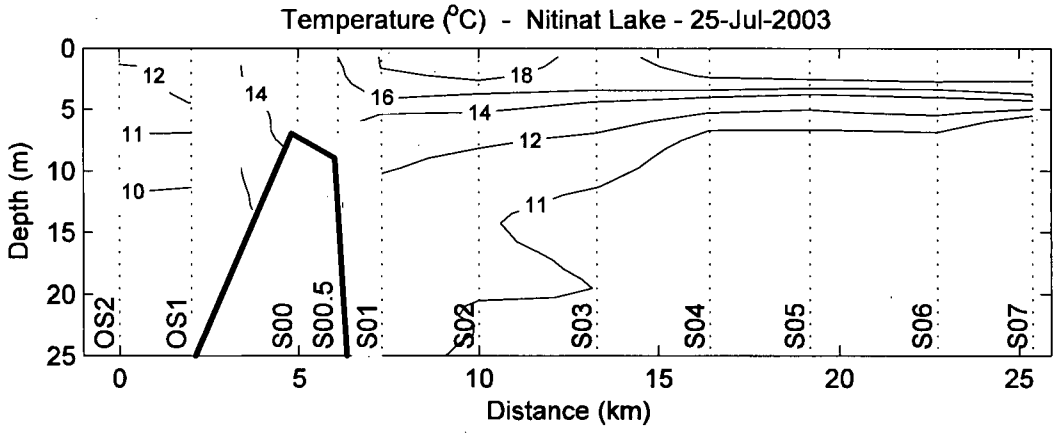

Figure 3.1.3 – Temperature contours on July 25, 2003. Ocean stations and sill are also shown. Heavy black line denotes bathymetry along thalweg. CTD cast locations denoted by doted vertical lines. Tide was incoming during this survey. A slow incoming current was observed when sampling at stations S00 and S00.5.

Two cross-lake transects were taken across the short axis of the lake at S06 (map, Figure 2.1.2) in the north basin (Figure 3.1.4). In the early morning of July 11 2003, there was no wind on Nitinat Lake and the surface was 'glassy' calm. It was at this time the first transect occurred. The second transect occurred in mid-afternoon with a strong sea breeze present. Noticeable changes were observed in the temperature structure of the lake during this time frame. In the early morning, there is no significant spatial variation across the short axis of the lake. By the afternoon the vertical temperature gradient had increased in comparison to the early transect, with a sharp change in temperature between 5 and 7m depth at SC1. On the other side of the lake at SC4 the depths of the temperature contours

are almost unchanged from the morning, although the surface water had become slightly cooler dropping from 18 to 17°C.

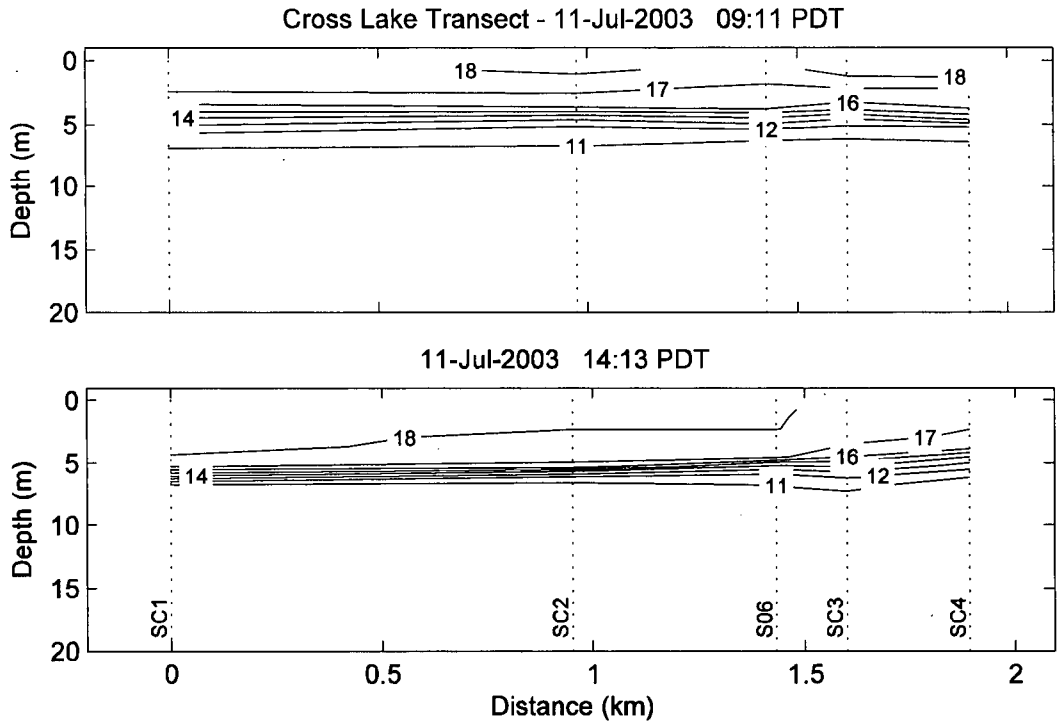

Figure 3.1.4 – Temperature contours in the upper 20m of the lake, taken perpendicular to the thalweg at S06. The two sets of contours are from different times on the same day: top plot shows temperature in the morning, bottom plot show temperature at mid-afternoon. Morning conditions were zero wind, and 'glass calm' lake surface while afternoon conditions were strong winds (>9 m/s) from the SW and 0.5m waves.

Wind driven surface currents were observed to be very strong during the afternoon transect at SC1, SC2, and S06 on July 11 (Figure 3.1.4). While the CTD was in the top 5m of the water column, the survey boat could drift with the wind and waves to maintain a vertical rope to the CTD. Once the CTD dropped below 8m in depth, it was necessary to actively keep station with the survey boat in order to maintain a vertical rope on the CTD. Surface drift was estimated to be approaching 1 m/s. However, at stations SC3 and SC4 the strong surface current was not observed, and the sea-state was altered (sharp short waves) suggesting a possible counter current existed at this time. The survey boat was not equipped to measure currents, so no conclusions are possible, but these observations may explain the spatial variations in the afternoon temperature contours in Figure 3.1.4.

Figure 3.1.4 suggests that wind forcing can significantly alter the temperature gradient in the surface layer. To examine temporal changes in temperature, two temperature sensor moorings were placed in the lake on July 21 and 22 respectively (Figure 3.1.5).

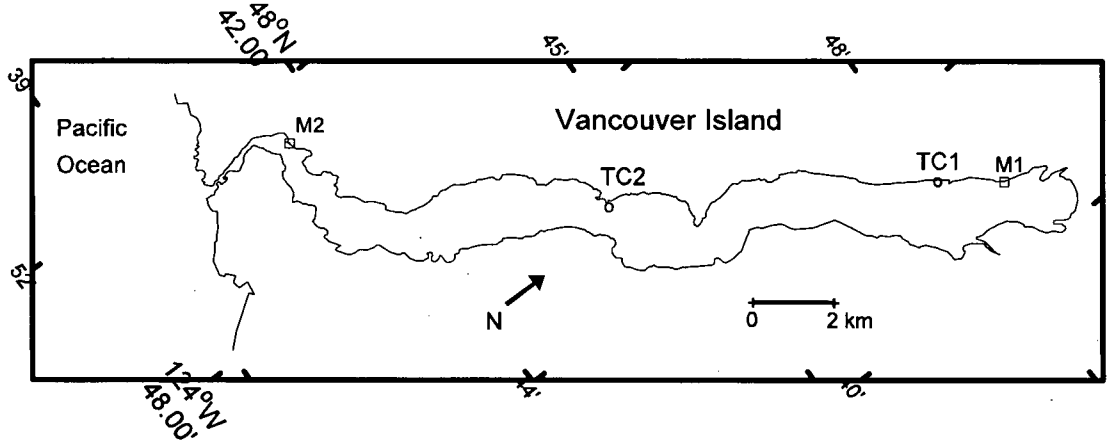

Figure 3.1.5 – Map showing location of temperature sensor moorings TC1 and TC2, as well as meteorological stations M1 and M2.

The summer sea-breeze was observed to mix the surface layer and push the surface waters towards the downwind (i.e. northeast) end of the lake. Figure 3.1.6 shows temperature data from four sensors (5m, 7.5m, 10m and 34m depths) on the TC1 mooring during two days in July when a strong sea-breeze was present. The uppermost sensor at 5m (heavy solid line, Figure 3.1.6) is seen to vary the most with temperatures between 11 and 19°C observed in a single day. The warmest temperatures are recorded in the late afternoon and evening, corresponding to the time of day when air temperatures are highest and the afternoon sea-breeze has developed. Temperature variation is significantly less at 7.5m depth (dash-dot line, Figure 3.1.6), with a daily range of 10.4 to 12.5°C for the same time period. At a depth of 10m, the daily temperature variation due to wind forcing becomes very small (thin solid line, Figure 3.1.6 and Figure 3.1.7) in comparison to the changes at 5m depth. Finally, at a depth of 34m there is no significant daily change in temperature (dashed line, Figure 3.1.6). However, it is interesting to note that the temperature at 34m is warmer than the temperature at 10m. This trend, with the coldest waters observed at a depth near 10m and a slight increase in temperature at a depth of 20-40m, was observed in CTD data from stations S05 to S07 during the month of July (Figure 3.1.2, July data).

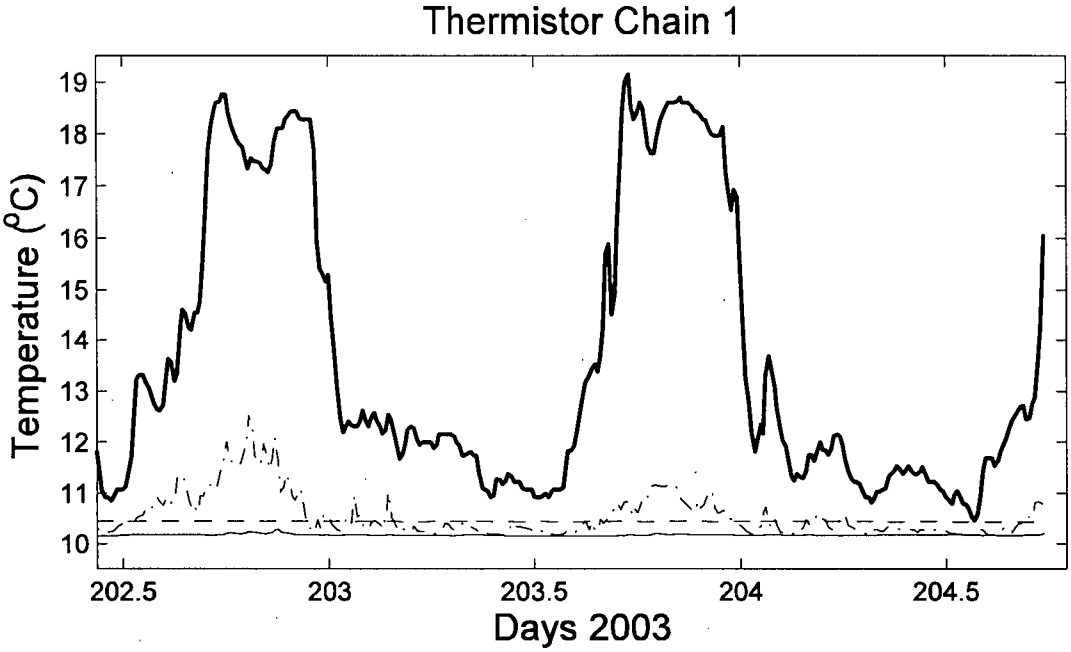

Figure 3.1.6 – Temperature data from thermistor mooring 1 from 10:30 PDT July 22 to 18:00 July 24. The t-sensors were located at 5m (thick solid line), 7.5m (dash-dot), 10m (thin solid line) and 34m (dashed) depths. Note the large temperature variations at 5m depth compared to the temperature variations at 10m. Also note that the temperature is higher at 34m than at 10m depth.

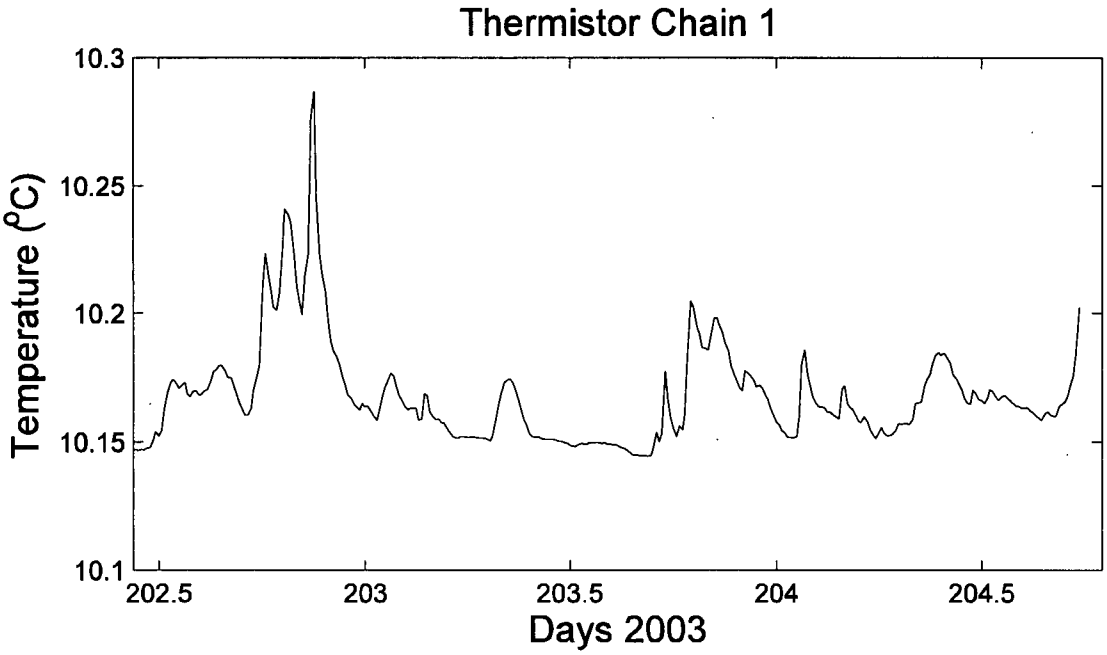

Figure 3.1.7– Temperature data from thermistor 6775 on mooring 1 from 10:00 PDT July 21 to 18:00 July 24. The t-sensor was located at 10m depth. Note the range of the temperature scale.

Figure 3.1.8 shows temperature data from sensors on TC2 during the same time period in July as shown in Figures 3.1.6 and 3.1.7 for TC1. The temperature sensors on TC2 shown in Figure 3.1.8 are at 5m, 10m and 38m depths. As at TC1, the uppermost temperature sensor is seen to have the greatest daily variation in temperature, while the deepest sensor shows the smallest variation. In contrast to TC1, the warmest temperatures are recorded in the morning at TC2, while the coldest temperatures were recorded in the evening. This is exactly opposite to the effect at TC1. The temperature variation at 5m depth at TC2 is also less than that at TC1, and there is more variation in the signal.

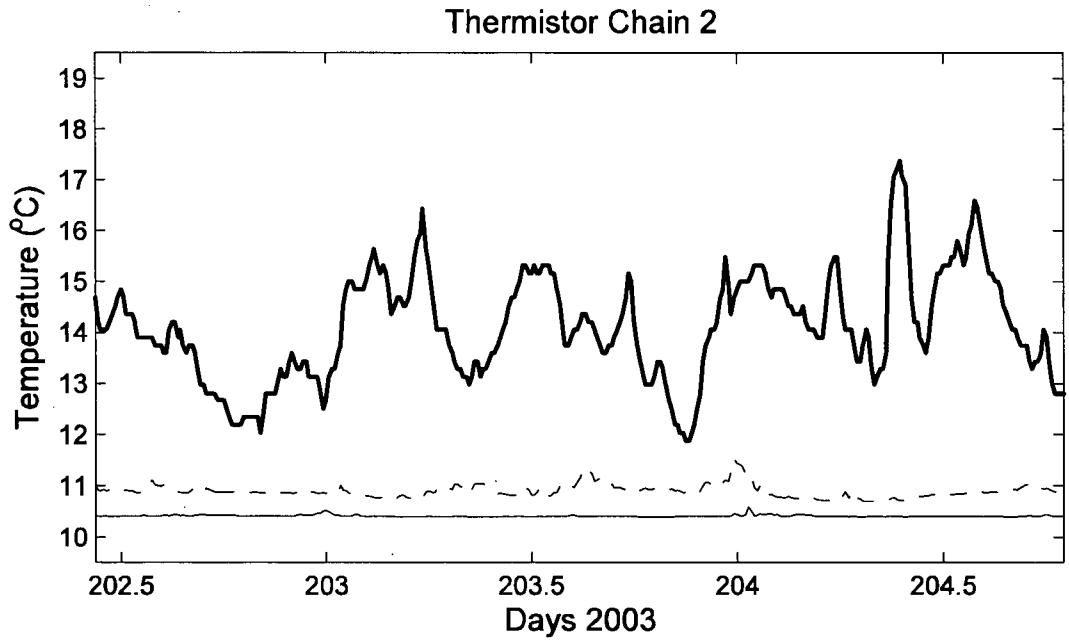

Figure 3.1.8 – Temperature data from thermistor mooring 2 from 10:30 PDT July 22 to 18:00 July 24. The t-sensors were located at 5m (thick solid line), 10m (dashed), and 38m (thin solid line) depths. Note the large temperature variations at 5m depth compared to the temperature variations at 10m. Maximum surface temperatures at TC2 are less than at TC1 (Figure T5) during this time period.

Looking back to Figure 3.1.2, it is clearly seen that the shape of the profile near S02 is significantly different than that near S06. The profile for July from the south basin reveals a cooler surface temperature and near constant temperatures down to a depth of 4m, whereas at S06 during the same time period temperatures in the top 4m showed significant variation. Furthermore, at a depth of 10m the temperature in the south basin is warmer than the temperature at the same depth in the north basin in July, and below 10m

in depth the temperature in the south basin shows oscillations between 10.5 and 11°C. Comparisons between TC1 and TC2 for the same time period should be made cautiously, as a change in depth of the pycnoclines may not be directly proportional to temperature for both locations. The relationship between temperature and density in Nitinat Lake is further studied in section 5.2.4.2.

Figure 3.1.9 shows temperature profiles obtained with the CTD in the immediate vicinity of the temperature moorings. The profiles highlight the differences in the temperature structure that are seen in Figures 3.1.6-3.1.8, most striking that the temperature at 10m depth near TC1 is less than the temperature at 40m. This is not the case at TC2.

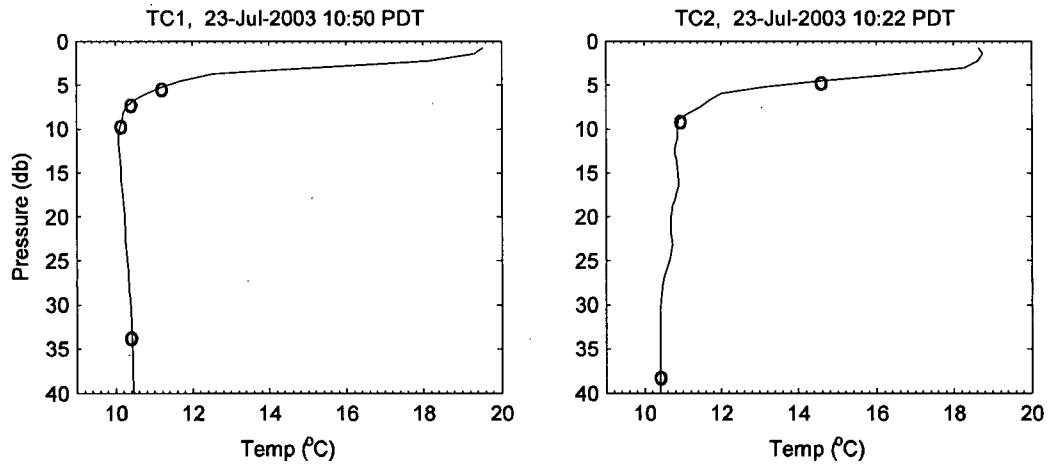

Figure 3.1.9 – Temperature profiles from CTD data obtained near TC1 and TC2 temperature sensor mooring. The circles represent the depth of the temperature sensors on the thermistor chains.

Figure 3.1.10 shows three profiles taken at the same location over the course of a single day. These profiles highlight the temporal variation in the temperature structure that occurred during the summer due to wind stress on the surface 'pushing' the surface layer towards the downwind end of the lake and forming a standing internal wave. These data confirm the data obtained by the temperature sensor moorings. Between 5 and 7m the water experienced the greatest variation in temperature with daily changes of over 7°C. At the surface, and below 13m, there is no discernable variation in water temperatures during the day.

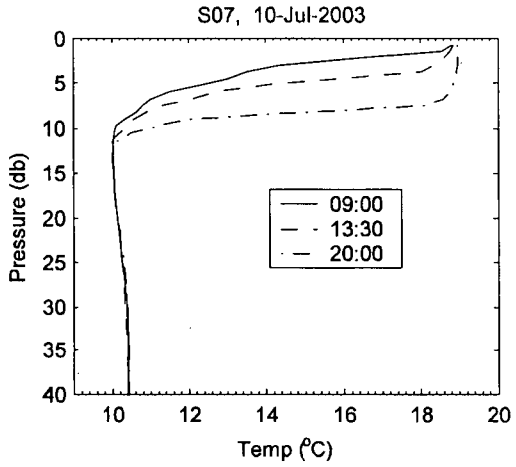

Figure 3.1.10 – Temperature profiles from CTD data obtained at S07 during three different times on July 10, 2003. A strong sea-breeze mixed the surface layer on this day, beginning at 10:00am and continuing until 19:00 PDT in the evening.

Up until this point, the focus has been on spatial and temporal changes in temperature in the upper 30m of the lake. In comparison to the upper layer, the bottom layer of water could be considered at a constant temperature. However, a close examination of deep water temperatures at two stations with in the lake reveals some minor variation between the July and November sampling periods. Figure 3.1.11 shows temperatures at stations S02 and S05 between 40 and 200m depths (although it should be noted the lake is only 138m deep at S02). The temperature scale on these plots is just 0.7°C in order to highlight the subtle differences in temperature over depth.

At station S02 it is observed that all of the July data (dashed lines) have a similar profile, ranging from near 10.4°C at 40m and slowly cooling to 10.2°C near the bottom of the lake. By November (solid lines) the deep water temperature structure has changed. At 40m, the temperature in November has increased to 10.6°C, with even warmer temperatures observed towards the bottom.

At station S05 a similar trend was observed between the July data and the November data, with an increase in the deep water temperatures in November. Between 40 and 120m depth at S05 there is no significant change between the two time periods, but below 130m there is a marked shift in the November data. At 145m there appears to be a distinct 'step' in the temperature profile (which is, oddly, a temperature inversion as well) and

below this depth temperatures gradually increase towards the bottom of the lake. If the water was homogeneous, these temperature profiles with their inversions would be very unstable, suggesting that salinity is more powerful in controlling the density stratification in this lake. The profile in Figure 3.1.11 would also suggest that there was some renewal or change of the deep water in Nitinat Lake between July and November of 2003.

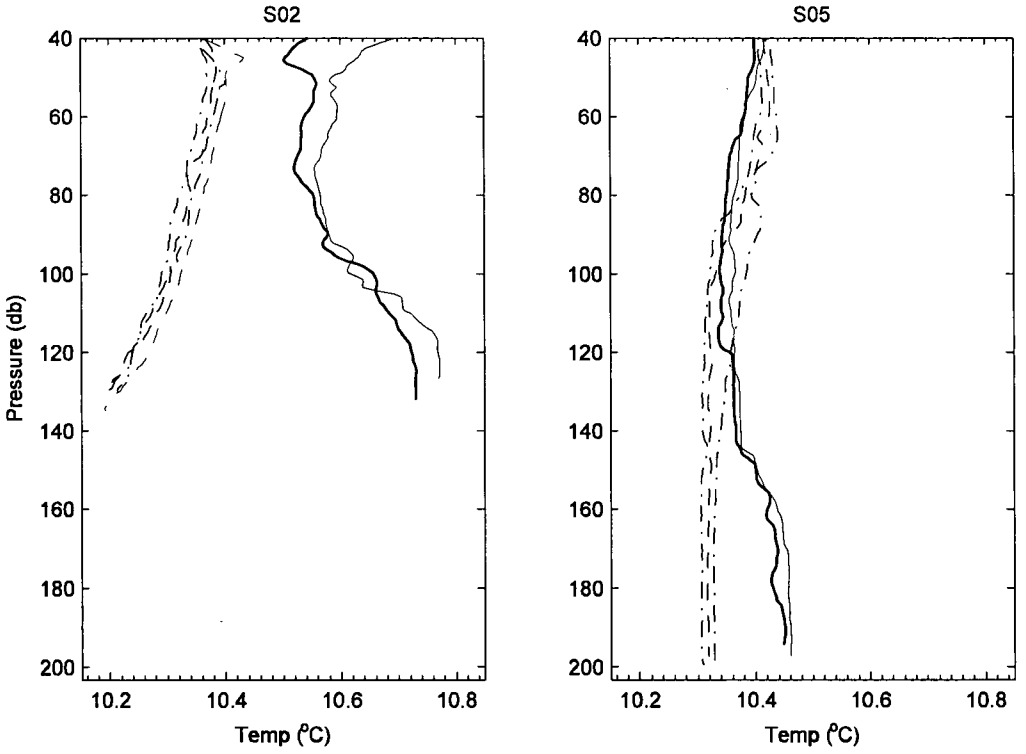

Figure 3.1.11 – Deep water temperature profiles for stations S02 and S05 during 2003. Dashed lines represent data from July sampling period, while solid lines indicate data from November. Note temperature range on plot is from 10.15°C to 10.85°C.

3.2 River Temperatures

Temperature sensors were places in three of the major tributaries that feed into Nitinat Lake during the 2003 study period. The three rivers represent drainage areas of significantly different sizes: Nitinat River drainage is roughly 800 km^2, Caycuse is approximately 150 km^2, and Hobiton just 35 km^2.

The Nitinat River is the largest river, and meanders over large gravel beds as it approaches Nitinat Lake. During the summer months the flow is very low, and large

pools form between gravel beds. It is not possible during summer months to bring a boat up this river without frequent portages. In the winter months the river is several meters higher on average, and on rare occasion much more. During the October 16 flood of 2003, river levels increased by more than 9m from summer levels at the Nitinat Hatchery pump house. (During instrument recovery in November, Salmon carcasses were observed in the lower branches of trees along the river banks). Figure 3.2.1 shows temperature for the Nitinat River between 23 July and November 17. The solid line represents the actual recorded temperature, once every 15 minutes in the river, while the solid dots are the daily average temperature. There is a strong daily variation in temperature up until early October, due primarily to the combination of low flows at this time of year and good sun exposure to the shallow waters flowing over the gravel beds.

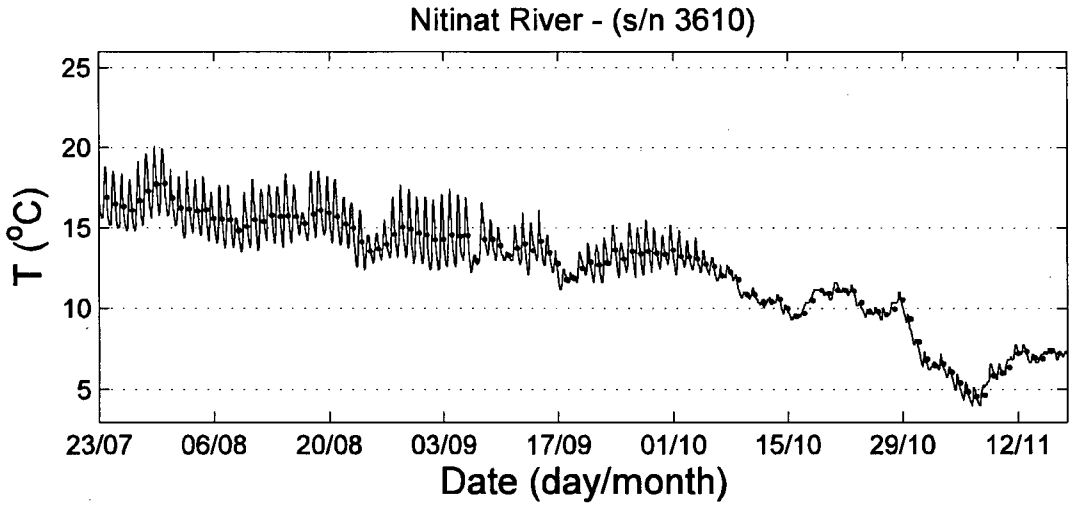

Figure 3.2.1 – Temperature record from Nitinat River during 2003 study. The sensor was located at N 48° 49.60' W 124° 40.21'. Temperatures were recorded once every 15 minutes in the river, and these data are shown as a solid line. Daily average temperature is shown as a dot.

The average daily temperatures in the Caycuse River are almost identical to that of the Nitinat River, although the daily temperature range was smaller (Figure 3.2.2). This is likely due to the fact that the Caycuse River is smaller than the Nitinat River, with significantly more shade. Gravel beds on the Caycuse exist at the river mouth and continue upstream for about 1.3km, but upstream of this the river runs through a deep and narrow gorge.

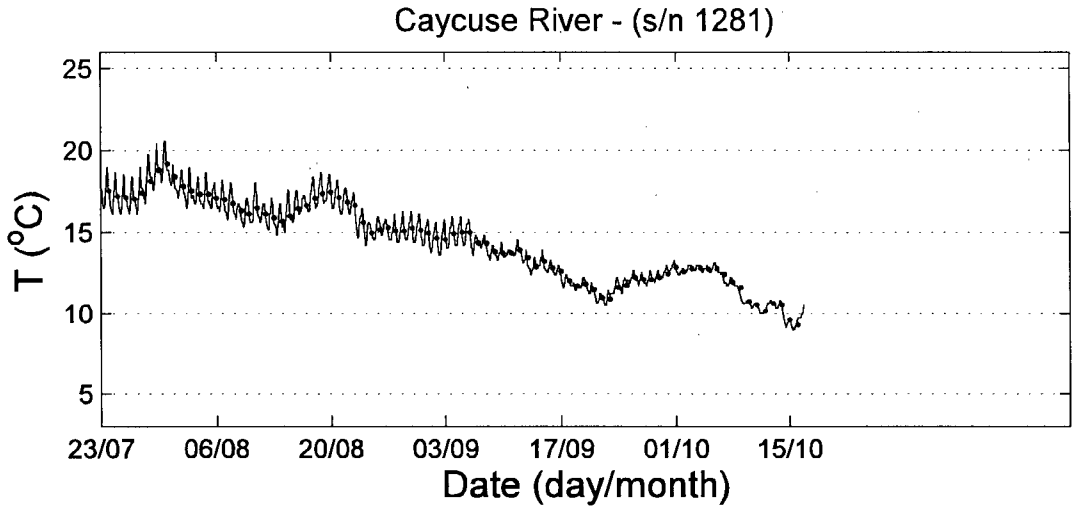

Figure 3.2.2 – Temperature record from Caycuse River during 2003 study. Sensor was located at N 48° 47.97' W 124° 38.44'. Temperatures were recorded once every 15 minutes in the river, and these data are shown as a solid line. Daily average temperature is shown as a dot. This sensor was recovered with a small amount of water in the housing, and was found to have no data beyond the date of the flood on October 16, 2003.

As on the Caycuse, the Hobiton River (Figure 3.2.3) daily temperature range is smaller than in the Nitinat River due to the small size of the river and dense vegetation that provides shade for most of the river. The Hobiton River and Hobiton Lake exist within the boundaries of Pacific Rim National Park. The Hobiton River drainage area is smaller and closer to the coast than the other two rivers, and the temperatures in this river were seen to be about 5°C warmer than daily averages in the other rivers. In the summer time this could be explained due to the extremely low flow rates in this river, and to the fact that this river drains from the surface of a lake. In summer, it is likely that this fresh water lake is thermally stratified and the surface layer is heated by solar radiation. During the winter time, warmer temperatures in the Hobiton may be explained by the fact that the Hobiton drainage area is smaller, closer to the coast and at a lower elevation than the larger drainage areas of the other rivers. In mid November of 2003, both the Nitinat and Caycuse rivers had melting snow in their upper watersheds while this was not the case for the Hobiton watershed. Furthermore, the Hobiton River is draining a small lake and Hobiton Lake, which is probably monomictic, mixes during the fall and buffers some of the cooler temperatures.

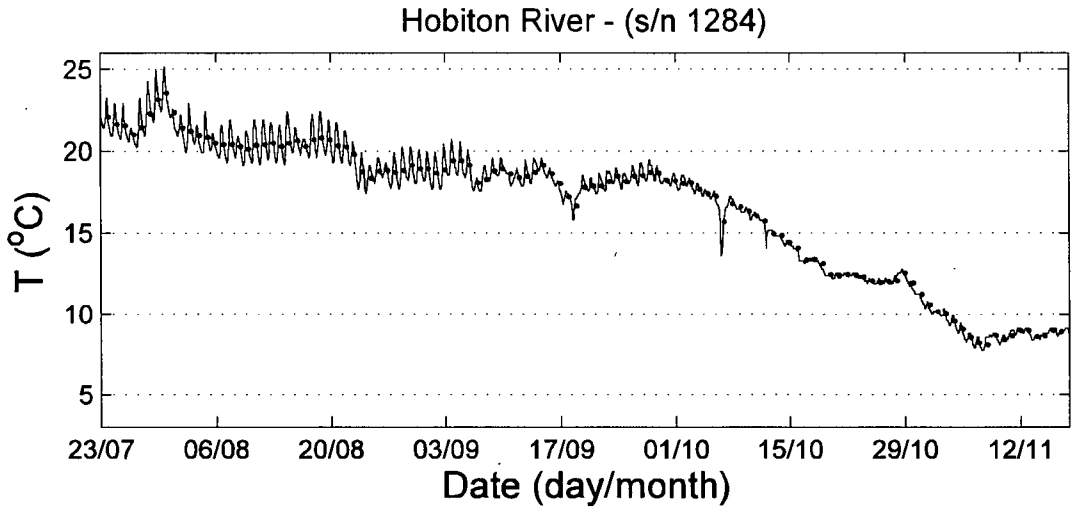

Figure 3.2.3 – Temperature record from Hobiton River during 2003 study. Sensor was located at N 48° 46.47' W 124° 44.35'. Temperatures were recorded once every 15 minutes in the river, and these data are shown as a solid line. Daily average temperature is shown as a dot.

3.3 Salinity

Sea water is composed of 96.5 % pure water plus a mixture of salts, dissolved gases, and organic substances. Salinity is a term that refers to the concentration of salt per unit of sea water. Sea salt is comprised of six main elements (sodium, chlorine, calcium, potassium, magnesium, and sulphur) that account for 99% of the total sea salt. Of these six elements, sodium and chlorine compose about 86% in seawater (Thomson, 1981). These elements exist as ions in the water, and can carry an electrical charge. Ocean water is chemically renewed over long time periods (millions of years) by the hydrologic cycle and by passing through the earth's crust, and the relative proportions of these ions in sea water remains constant over time due to 'relatively' quick mixing processes within the oceans.

Salinity has historically been defined as the total weight of salts in grams dissolved in one kilogram of water at a temperature of 15°C (UNESCO, 1969). However, the original practice of evaporating seawater in order to weigh the salt residue to determine salinity was time consuming and prone to error. Once technology came available to perform in-situ measurements of conductivity, this became the preferred method of salinity determination. In response to new measurement technology, salinity was redefined as a

ratio of the electrical conductivity of the seawater to the electrical conductivity of a standard concentration of potassium chloride solution (Segar, 1997). Known as the Practical Salinity Scale and given in units of Practical Salinity Units (PSU)

Nitinat Lake salinity was calculated from measured conductivity, temperature, and pressure using the 'practical salinity scale' or PSS-78 (UNESCO 1981a. The Practical Salinity Scale 1978 and the International Equation of State of Seawater 1980). The relationship between Practical Salinity Units and older measures of salinity (typically measured in parts per thousand) is very close to 1:1. It should be noted that practical salinity has no units as it is a ratio, but is commonly denoted by PSU (practical salinity units). All salinity values calculated for Nitinat Lake from recent field measurements are in PSU.

Nitinat Lake contains seawater due to a narrow channel that connects the lake to the ocean. However, mixing of incoming seawater with outgoing lake water in the shallow channel reduces the salinity of ocean water entering the fjord, resulting in the deep water in Nitinat Lake being less saline than the ocean water in the Strait of Juan de Fuca. On July 10, a survey of the lake and ocean immediately seaward of the sill (Figure 2.1.1) observed salinities near 32 PSU, while deep water maximum salinities observed during July were 31.28 PSU in the south basin, and 31.3 PSU in the north basin (Figure 3.3.1).

The salinity distribution in the surface layer of Nitinat Lake is influenced by a variety of factors such as precipitation, river runoff, tides, and wind mixing of the surface layer. Of these, it was observed that precipitation (and related river inflow) has the single biggest effect on the salinity gradient as seen by comparing seasonal variations in the surface layer. Figure 3.3.2 shows salinity contours for the upper 25m of Nitinat Lake along the thalweg between February 2003 and February 2004.

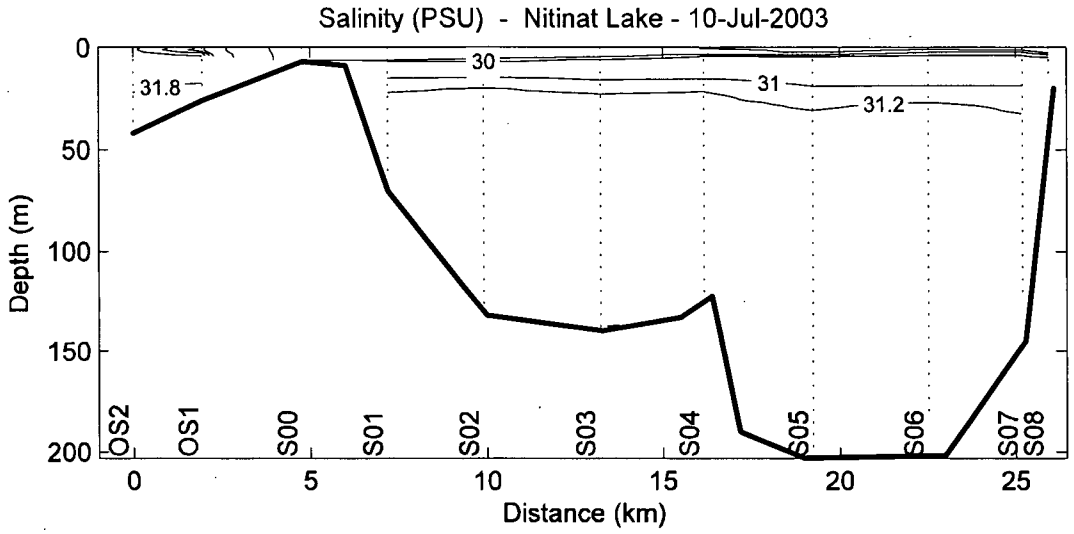

Figure 3.3.1– Salinity contours on July 10, 2003. Ocean stations and sill are also shown. Heavy black line denotes bathymetry along thalweg. CTD cast locations denoted by doted vertical lines. Tide was outgoing during this survey.

A close inspection of Figure 3.3.2 reveals the state of the salinity gradient within the lake at different times of the season. In February of 2003, there was a strong salinity gradient present in the upper 5m with salinities less than 5 PSU recorded at the surface in the northeast basin. In the southwest basin, surface salinities were slightly higher, ranging between 5 and 10 PSU. Salinity increased quickly with depth below the surface, with the 25 PSU contour observed near 5m depth. Below this depth, the gradient weakened, and did not reach 30 PSU until a depth of 15m.

In July of 2003 the salinity gradient within the lake had changed significantly from that observed in February. Surface salinities were observed to be significantly higher, and the accompanying gradient between the surface layer and the bottom waters was thus weaker. As in the winter, there was some spatial variation in the salinity of the surface water with the northeast basin having a slightly lower salinity (between 20-25 PSU) at the surface as compared with the southwest basin (25-30 PSU).

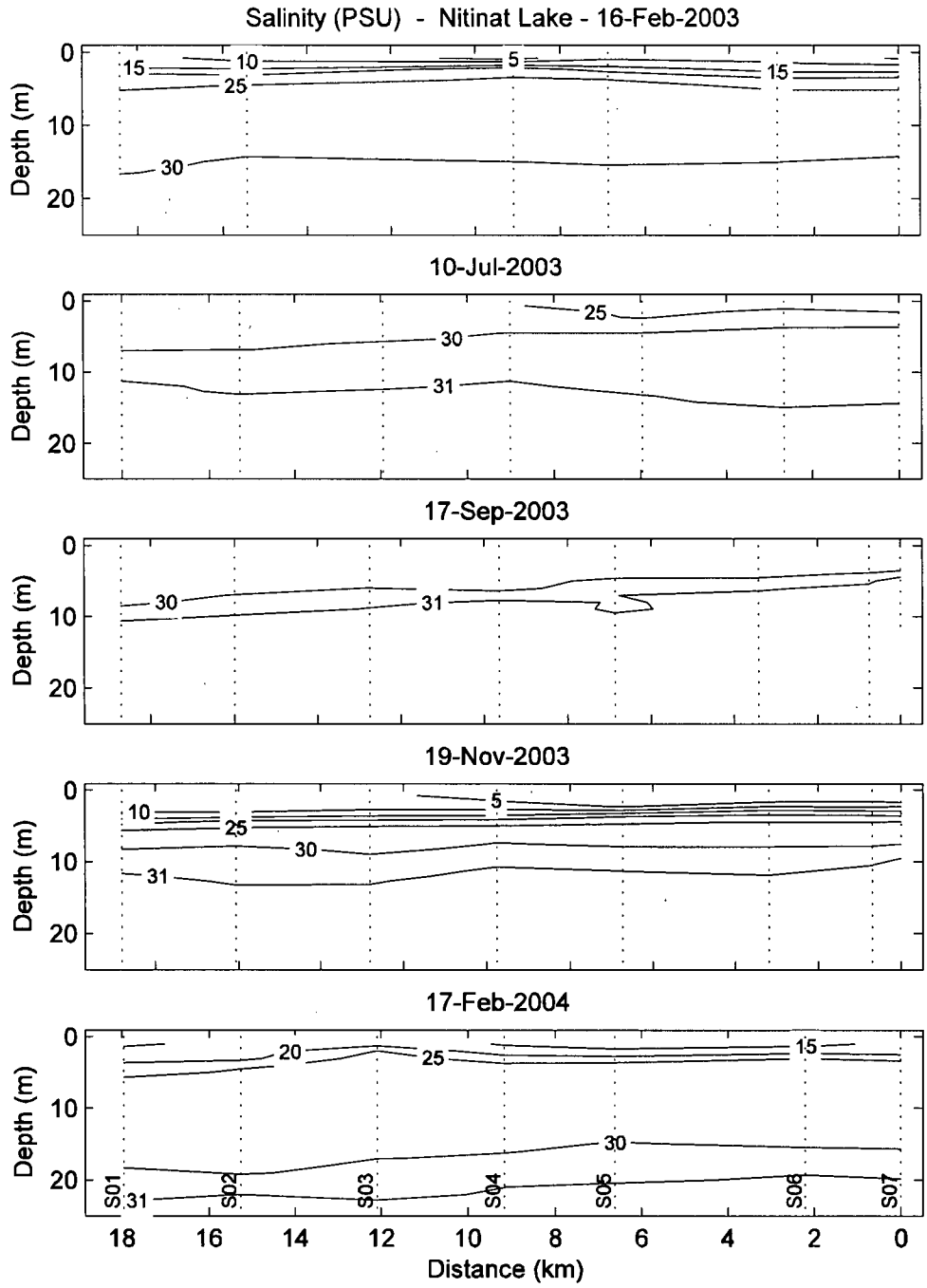

Figure 3.3.2 – Salinity contours for the top 20 m of Nitinat Lake, from February 2003 until February 2004. Contours shown are set at 5, 10, 15, 20, 25, 30, 31 PSU intervals. Weakest stratification was recorded in September, while the strongest stratification was in November following a period of heavy rainfall. Surface salinity tended to increase from the inland (S07) to the ocean (S01) end of the lake.

In July it is also notable that the 30 PSU contour has shifted upwards, and developed a spatial variation as compared with February. In the northeast basin, the gradient between 25 and 30 PSU is much more pronounced than in the southwest basin, with the depth of the 30 PSU contour slowly increasing as it approaches the sill. Curiously, the 31 PSU contour has the opposite slope, and is deeper at the northeast end of the lake than the southwest.

In September the vertical salinity gradient is at its weakest with the highest surface salinities recorded during the entire year, as expected following dry summer months. Salinity in the top 1m of water was recorded between 27 and 29 PSU, increasing relatively quickly with depth towards the deep water salinity levels of 31.2 PSU. Again in September there is a horizontal spatial variation in the salinity stratification, with salinity levels increasing at depth from the inland to the ocean end of the lake.

A strong vertical salinity gradient is again present in November as heavy rains in October and November provided a high inflow of fresh water into the lake. Contours lines between 10 and 25 PSU are tightly spaced near the 5m depth, while water below 10m in depth is observed to be greater than 30 PSU. Surface waters at the inland (northeast) end of the lake are very fresh, below 5 PSU, while in the southwest basin surface salinity increases slightly. In comparison to summer months, the lake in November does not exhibit any significant horizontal spatial variations in salinity below the strong halocline.

Finally, February of 2004 has similar profiles to those observed a year previous, with the exception of the surface water having slightly higher salinities. This may simply be due to the fact that sampling in February of 2003 occurred immediately after several days of rainfall in the area. Both the 25 and 30 PSU contours are in very similar locations as observed between to the two years.

Figure 3.3.3 shows salinity profiles at two stations during various times of the year. In these profiles it is clearly shown that there is a large variation at the surface, while at 20m depth the seasonal variation at each station is very small. It is also noticeable in Figure 3.3.3 that the surface salinity is slightly lower at S06 than S02, and that the halocline is

roughly 3-4m shallower at S06 than at S02 during the summer (July and September) months. One possible explanation is that as incoming tidal water propagates inland, it mixes and becomes entrained with surface waters flowing towards the sill (estuarine circulation model). This mixing serves to weaken the stratification gradient near the ocean end of the lake in comparison to the inland end of the lake.

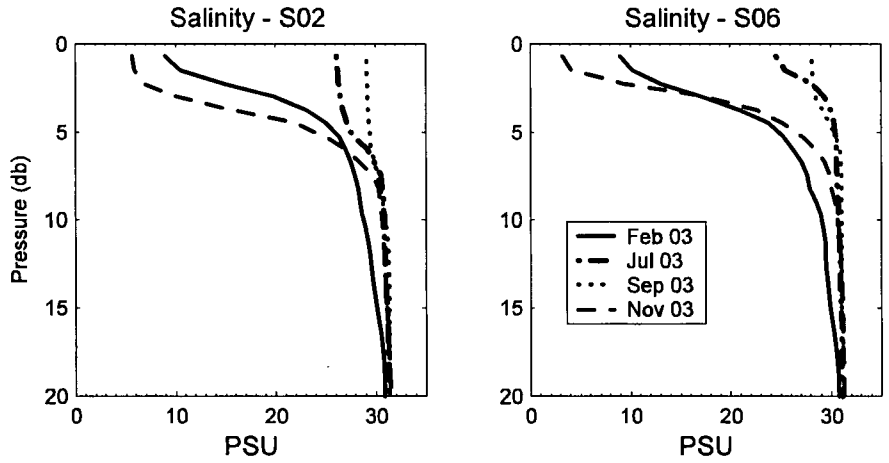

Figure 3.3.3 – Salinity profiles at stations S02 and S06, showing seasonal variation in surface layer.

Surface salinity often shows a spatial variation between the inland and ocean end of the lake, with the lowest lake salinities recorded at S07 (Figure 3.3.4). The salinity gradient over depth is usually seen to be strongest in the northeast basin between S05 and S06. This gradient is generally weaker in the southwest basin. Similar spatial variations between the two ends of the lake are evident in Figures 3.3.2 and 3.3.3 during summer months.

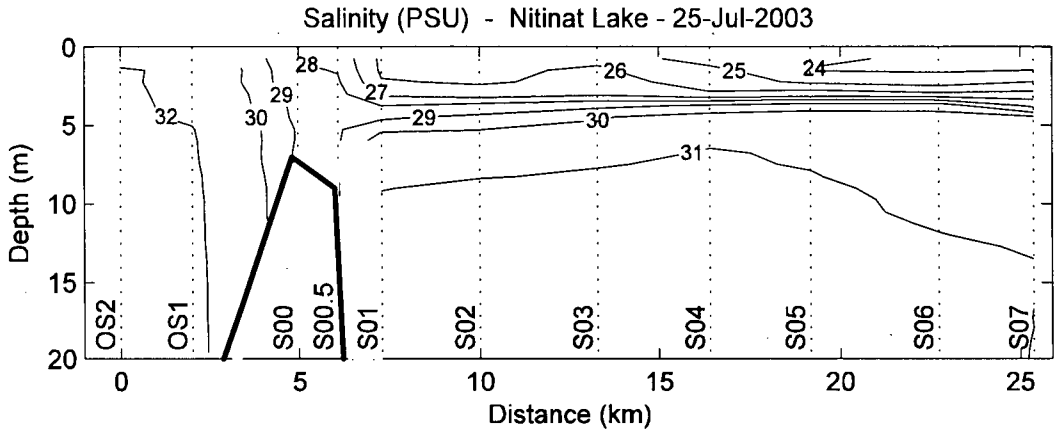

Figure 3.3.4 – Salinity contours on July 25, 2003. Ocean stations and sill are also shown. The heavy black line denotes the lake bottom in the vicinity of the sill. Salinity on sill was found to be ≈28 PSU, while salinity at OS2 was seen to be greater than 32 PSU. Survey began at 9:00am (PDT) at S07, and concluded at 11:30am (PDT) at OS2. Low tide (0.8m) occurred at 5:05am, while a high tide of only 2.3m occurred at 11:38am. A slow incoming current was observed when sampling at sill.

Figure 3.3.4 shows salinity contours of the entire lake, the sill, and two ocean stations for the top 20m of the lake. At the furthermost ocean station (OS2) the salinity is higher than 32 PSU with the exception of the top meter. Closer to the entrance to Nitinat Lake (OS1), the water in the top 5m is between 31 and 32 PSU, while below that it is greater than 32 PSU. On the sill (S00) the salinity of the water is between 28 and 29 PSU. These profiles would suggest that, as expected, outflow from Nitinat Lake affects the salinity concentrations in the ocean waters immediately surrounding the entrance to Nitinat Lake.

Tidal exchange through a channel has been previously discussed by *Wheless and Valle-Levinson* [1996]. In this paper they present a conceptual model where, on an ebb tide, water is drawn uniformly from an embayment and is accelerated through a narrow channel. The momentum gained in the narrow channel causes the flow outside of the channel to behave similar to a jet. The reverse occurs on the following flood tide, where water is drawn uniformly from the surrounding ocean and enters the narrow channel. The result is that some of the water that exits the embayment on the ebb tide does not return on the subsequent flood tide, leading to a net exchange of water within the embayment over time. The narrow channel connecting Nitinat Lake and the Pacific Ocean experiences strong currents during high and low tide, and it is probable there is a 'quasi-potential flow on one side of the channel and jet-like flow on the other". Furthermore, to

maintain a constant average lake height, there must be a net flow over time from Nitinat Lake to the ocean to account for river and precipitation inflows. Given this, it is safe to presume two things: not all of the water that exits Nitinat Lake during low tide returns on the subsequent high, and ocean water that enters Nitinat Lake has a lower salinity than the average surface salinity in the Strait of Juan de Fuca. (Further discussion of the sill and tides is found in section 3.8.)

On July 25 (Figure 3.3.4) the salinity on the sill was observed to be 28 to 29 PSU at S00 during a weak incoming flood. The relatively low salinity of the incoming water on this day is likely due to the fact that sampling occurred shortly after slack water in the channel and early in the development of the flood tide. On other days, measurements were taken on the sill at maximum flood, and salinities as high as 31 PSU were recorded.

In addition to transects along the thalweg, two cross-lake transects were taken across the short axis of the lake at S06 in the north basin (Figure 3.3.5). In the early morning of July 11 2003, there was no wind on Nitinat Lake and the surface was 'glassy' calm. There is a strong salinity gradient present in the upper 5m, with a slight horizontal spatial variation noted in that the surface salinity is slightly less than 25 PSU along the south side of the lake, and is greater than 26 PSU along the north side of the lake. This is explained by the Caycuse River mouth being present near station SC4.

A second transect was done in the early afternoon when winds were strongest, and noticeable changes were observed in the salinity structure of the lake from the early morning. The halocline had been strengthened, with a tight gradient occurring near the 5m depth across the lake. Above this depth the salinity was generally between 26 and 27 PSU, while below 5m the salinity was greater than 30 PSU, and gradually increased with depth to a maximum value of 31.2 PSU. The homogeneity of the surface layer is the result of wind induced surface stress 'pushing' the surface layer towards the downwind (northeast) end of the lake. The horizontal spatial variation in the surface layer is different in the afternoon than during the morning, with the lowest salinity recorded at SC2 and highest surface salinity recorded at SC4. The asymmetry of the depth of the 27 PSU contour line is likely caused by the fact that the SC3 and SC4 stations are located in

a slight embayment on the south side of the lake that is slightly sheltered from the summer afternoon sea breeze. It has been noted by the author when windsurfing that this embayment usually has lighter winds than in the middle of the lake, and that the downwind current which is often strong in the center of the lake is not present here.

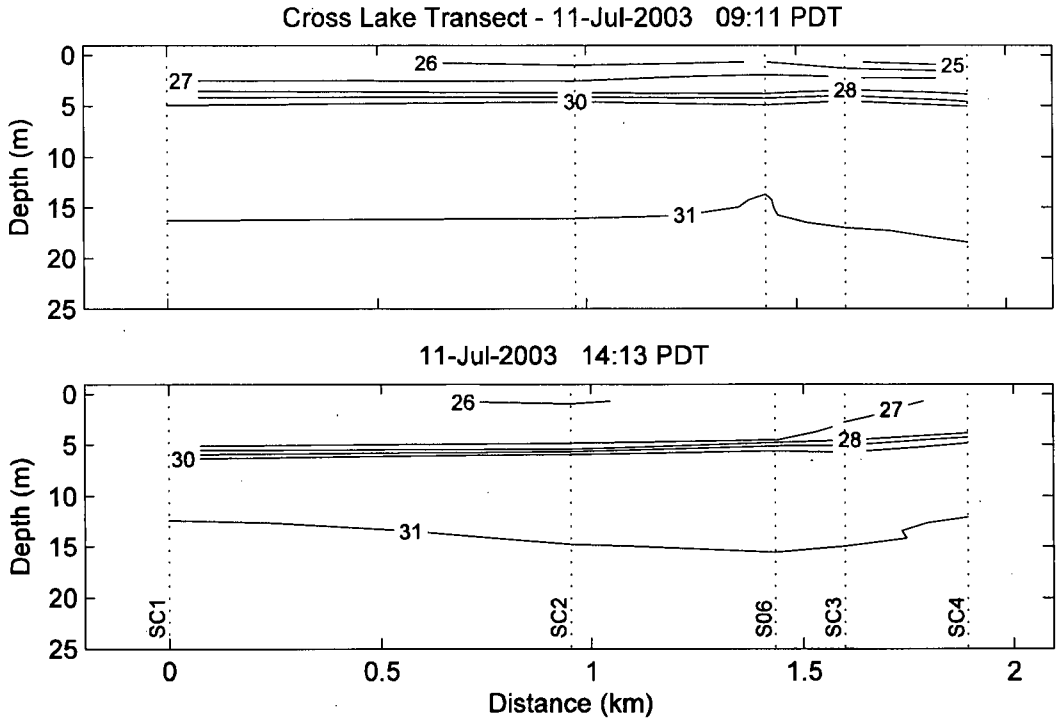

Figure 3.3.5 – Salinity contours in the upper 25m of the lake, taken perpendicular to the thalweg at S06. The two sets of contours are from different times on the same day: top plot shows salinity in the morning, bottom plot show salinity at mid-afternoon. Morning conditions were zero wind, and 'glass calm' lake surface while afternoon conditions were strong winds (>9 m/s) from the SW and 0.5m waves.

Hourly variations in the salinity gradient were observed on two separate occasions during the month of July at two separate locations within the lake. These observations showed that the salinity gradient changes on an hourly scale.

Figure 3.3.6 shows salinity profiles obtained during the night of July 23/24 near S07 after a day of very strong winds from the ocean. The wind from the ocean stopped during the night and reversed into a light offshore breeze and this reversal is seen as the surface layer forcing relaxes (Figure 3.3.7). The profiles displayed in Figure 3.3.6 were obtained over an 11 hour period beginning at 9:10pm (PDT) on July 23. Only the top 10m of the

lake are shown in the plot as deep water salinities remained constant near 31 PSU throughout the sampling period.

At the beginning of the sampling the water in the top 1.5m was at its lowest salinity, with values near 15 PSU, while at the end of the sampling period surface salinities had increased to values of 24 PSU (Figure 3.3.6). This is likely due to the fact that the wind forcing created surface currents during the day that 'pushed' the surface layer towards the downwind end of the lake, and thus the fresh water that flowed into the lake from the Nitinat river during the day was temporarily trapped. Once the wind forcing relaxed near midnight (between 6-7 hours on the time scale in Figure 3.3.6) the surface currents reversed, and fresh water on the surface was able to begin moving towards the ocean end of the lake.

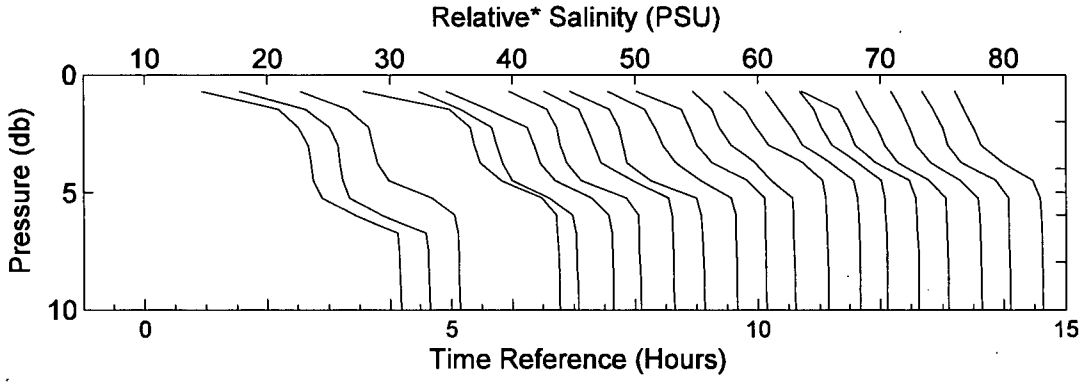

Figure 3.3.6 – Salinity profiles recorded near station S07 between 9:10pm (PDT) on July 23 and 7:40am on July 24, 2003. Casts were performed once every 30 minutes, although one full hour of sampling was missed due to equipment problems. Data have been depth averaged into 0.75m bins and salinity values increased by 5.05 PSU/hour for the purpose of displaying data. Both the halocline and surface salinity are seen to increase during this time period. Afternoon winds on July 23 were very strong, pushing the surface layer towards the inland end of the lake, and deepening the pycnocline.

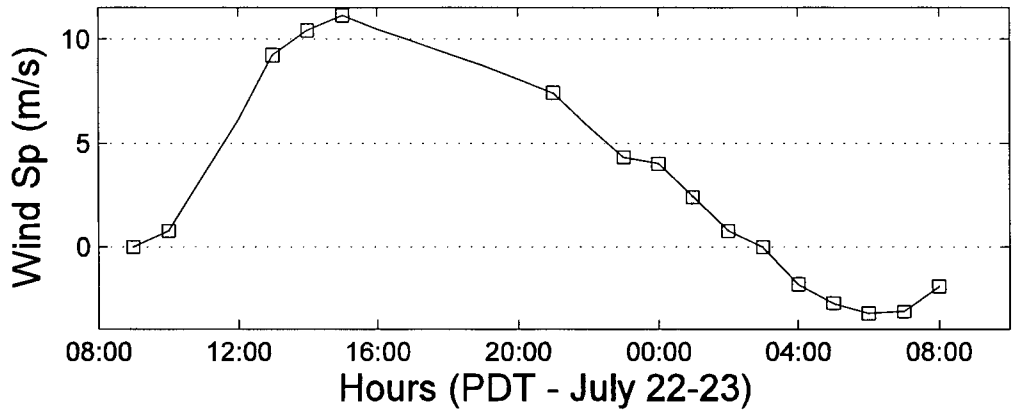

Figure 3.3.7 – Wind data from the morning of July 22 to the morning of July 23, 2003. Collected near S07, boxes represent actual wind measurements, obtained using a hand-held anemometer, and corrected to U_{10}.

On July 14, CTD casts were performed once every half hour between 9:30am and midnight at station S04 (Figure 3.3.8). The changes in Figure 3.3.8 are more subtle than those in Figure 3.3.6, due to that fact that S04 is located in the middle of the lake and winds were lighter on July 14 than on July 23. Examining Figure 3.3.8 closely reveals that the salinity profiles have a distinct 's' shape above 6m for the first ten casts (9.5 to 14 hrs) while the afternoon profiles have a more linear slope in the top 6m, particularly near hour 17.

Winds for the day were generally light at S04, partly due to the wind sheltering that was commonly observed in this part of the lake. Morning winds were less than 5m/s while afternoon winds were recorded between 5 and 7m/s from the SW. During the afternoon the appearance of whitecaps was observed in the area of station S05, suggesting that winds were stronger in the northeast basin than at station S04.

In Figure 3.3.8, the salinity profile recorded at hour 22 is significantly different than the profiles recorded before and after. It is possible that when the south-westerly sea breeze stopped shortly after sunset (hour 21) the relaxation of the surface layer from the wind stress produced an internal bore that was recorded propagating down the lake. Unfortunately, no other sensors were in the lake during this time to confirm this possibility.

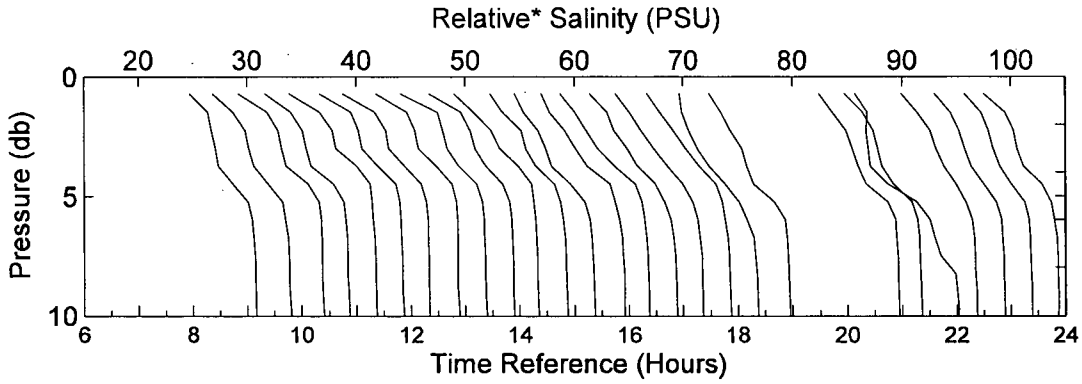

Figure 3.3.8 – Salinity profiles recorded at station S04 between 9:30am (PDT) and midnight on July 14, 2003. Casts were performed once every 30 minutes, although a shore break was taken between 6:30 and 8:30pm. Data have been depth averaged into 0.75m bins, and salinity values increased by 5.05 PSU/hour for the purpose of displaying data. Low tide (-0.1m) occurred at 7:53am, followed by a high tide (2.8m) at 2:23pm and another low (1.3m) at 7:36pm. A high tide of 3.5m occurred at 1:38am on the morning of July 15.

3.4 Density

The density of water is controlled by three factors: pressure, temperature, and the concentration of dissolved salts (Segar, 1997). Water is generally considered to be incompressible, but deep in the ocean the density of water increases by up to 2 percent due to the high pressures. In a shallow body of water such as Nitinat Lake, the density changes due to pressure are small. However, the density gradients in the deep waters of Nitinat Lake are also small. Temperature affects density through increasing or decreasing the energy of the molecules, which in turn affects the distance between the molecules. In general, as temperature increases the density decreases. But water is unique in that the solid form (ice) is less dense than the liquid form, and the temperature of maximum density for pure liquid water is 4°C (Segar, 1997). For sea-water, with salinities greater than 20 PSU, the maximum density occurs at the freezing point. In Nitinat Lake, no water was measured to be less than 5°C, thus the general statement that water density decreases with increasing temperature and increases with increasing salinity holds true. Salts dissolved in water increase the water density as the dissolved ions have a higher density than the water molecules.

For seawater, the relationship between temperature, salinity, and density is shown in Figure 3.4.1. From this plot it is observed that raising the temperature of seawater (35 ppt) from 5 to 20°C decreases the density by about 0.3 percent. Comparatively,

maintaining a constant temperature of 10°C and increasing the salinity from 5 ppt (parts per thousand) to 35 ppt increases density by about 2.3 percent. Thus, within the range of conditions found in Nitinat Lake, it is expected that salinity will most strongly govern density where there are large variations in salinity, such as the surface layer.

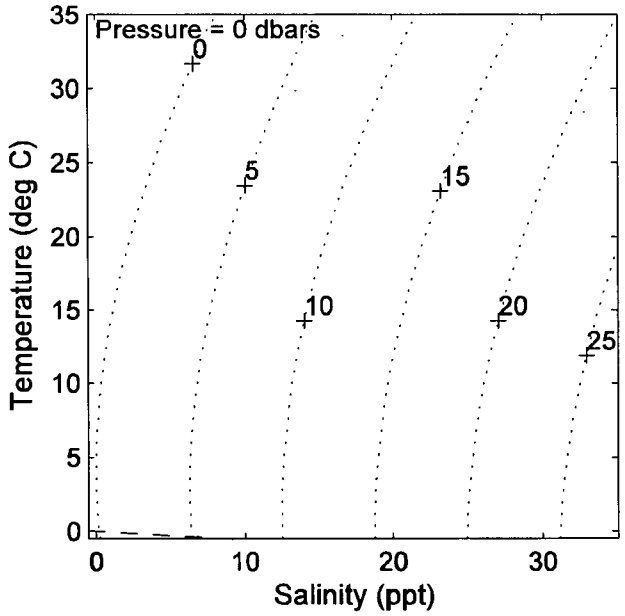

Figure 3.4.1 – Temperature salinity plot for sea-water with lines (dotted) of constant density.

Figure 3.4.2 is another temperature and salinity plot, but with Nitinat Lake data from two separate times of the year shown. The data are a compilation of depth bin-averaged CTD data from July (crosses) and November (circles) 2003 from stations S01 to S08 inclusive. The July data stretch in a band from cooler and saltier water to warmer 'fresh' water at the surface. Outlying data close to 15 ppt and 19°C were recorded near the mouth of Nitinat River on the evening of July 23, following a day of strong south westerly winds. The plot of winter data (circles) has a distinctly different shape due to the temperature inversion in the surface of the lake. In November, surface waters were significantly fresher than during the summer months, and surface temperatures were generally between 6 and 7.5°C.

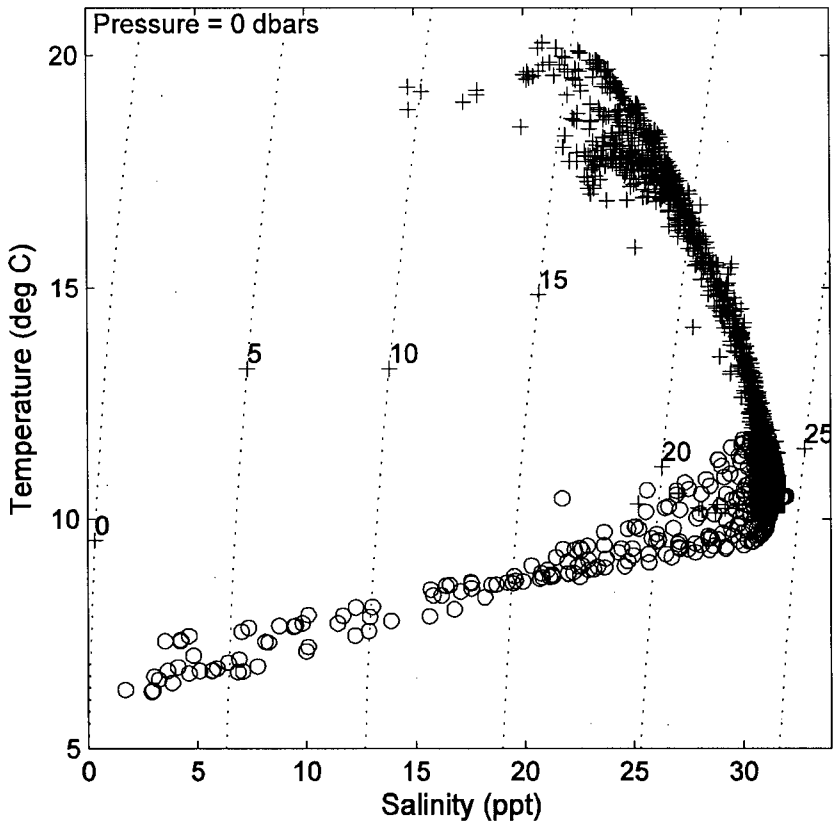

Figure 3.4.2 – Temperature salinity diagram showing water in Nitinat Lake from July (+) and November (o). Constant density curves (0,5,10,15,20,and 25 sigma-t) are shown as dashed lines. Deep water in Nitinat Lake is relatively constant near 10°C and 31 ppt salinity while surface water is seen to vary from near 20°C in July to near 7°C in November. Surface waters in November are significantly fresher than during summer months.

The relationship between temperature, salinity, and density in Nitinat Lake can be seen in figures 3.4.3 and 3.4.4. These figures show profiles of all three properties on the same plot. In Figure 3.4.3, the top 30m of the lake is shown at station S02 at two times of the year; July and February. The surface water in February is both colder and less saline than the surface water in July, as would be expected. The density profile is seen to approximate the shape of the salinity profile, confirming that salinity is far more dominant than temperature in determining density. Also of note in Figure 3.4.3, it appears that the depth of the surface layer at S02 in July is about 10m while in February it is just over 20m, if one visually defines the surface layer as the region where temperature and salinity vary significantly from deep-water values.

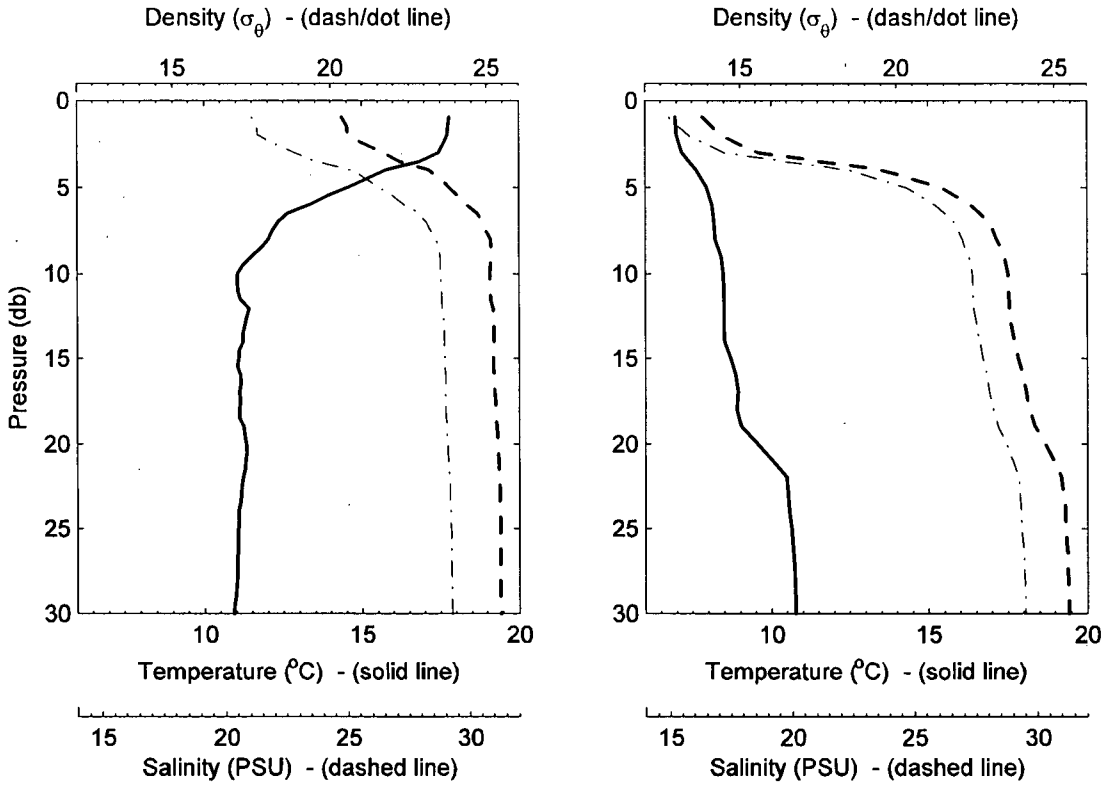

Figure 3.4.3 – Temperature (solid), salinity (dashed), and density (dash-dot) profiles at S02 in July of 2003 (left plot) and February 2004 (right plot) for the top 30m depth. These plots show the relative influence of both temperature and salinity on the density of the water.

Figure 3.4.4 shows two CTD profiles of temperature, salinity and density for the deep water in the lake at two stations (S02 and S05) on the same day. Station S02 has a maximum depth of 133m while station S05 has a maximum depth of 200m. Again the density profile is seen to more closely match the salinity profile, although temperature affects become more significant as changes in salinity decrease with depth. At station S02 (Figure 3.4.4, left plot) there is very little change in salinity between 80 and 130m depth, yet density increases due to a drop in water temperature. At station S05, a small increase in salinity occurs between 70 and 80m depth, but the sharp increase in temperature at these depths causes the density to continue to decrease.

The most striking thing about the deep water profiles as compared to the surface profiles (such as in Figure 3.4.3) is the lack of variability. The temperature changes 7°C between 0 and 10m at station S02 on July 16, while only changes 0.16°C between 40m and 120m.

Similarly, the change in density in the upper 10m is greater than 6 kg/m^3 while the change in the bottom 90m is just 0.05 kg/m^3.

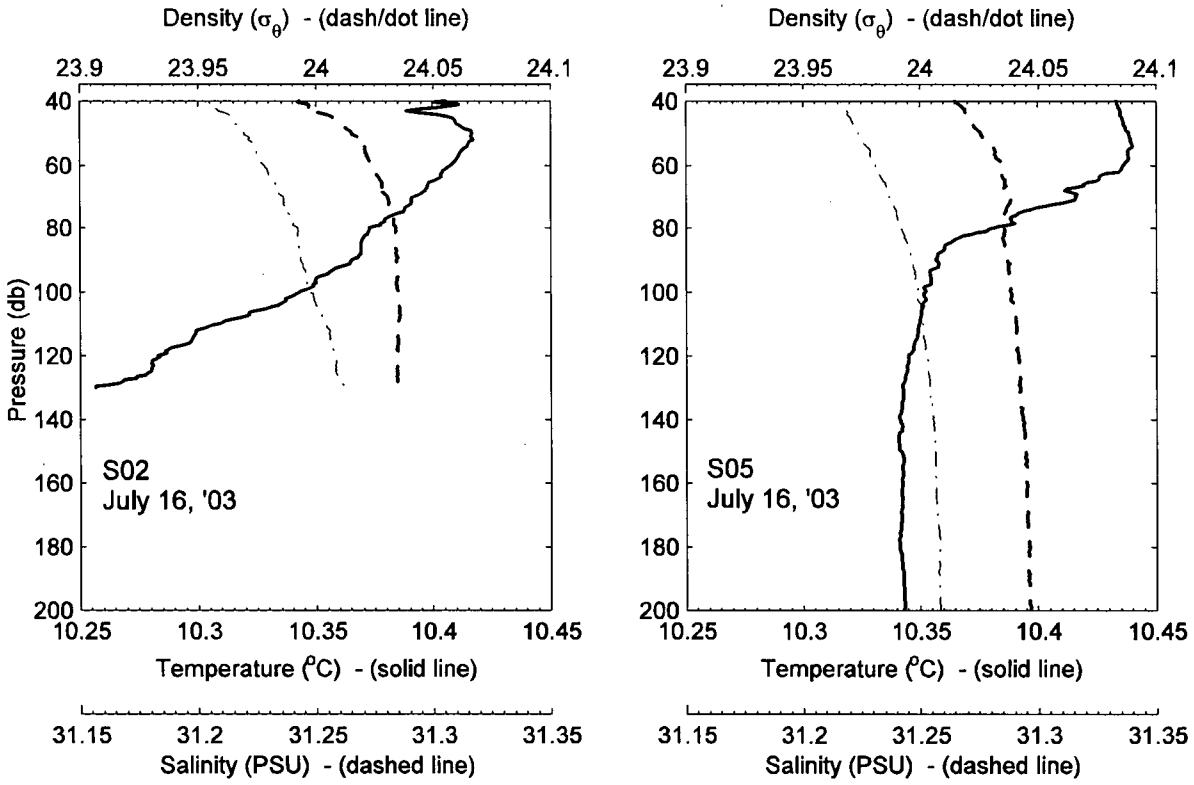

Figure 3.4.4 – Temperature (solid), salinity (dashed), and density (dash-dot) profiles at S02 (left plot) and S05 (right plot), for water below 40m depth on July 16, 2003. These plots show the relative influence of both temperature and salinity on the density of the water. Note the scaling of the axis: depth is from 40 to 200m and the temperature, salinity, and density ranges are very small.

Horizontal spatial variations in density within the lake are confined primarily to the surface layer, as seen in Figures 3.4.5 and 3.4.6. Figure 3.4.5 shows density contours within the entire lake, while Figure 3.4.6 focuses on the top 30m depth. In Figure 3.4.5 it is seen that there is little change in density below 30m depth, with lake water recorded between 1023.9 and 1024.1 kg/m^3. The 1024 kg/m^3 contour line is generally horizontal with the exception being at stations S04 and S07 where the depth of the 1024 kg/m^3 is seen to increase slightly. Unfortunately the CTD casts only provide a 'snapshot' of the state of the lake, and no permanent moorings were placed at this depth to observe temporal changes that might give more clues to the structure and temporal changes in the density stratification at this depth.

Horizontal spatial variation in the surface layer is significant, with water less than 1015 kg/m^3 observed at station S06, while density levels generally increased at the surface moving towards S01 and the ocean. Of note in Figure 3.4.6 is that the 19 and 21 σ_θ contour lines are very horizontal while deeper contour lines such as 23.7 and 23.9 σ_θ show a distinct jump between station S04 and S05.

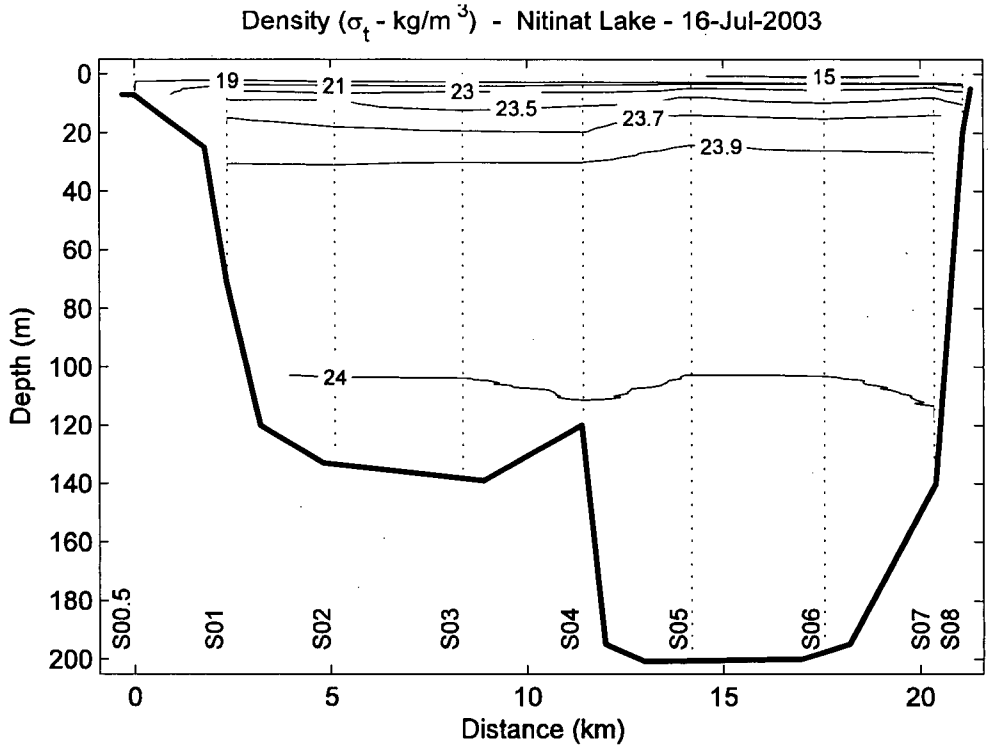

Figure 3.4.5 – Density contours of Nitinat Lake taken on July 16, 2003, using SBE-25 CTD instrument at nine locations in the lake. (Data courtesy Rich Pawlowicz)

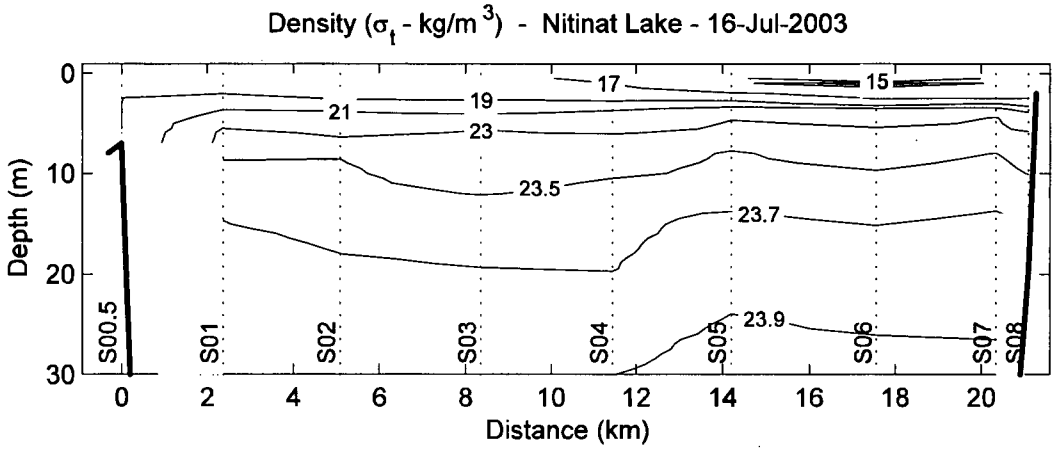

Figure 3.4.6 – Density contours of Nitinat Lake taken on July 16, 2003, using SBE-25 CTD instrument at nine locations in the lake. (Data courtesy Rich Pawlowicz) Only the top 30m is shown.

Figure 3.4.5 reveals density contours that are horizontal, while temperature and salinity contours shown in Sections 3.1 and 3.3 were not always horizontal. Variations in both temperature and salinity are not reflected in the density data due to the fact that they compensate for each other. This is seen clearly when contours from the same data set are compared. Figures 3.4.7 and 3.4.8 show temperature and salinity contours respectively for July 16, 2004. By comparing these contour plots with Figure 3.4.5 it is possible to clearly see the relation. At the 20m depth, temperatures are higher at S01 than at S07, while salinity is lower at S01 than at S07 at the same depth. Thus, temperature and salinity changes are inversely related in order to maintain a constant density at a given depth.

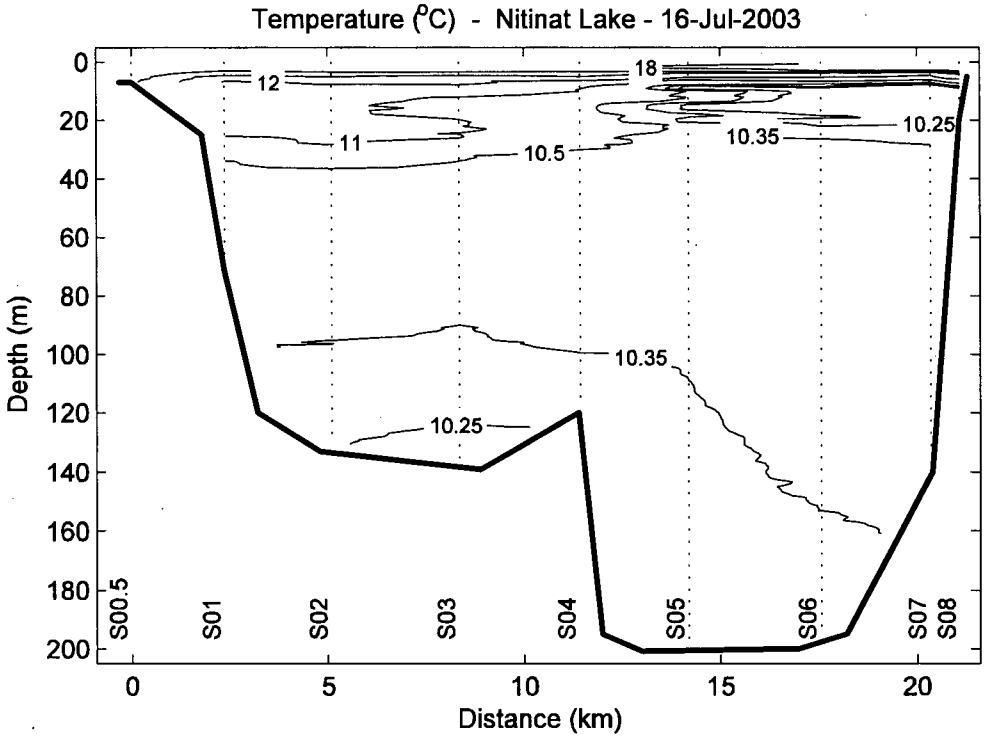

Figure 3.4.7 – Temperature contours of Nitinat Lake taken on July 16, 2003, using SBE-25 CTD instrument at nine locations in the lake. (Data courtesy Rich Pawlowicz)

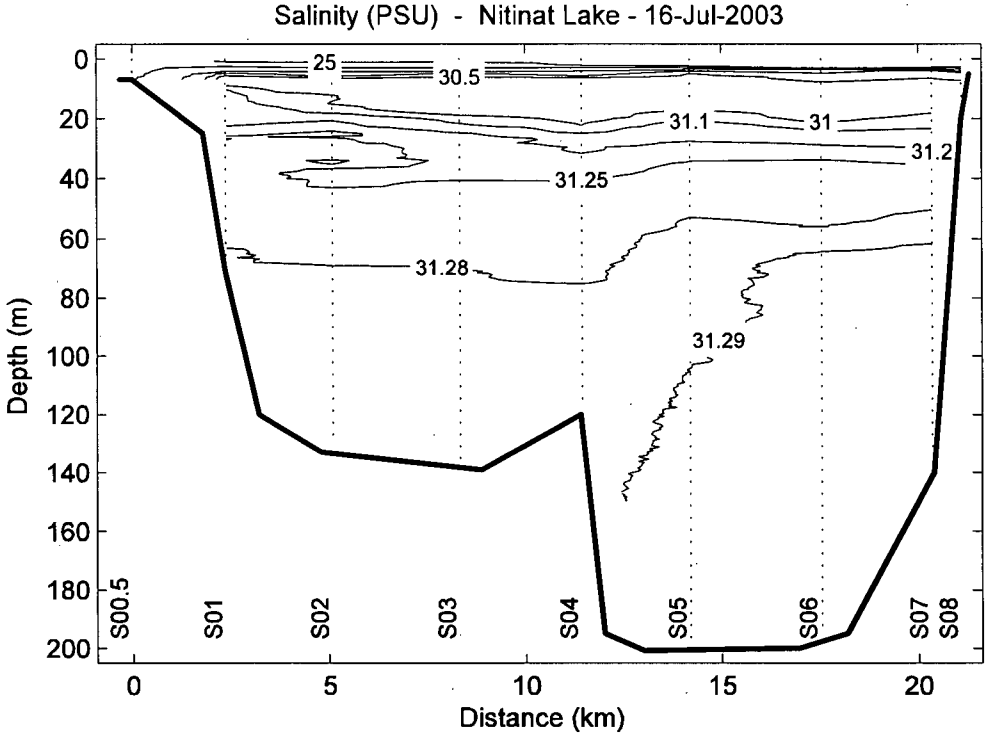

Figure 3.4.8 – Salinity contours of Nitinat Lake taken on July 16, 2003, using SBE-25 CTD instrument at nine locations in the lake. (Data courtesy Rich Pawlowicz)

3.5 Dissolved Oxygen

Perhaps the most striking feature of Nitinat Lake is the complete depletion of oxygen (anoxia) in the deep waters of the lake. Anoxic conditions typically occur in areas where the transport rate is low compared to the rate of supply of organic matter (Segar, 1997). Nitinat Lake, which appears to be permanently anoxic (Northcote et. al., 1964), is an extreme example with a relatively shallow surface layer and a deep anoxic bottom layer. The deep water in Nitinat Lake is restricted from mixing with ocean waters due to the very shallow, narrow and long sill that connects the lake to the ocean, similar to deep Norwegian fjords that are also found to be anoxic (Ozretich, 1975). If the oxygen transport rate into the deep water is less than the rate of respiration within the basin, permanent anoxic conditions will occur even in the presence of a continual, but slow, renewal of this deep water. Fresh water inputs from rivers and tributaries, tidal mixing across the sill, and wind mixing of the surface layer all work to maintain oxygen levels in the surface layer of the lake.

Oxygen consumption is commonly caused by either respiration or chemical reactions (Segar, 1997). In the surface layer, photosynthesis produces organic material that eventually falls to depth. Typically this material is consumed by aerobic organisms such as zooplankton and bacteria. However, in the absence of oxygen, anaerobic bacteria are present which derive their energy either by anaerobic respiration or by fermentation. Excluding dissolved oxygen, the main inorganic hydrogen acceptors in seawater are nitrate, sulfate, and bicarbonate. Measurements made of the level of reduced sulfur in the water column by Broenkow (1969) found a "persistent increase with depth near the bottom... suggesting that one source of H_2S to the water column in Nitinat Lake is from sediments."

The coexistence of oxygen and hydrogen sulfide in aqueous solution is chemically unstable, and if the two are to coexist at an interface, a dynamic balance must be maintained between their rates of supply and removal (Broenkow, 1969). In Nitinat Lake the oxygen-sulfide interface occurs in the photic zone, which is not always the case for anoxic basins. As a result, the various chemical and biological processes that occur in the oxygen-sulfide interface zone include photosynthetic production of oxygen, photosynthetic oxidation of hydrogen sulfide, chemolithotrophic oxidations of hydrogen sulfide, the reduction of sulphate by bacteria, and sulfide removal through the formation of insoluble metal sulfides (Broenkow, 1969). Advection and diffusion near the interface are important in supplying oxygen and sulfide. If the oxygen-sulfide interface slopes significantly, horizontal advection can also affect distribution near the interface. Wind driven and thermohaline circulations in the surface layer also affect the distribution of oxygen and sulfide near the interface. In this study, dissolved oxygen concentrations were recorded on several occasions, but no measurements were made of hydrogen sulfide levels.

Figure 3.5.1 shows DO contours for the upper 40m of the lake between station S01 and S08 on July 16. The contours indicate that below 30m in depth there is no appreciable DO anywhere in the lake. Spatial variation in the levels of DO at a specific depth are notable between the south and north basins of the lake. Stations S01-S03 in the south basin are near the ocean sill, and show dissolved oxygen levels to be generally higher

with depth than in the north basin. For example, at S01 it is observed that the DO level at a depth of 10m is near 3 ml/l, while at S07 the DO at 10m is less than 1 ml/l. This is likely caused by highly oxygenated ocean water entering the lake across the sill and then propagating up the lake at a depth between 5-15m (depending upon the density of the incoming ocean water and the density of the lake water) on an incoming tide. It is also possible that there are temporal changes in the DO contours on the order of hours, but these would not be detected with a single CTD transect.

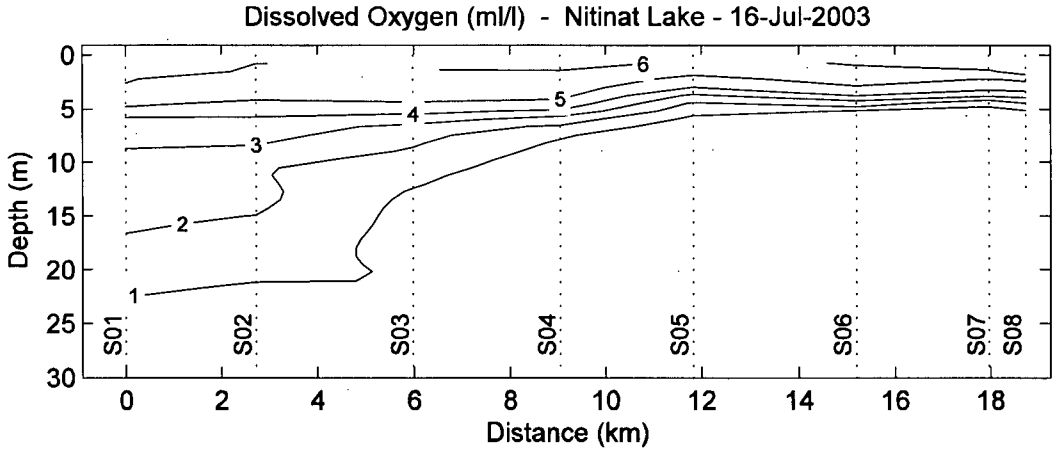

Figure 3.5.1 – Dissolved oxygen contours (ml/l) in Nitinat Lake on July 16, 2003.

Figure 3.5.2 and Figure 3.5.3 show DO contours for November of 2003. The spatial structure is similar to July 2003 (Figure 3.5.1), with slightly higher DO levels for a given depth at S01 than S07. Of note is that surface DO levels are higher in November than July, with maximum recorded value in excess of 8 ml/l, in conjunction with cooler surface water temperatures in November than July. Changes in the contours are noted between November 17 and November 20, which would suggest that the gradient is influenced by external factors in the short term. However, while the gradient contours may change slightly in the surface layer in the short term, is should be noted that the depth of the 1 ml/l contour remains relatively constant during this same time period.

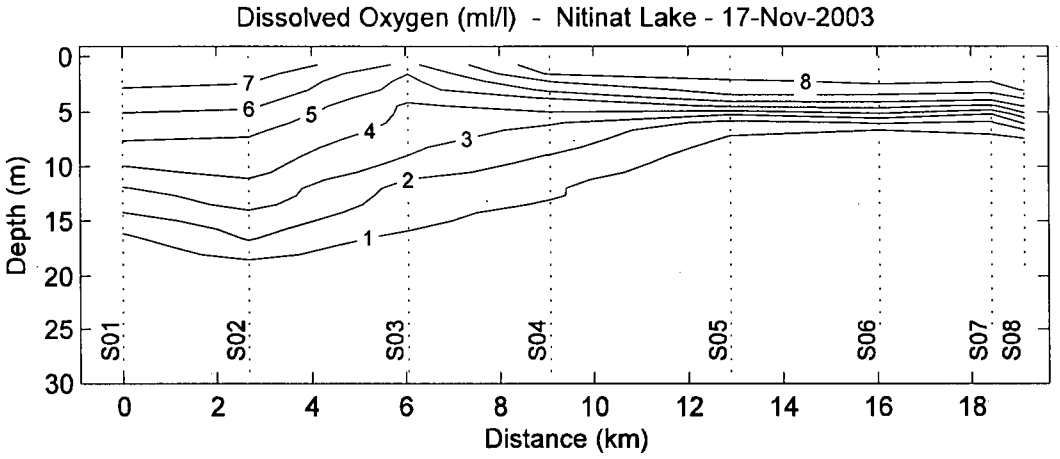

Figure 3.5.2 – Dissolved oxygen levels on November 17, 2003

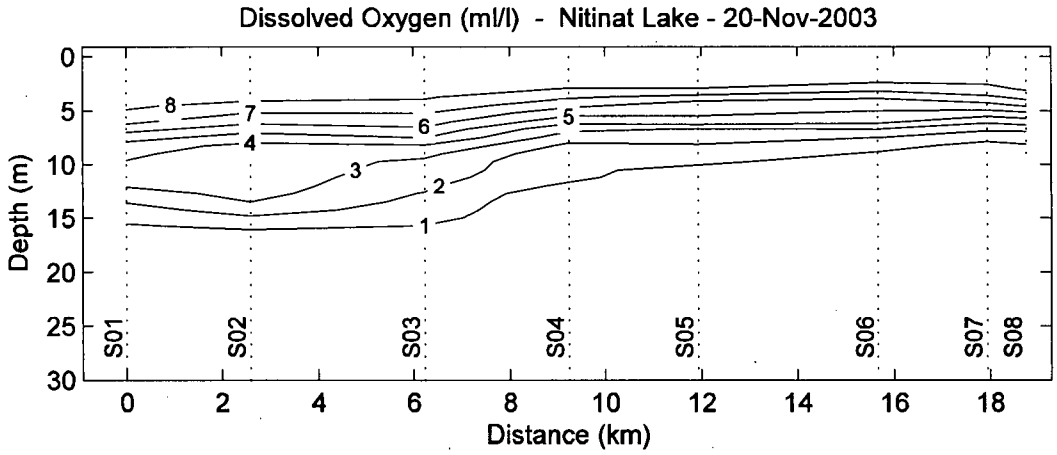

Figure 3.5.3 – Dissolved oxygen contours in Nitinat Lake on November 20, 2003.

It is interesting to note that there was not a significant increase in dissolved oxygen within the lake in November, despite there being a significant flooding event that raised lake levels by several meters in October. This would suggest that rather large and significant changes can occur to the surface layer without significantly impacting upon the bottom layer, or the oxygen-sulfide interface.

A third transect of the lake was done with a CTD equipped with an oxygen sensor in February of 2004 (Figure 3.5.4). In February of 2004, DO levels are similar to those of November 2003. Spatial variations between S01 and S07 remain as evident by the 5 ml/l contour line which is at a depth of 13m near S01 and rises to almost 3m depth at S07.

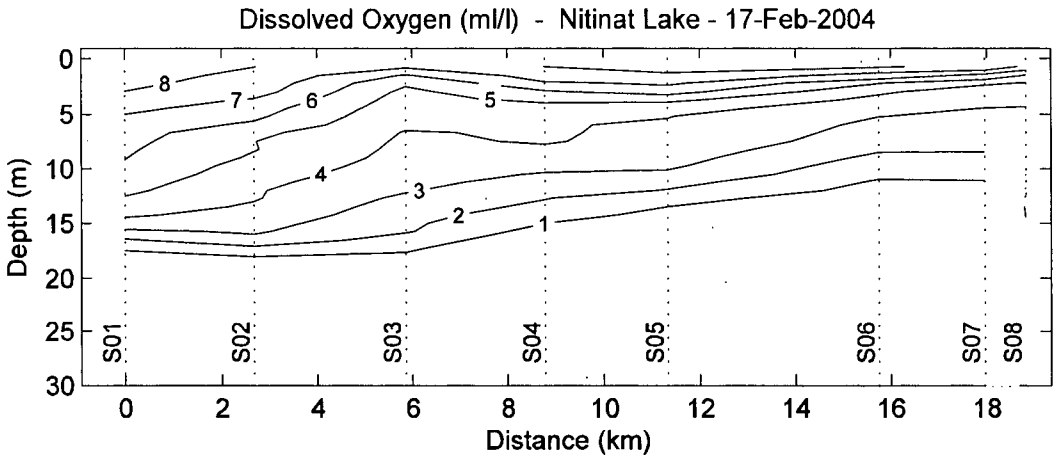

Figure 3.5.4 – Dissolved oxygen contours in Nitinat Lake on February 17, 2004. (Data courtesy Rich Pawlowicz)

3.6 Relative Chlorophyll Concentrations

The CTD probe used to perform vertical water sampling at lake stations was equipped with a pumped WETstar Fluorometer. This device was used to record the relative chlorophyll in the water column.

A Fluoromter directly records the amount of fluorescence emission from a given sample of water, and uses this to determine the relative amount of chlorophyll in the water. (Chlorophyll is known to emit florescence at a given wavelength when excited by an external light source). The WETstar Fluoromter emits light using two light emitting diodes centred near 470nm and modulated at 1 kHz to excite the chlorophyll (WET Labs Wetstar User Guide, Revision K). A voltage signal is sent to the data logger on the CTD that records the relative chlorophyll concentration on a scale of 0-5 V, with zero V representing water with no chlorophyll. For this study, the WETstar instrument was not calibrated against a specific concentration of chlorophyll, thus all data presented in this paper is as a voltage giving only a relative indication of the location and concentration of chlorophyll in Nitinat Lake.

Figure 3.6.1 shows contours of the relative chlorophyll concentration in Nitinat Lake at three times during 2003. In February of 2003 the lake contained the most chlorophyll,

with most concentrations recorded between 5 and 10m in depth. Of note, the chlorophyll concentrations decrease near S01 in February, but are strong in the remainder of the lake.

In July there is a significant decrease in the concentrations of Chlorophyll within the lake from February. At S01 concentrations were below 1V at all depths, while in general chlorophyll increased between 5 and 10m depth moving from the ocean end (S01) to the inland (S07) end of the lake. In November, no significant chlorophyll concentrations were recorded.

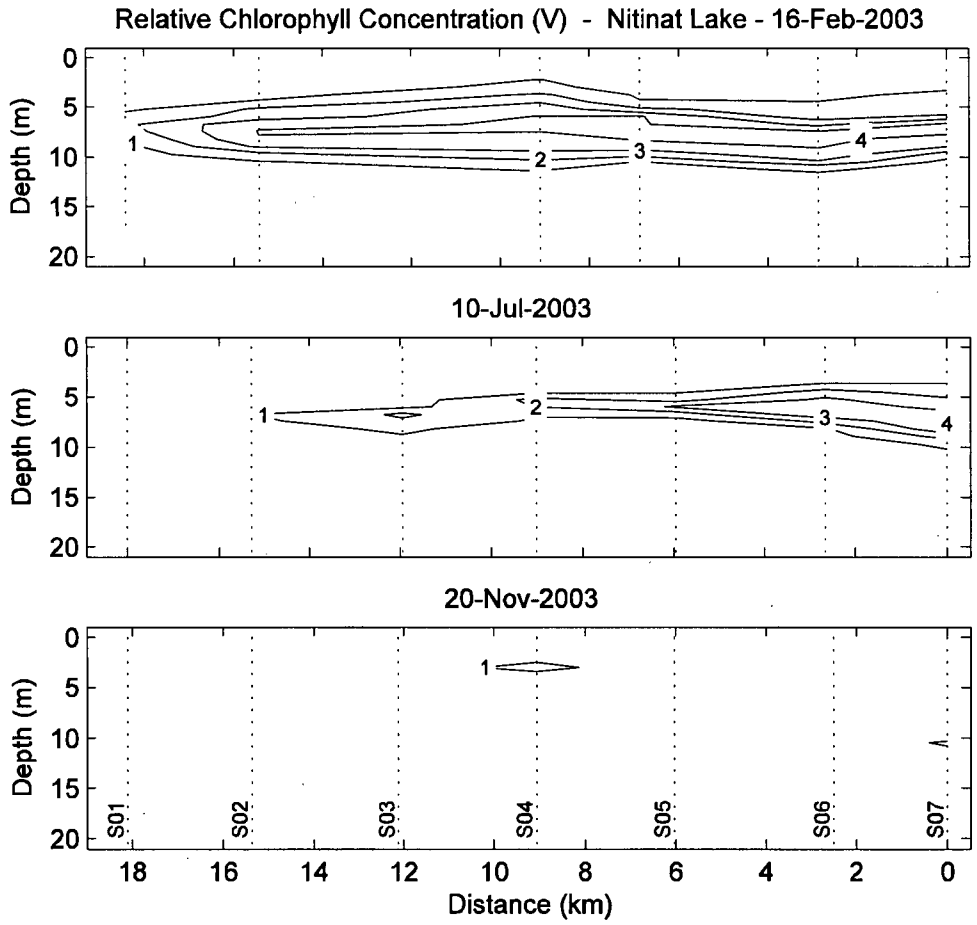

Figure 3.6.1 – Contour plots showing the relative concentrations of chlorophyll in volts as recorded during three different seasons on Nitinat Lake, 2003.

3.7 Turbidity and Transmittance

The CTD profiler used primarily in the Nitinat Lake study was fitted with two instruments for measuring suspended particles, phytoplankton, bacteria and dissolved

organic matter in the water column. A Wetlabs C-Star Transmissometer was used to measure light transmittance, and a Seapoint Sensors Inc. Turbidity meter detected light reflected from particles suspended in the water.

The transmissometer had a path length of 25 cm separating the light emitter and receiver, and was oriented parallel to the main axis of the instrument (WET Labs C-Star User's Guide, Revision K). A transmissometer works by projecting a collimated beam of light through the water and into a focused receiver. The ratio of light gathered by the receiver to the amount originating at the source is known as the beam transmittance (Tr), and is measured as a voltage that is output from the instrument. The voltage output of the instrument is between 0 and 5 V-DC, with a value near five indicative of clear water and a value near zero indicative of water that absorbs or scatters all of the light.

The turbidity meter, also referred to as a backscatter meter, works by emitting a pulse of light, and then recording the amount of light that is reflected back by particles in the water. The Seapoint Sensor also outputs a voltage signal that is indicative of the amount of light reflected back to the instrument (Seapoint Turbidity Meter Datasheet, 2000). Thus, a low voltage reading indicates clear water with little suspended particulate, while higher voltages indicate increasing levels of turbidity.

Figure 3.7.1 shows profiles of both transmissivity and turbidity (backscatter) for the upper 50m of the lake at two stations. As expected, the voltage decreases for the transmittance and increases for the turbidity at corresponding depths, indicating a higher level of suspended particles in the water column at those depths.

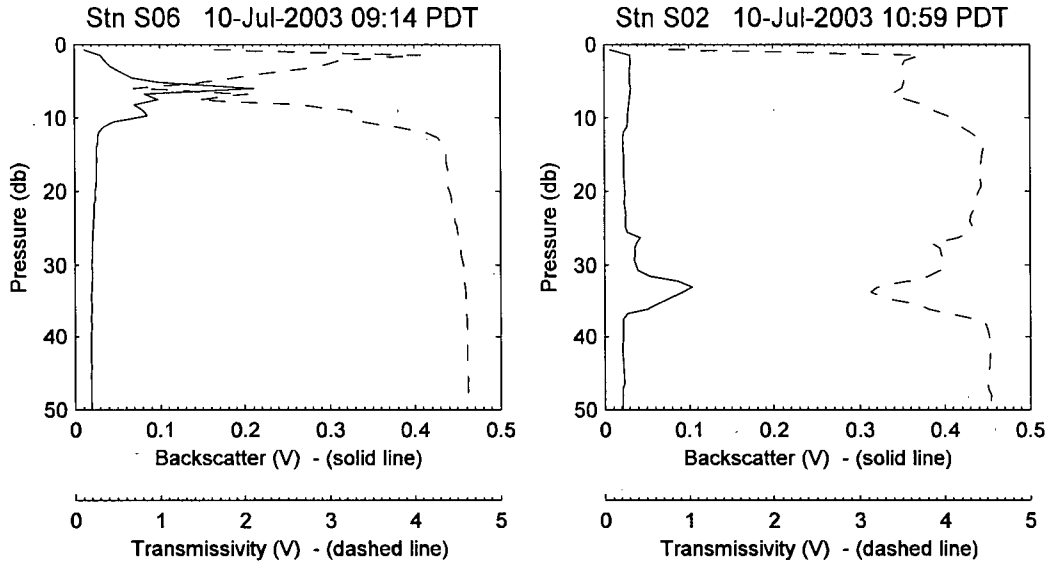

Figure 3.7.1 – Backscatter and transmissivity profiles for stations S06 and S02 on July 10, 2003.

Although the two measurements show peaks at the same depth, they do not perfectly mirror each other. For example, at station S02 on July 10, the transmissometer records a notable signal in the upper 10m of the lake while the signal recorded by the turbidity meter for the same depth is much less. This would seem to indicate that the upper 10m at station S02 contained a significant amount of material that absorbed but did not reflect light at the wavelength measured by the turbidity meter.

Figure 3.7.2 shows profiles of both transmissivity and turbidity from November 2003. The profiles are of only the upper 50m of the lake. The two signals more closely mirror each other than those from July. At station S06, there are notable spikes in both signals at the surface of the lake, and at a depth near 12m. In comparison, at station S02, the signal at the surface layer is weaker, and there is no strong signal at 12m. At S02 there are two strong spikes in both signals at depths of 20m and 42m.

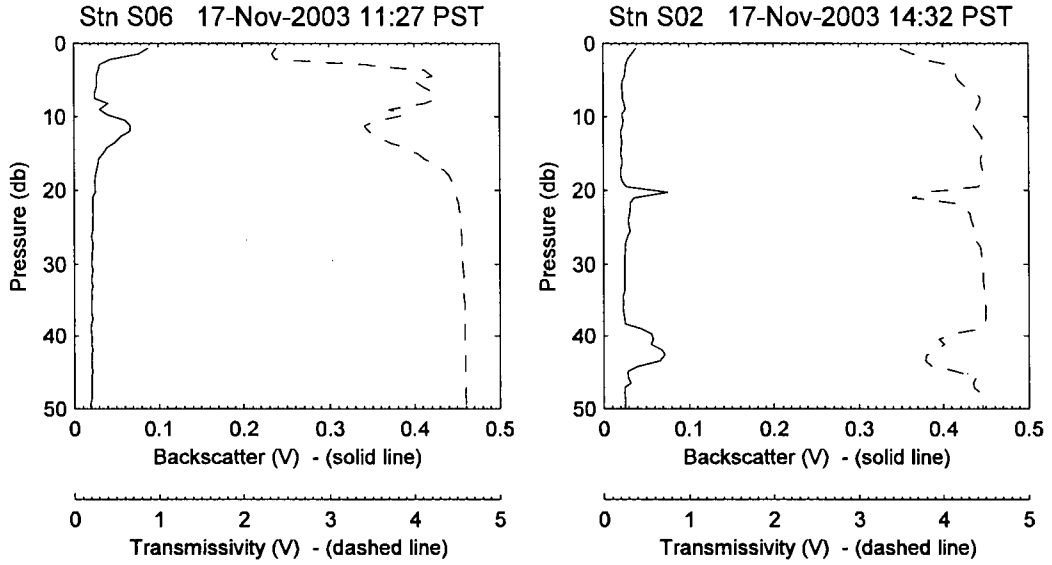

Figure 3.7.2 – Backscatter and transmissivity profiles for stations S06 and S02 on November 17, 2003.

Examining the dissolved oxygen contours for the same day (Figure 3.7.3), it is seen that there is some correlation between the depths of the spikes in Figure-3.7.2 and dissolved oxygen levels. The spike near 12m depth at S06 and the spike at 20m depth at S02 both correlate well to DO levels between 0.25 and 0.5 ml/l, or the upper reaches of the anoxic waters. However, there is no correlation between the spike in turbidity seen between 40 and 45m at S02 on November 17 and dissolved oxygen levels.

3.8 Tides

The mean water level on Nitinat Lake is below the maximum ocean tidal height on the west coast of Vancouver Island. As a result, ocean water enters Nitinat Lake at high tide through the narrow shallow sill that connects Nitinat Lake to the Pacific Ocean (Figure 3.8.1). The narrow sill runs north from the ocean before widening and turning west towards the lake. Large gravel bars that are exposed during low tides are found at the north end of the narrow channel; while the ocean mouth features a shallow sand bar that often has breaking waves except during very calm summer conditions. Depths in the narrow channel vary from just 2m to almost 8m, with average depths around 5m at slack tide.

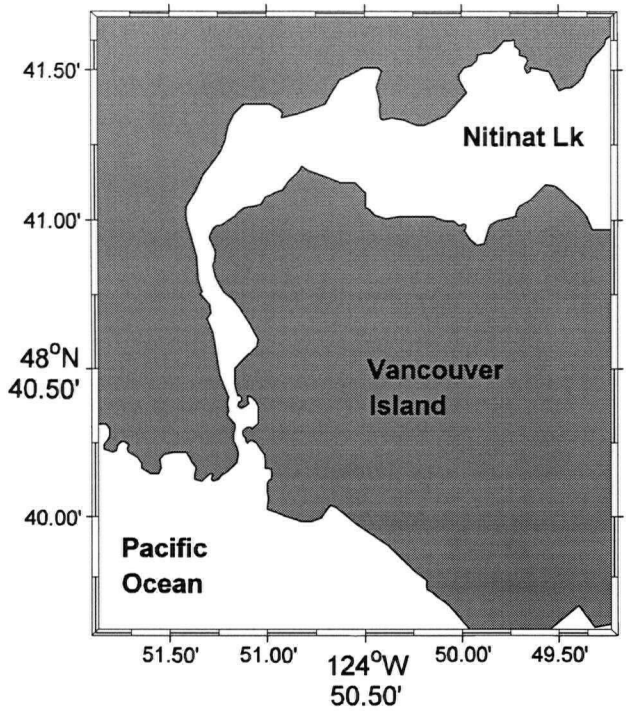

Figure 3.8.1 – Map of Nitinat Lake sill.

Due to the restriction of the sill, the tidal signal in Nitinat Lake is attenuated in comparison to the ocean signal (Figure 3.8.2 and Figure 3.8.3). Coastal tides are mix semi-diurnal with a range of 3.3m during spring tides. Nitinat Lake tides are also semi-diurnal, but with a range of just under 0.4m during spring tides. Slack water in the channel occurs when the ocean and lake levels are at the same height, about midway between high and low tide in the ocean. Conversely, tidal currents across the sill are greatest when ocean tides are at their daily maxima or minima.

The tidal prism is the volume of water exchanged between Nitinat Lake and the ocean during a single tidal period. A rough approximation of the tidal prism is obtained by multiplying the surface area of Nitinat Lake by the change in height to obtain the volume. In July of 2003 there was little rainfall and river input into the lake was near the minimum level. During this time, the maximum tidal range in the lake was observed to be 38 cm. Given that the surface area of Nitinat lake is approximately 27.7 km^2 (Northcote et al. 1964), then:

Tidal Prism = (Lake Surface Area) x (Delta h) = 10.49×10^6 m^3

When ocean water enters the lake, it mixes with lake water on the sill. This mixing acts to decrease the salinity of the incoming sea-water, depending upon the salinity of the surface layer in the lake. If the ocean level is only slightly higher than lake level, then the currents across the sill are weak and more mixing of sea water with lake surface water will occur at the sill and the incoming water will be fairly diluted by the time it reaches the lake. Alternatively, when the ocean level is significantly higher (more than 30cm) than the lake level, currents across the sill are high (up to 3.5m/s, Broenkow, 1969) and sea water fills the channel entrance to Nitinat Lake. In this instance, velocities will be highest in the narrowest section of the channel, and then decrease as the sill widens and turns to the west. Where the sill widens a tide line is often observed that indicates the boundary between sea water and lake surface waters as the incoming sea water sinks below the surface. After passing over the sill, incoming sea water on the high tide usually sinks to depths of 5-15m, depending upon salinity and temperature, before travelling up the lake. Deep water renewal is thought to occur only when dense ocean water is able to penetrate the sill during very high tides without becoming more dilute than the deep water in the lake (Ozretich, 1976).

The shallow and narrow sill not only limits the volume of ocean water that can enter into Nitinat Lake, it also restricts the rate at which lake water can exit. This effect is most notable during periods of heavy rainfall in winter months, as demonstrated during October of 2003 when heavy rains caused the lake level to rise 3.9m in a three day period. Lake levels peaked near midnight on the night of October 18 (day 290, 2003) before receding (Figure 3.8.4). Approximately 582 mm of rainfall fell in the Nitinat lake watershed from October 15 to 18 (Figure 3.8.5).

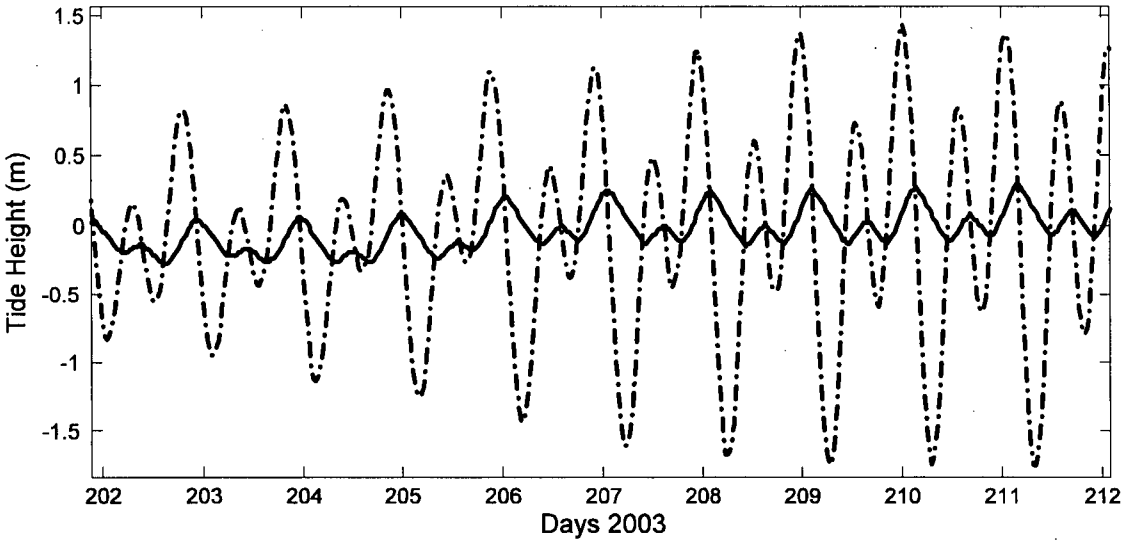

Figure 3.8.2 – Tidal signal from Bamfield Marine Station water level gauge 08545 (dash-dot line) with the water level signal from the pressure sensor on TC1 in Nitinat Lake (solid line). Period is from July 22 to Aug 1, 2003, showing mixed semi-diurnal tides. Tides in Nitinat are an order of magnitude smaller than ocean tides. The two sets of data do not share a common reference datum for height, and have been plotted together with zero representing the mean water value for each data set as recorded between July 21 and November 18, 2003. Flood water levels in October were omitted when calculating mean levels in the lake.

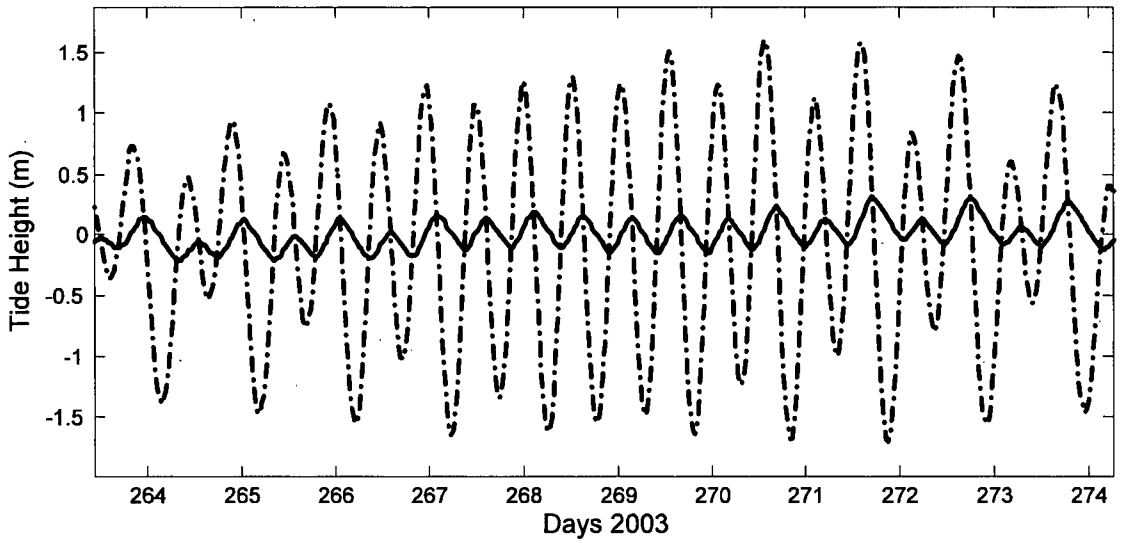

Figure 3.8.3 – Tidal signal from Bamfield Marine Station water level gauge 08545 (dash-dot line) with the water level signal from the pressure sensor on TC1 in Nitinat Lake (solid line). Period is from September 22 (day 264) to October 2 (day 274), 2003. Note the tidal signal between days 266-270 is almost perfectly semi-diurnal, as corresponding to the fall equinox. The two sets of data do not share a common reference datum for height, and have been plotted together with zero representing the mean water value for each data set as recorded between July 21 and November 18, 2003. Flood water levels in October were omitted when calculating mean levels in the lake.

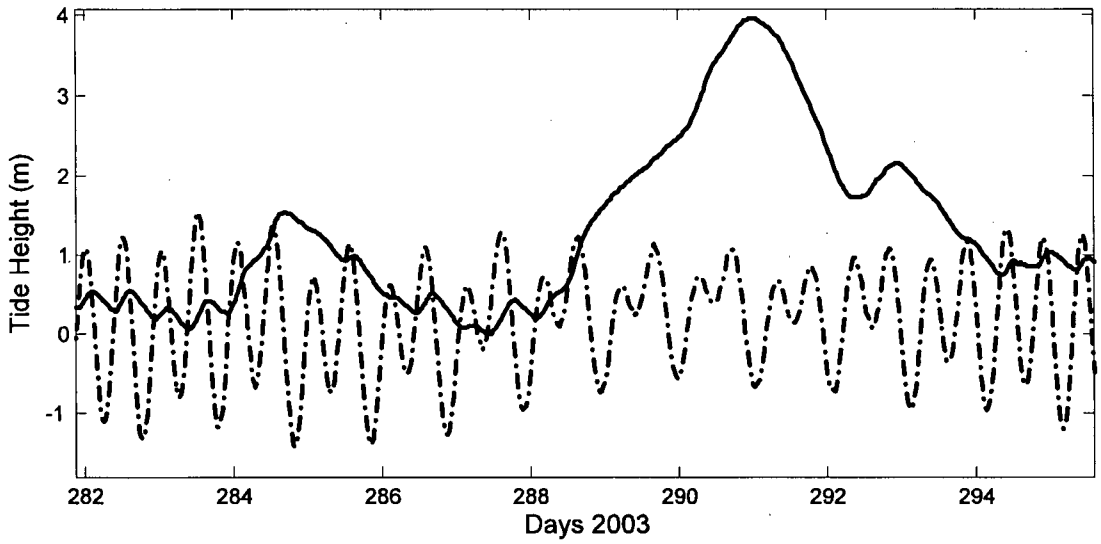

Figure 3.8.4 – Tidal signal from Bamfield Marine Station water level gauge 08545 (dash-dot line) with the water level signal from the pressure sensor on TC1 in Nitinat Lake (solid line). Period is from October 10 to October 23, 2003. Unusually heavy rains occurred during this time period, leading to an initial flood on day 284 (October 12) followed by a large flood beginning on day 288 (October 16) and peaking three days later. The two sets of data do not share a common reference datum for height, and have been plotted together with zero representing the mean water value for each data set as recorded between July 21 and November 18, 2003. Flood water levels in October were omitted when calculating mean levels in the lake.

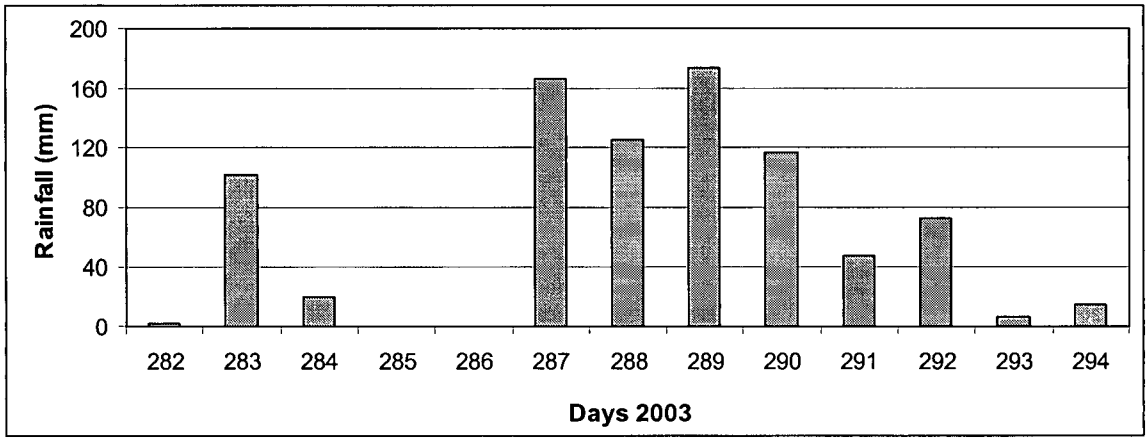

Figure 3.8.5 – Daily precipitation data (mm of rainfall) recorded at the Nitinat River Hatchery, between October 10 (day 282) and October 22 (day 294). Four day total for days 287 to 290 (October 15-18 inclusive) was 582 mm.

The Nitinat River watershed is roughly 800km^2, while the Caycuse, Doobah, and Hobiton watersheds together are estimated to be 250km^2 (Fedorenko, 1979). Assuming that the ground was already highly saturated from the earlier rainfall on October 11-12, the river

runoff may conservatively be estimated to be 70 percent of total precipitation at this time. If this estimate is reasonable, then for the October 15-18 time period the total river runoff into Nitinat Lake may have been as high as 428 $x10^6$ m^3 for this three day time period. (or 15 percent of the total estimated volume of Nitinat Lake) It is possible, given the saturated state of the soils in the watershed, and that November is a dormant growing season where root-uptake from vegetation is less, that the percentage of surface runoff might have been even higher than 70% of total precipitation.

3.9 Meteorological Data

This section presents meteorological data that were collect at Nitinat Lake during 2003. There were two study periods during which data was collected; July 7 to 24 and October 25 to November 19. During July data were collected at location M2, while during the fall data were collected at M1 (Figure 2.3.1). The original intention had been to collect data at M1 for the entire time period between July and November, but a flood event on October 19 damaged the data logger (see Sections 2.3 and 3.8 for further discussion of the flood event). The data collected at the meteorological stations included temperature, relative humidity, solar radiation, and wind speed and direction. Section 3.9.1 presents the temperature, relative humidity, and radiation data, while section 3.9.2 presents a selection of the meteorological station wind data corresponding to periods when water property data were collected on the lake.

3.9.1 Temperature, Relative Humidity, and Solar Radiation

As described in Section 1.5, Nitinat Lake is located in a temperate rainforest with a mild seasonal climate. The summer months are typically dry and warm, while the winter months see increased levels of precipitation and cooler temperatures. In general, the Pacific Ocean acts as a temperature regulator, minimizing coastal temperature variations between seasons (Thomson, 1981).

Figure 3.9.1 shows temperature, relative humidity, and solar radiation for the time period between July 7 and July 24 2003 at station M2. Daily maximum temperatures vary between 16.7 (July 8) and 25 °C (July 21) during this time period, while night time

minimum temperatures were observed to vary between 10.5 (July 17) and 16.1 °C (July 12). The daily average temperature at M2 was 16.87 °C for this time period.

Relative humidity (RH) at M2 during July was observed to be high, and most nights reached levels of 100% (Figure 3.9.1). The minimum RH was 49.7 % recorded on the afternoon of July 17, while on July 13 the RH remained high all day with a minimum daily reading of 95 %. For the time period that data were recorded, the mean RH was 91.2 %. Comparing the temperature and RH data presented in Figure 3.9.1, it is seen that warm temperatures are recorded on days when RH is lowest. Coastal fog in the Strait of Juan de Fuca was common during this time period, and was often observed to envelope the shore and southwest end of the lake during the late evening and early morning. Presumably, this fog was present during the entire night and was responsible for the high nighttime readings of RH.

Solar radiation at station M2 (Figure 3.9.1) reached its daily maximum near noon and was zero during the night as expected, with the highest recording of 1213 W/m^2 observed on July 24, shortly after the summer solstice. The lowest daily maximum recording was just 339 W/m^2 on July 13. The average solar radiation during the July study period was 203.5 W/m^2, which includes the night periods when zero radiation was present. July 12 and 13 accounted for 83% of the total precipitation (Nitinat River Hatchery, DFO/Environment Canada data, unpublished – Figure 5.1.1) during the month of July, and the low solar radiation levels on these days are due to the passing weather system that was present in the area. Light rain also occurred on July 8.

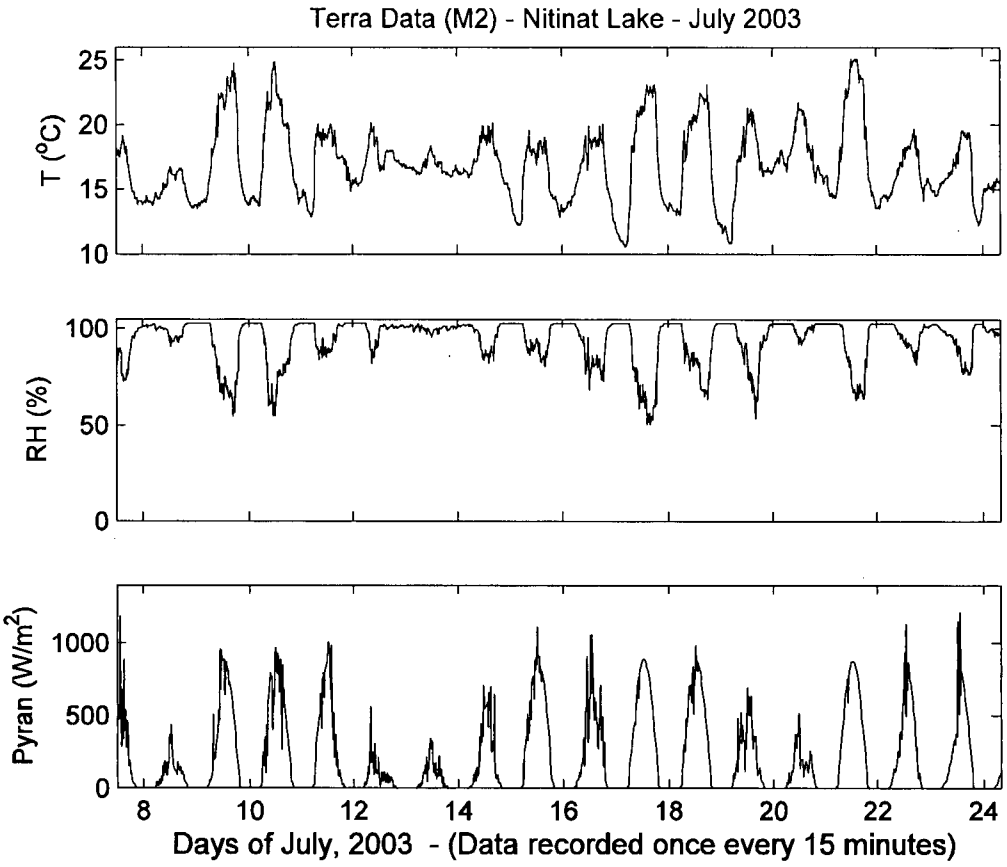

Figure 3.9.1 – Air Temperature (°C), Relative Humidity (%) and Solar Radiation (W/m^2) from station M2 during July of 2003 at Nitinat Lake. Days are indicated, beginning at midnight on every second day.

Figure 3.9.2 shows temperature, relative humidity, and solar radiation during the fall when daily average air temperatures were decreasing. Data in Figure 3.9.2 were recorded between October 25 and November 19, 2003 at station M1, located 17 km inland from the coast on the north shore of Nitinat Lake (Figure 2.3). An examination of the weather history during this time period shows that a series of coastal disturbances, which brought significant precipitation to the coast, moved over the area from the west during the second and third weeks of October 2003. The warm temperatures on October 25 are a result of this weather pattern. In early November, the Jet Stream had shifted and a high-pressure area in the middle of the province, coupled with a low-pressure area to the southwest, brought arctic outflow winds to the southern coast of British Columbia, leading to below seasonal temperatures. (Weather history obtained from Environment Canada forecasts; noted by Author during this time period.)

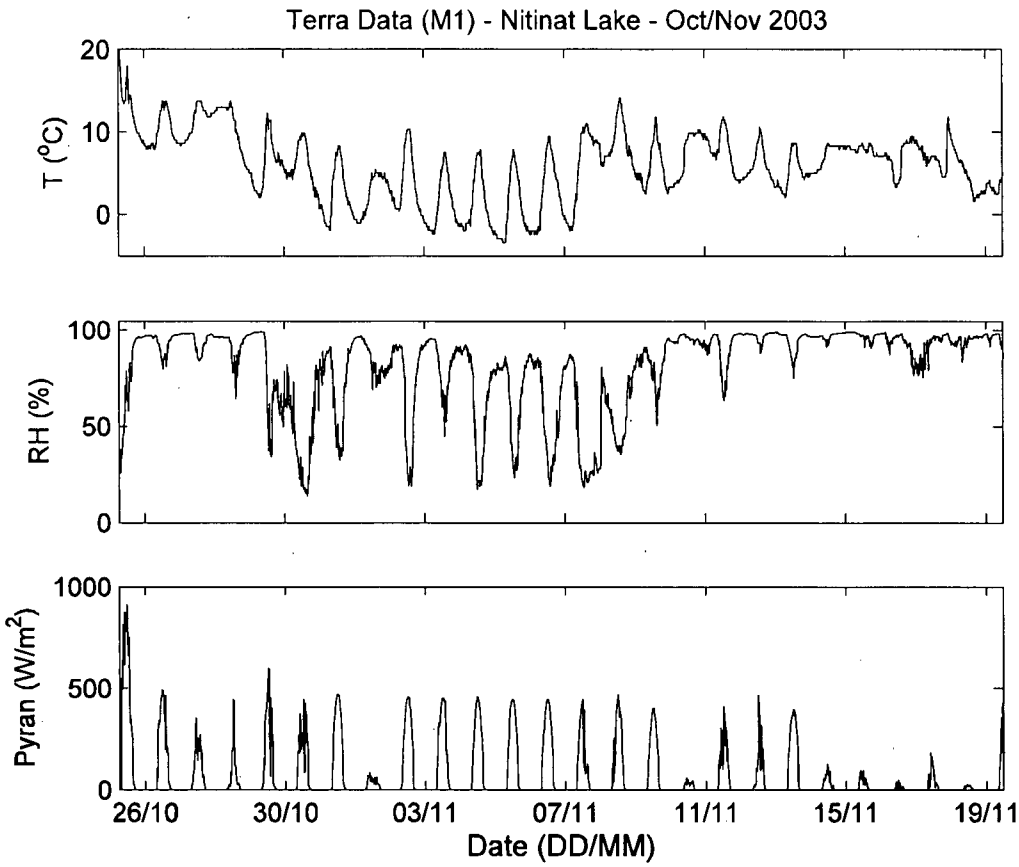

Figure 3.9.2 – Air Temperature (°C), Relative Humidity (%) and Solar Radiation (W/m^2) from station M2 during October and November of 2003 at Nitinat Lake. Days are indicated, beginning at midnight on every fourth day.

Between October 25 and November 19 the temperature is seen to vary significantly at Nitinat Lake (Figure 3.9.2). The maximum air temperature recorded during this time period was 19.8 °C during the early afternoon of October 25, while the coldest temperature recorded was -3.4 °C during the early morning hours of November 5. The mean temperature during this time was 5.87 °C.

Relative humidity (RH) was found to be lower, on average, during the second study period than the first. However, with two variables (season and location) being changed it is impossible to say which factor, the different season or the change in location, is responsible for the change in RH. The average RH recorded during the fall was 81.0 %, while during July at location M2 it was 91.2 %. The highest RH recorded during the fall

was 98.9% during the early morning hours of October 29, while the lowest RH was just 13.9 % on the afternoon of October 30 (Figure 3.9.2).

Solar radiation was less during the fall equinox than during the summer solstice, as expected. Average daily solar radiation was 79.9 W/m^2 with a maximum reading of 1137 W/m^2 on October 25. On most days, the maximum daily reading was near 450 W/m^2 while on rainy or overcast days the daily maximum was sometimes less than 100 W/m^2. Unusually low readings on November 16 and 18 may be attributed to snow accumulations on the sensor, as light snow fell at the lake on these days.

3.9.2 Wind Data

Wind data are discussed in further detail with respect to shear stress of the surface layer in Section 5.2. This section presents samples of wind data collected by the meteorological stations deployed at stations M1 and M2 during July and October/November 2003. Wind data in this section is presented from dates when on-water sampling of water properties occurred.

Figure 3.9.3 shows compass plots of wind from various days in July 2003 at location M2. The scale is such that a 5 m/s wind vector would touch the outer ring of the compass plot, while vectors are aligned to point in the direction that the wind is travelling to. On July 9-11 the strongest winds are from the west, blowing to the east while on July 12 and 13 the winds were weaker and generally blowing towards the northwest. On July 9-11 the weather conditions were warm and sunny, and strong afternoon sea breezes were noted. On July 12 and 13 a rain front moved over the area, and disrupted the stable weather pattern. It should be noted that winds were observed, in general, to be weakest near M2 and strongest near M1 during the summer observation period. As such, the winds at location M2 during July represent a lower limit on the lake winds during the time period. (Further comment on spatial variations in wind strength is made in section 5.2.1.)

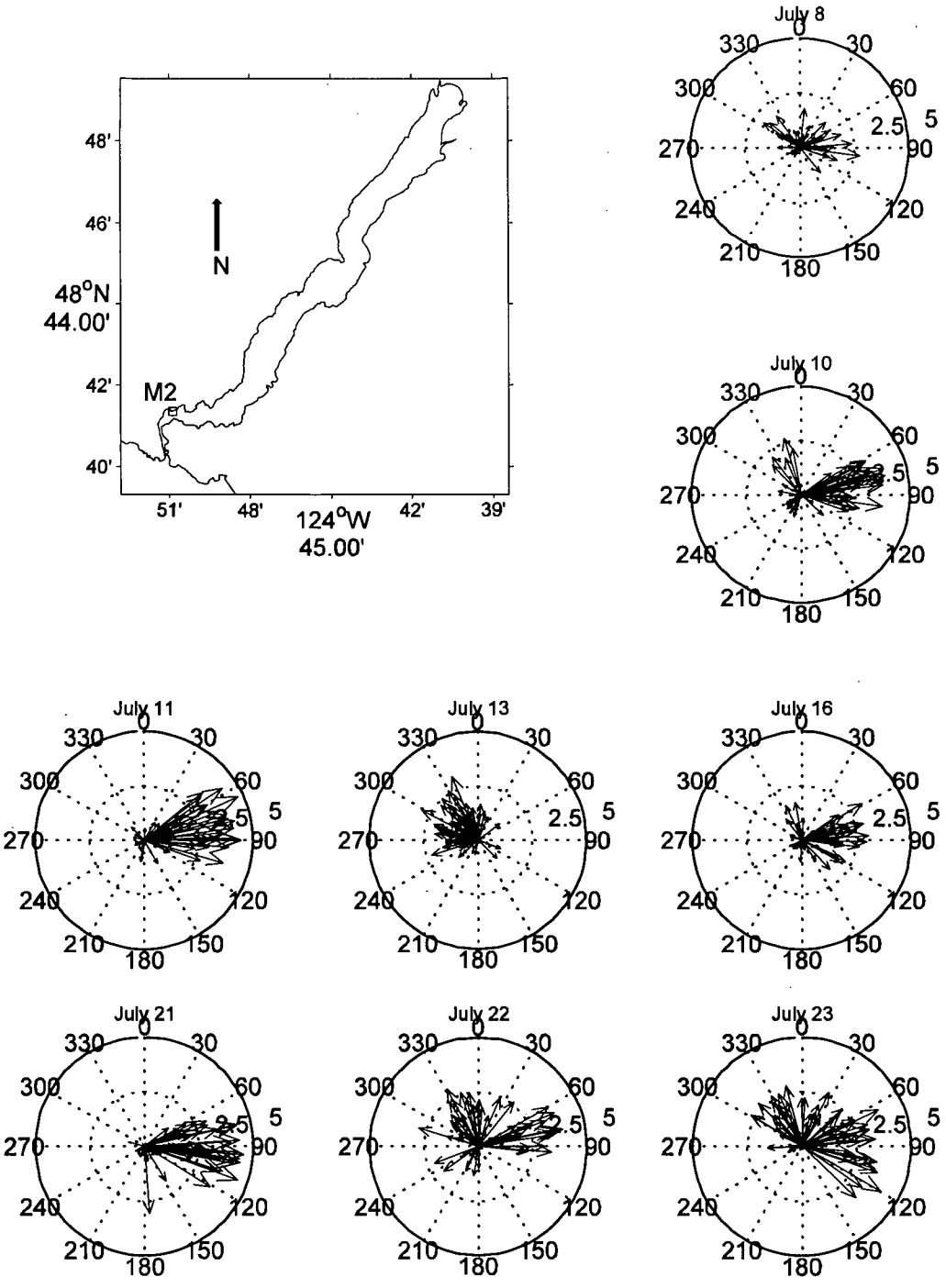

Figure 3.9.3 – Compass plots of daily wind data for M2. Inner ring represents a scale of 2.5 m/s, while the outer ring represents a scale of 5 m/s wind speed. (Note: 0 degrees equals true north, an arrow pointed at 90 degrees equals a wind blowing from the west to the east).

Figure 3.9.4 shows compass plots of the winds from mid-November 2003 at location M1. The scale is different in this figure than in Figure 3.9.3, as the outer ring of the compass plot represents a wind velocity of 10 m/s. Between November 15 and 18 the strongest winds are seen to blow from the south to the north. This corresponds to a wind blowing along the long axis of the lake. Unlike the summer months, when the winds were primarily driven by temperature gradients between the ocean and the warm valleys in the center of Vancouver Island, the winds in the fall were driven more by weather fronts moving across the area, and no discernable daily patterns were present. On November 4, cold outflow winds were present (Figure 3.9.2). The fact that the winds in Figure 3.9.4 are in general of a higher velocity than the winds in Figure 3.9.3 does not necessarily imply that the winter winds at Nitinat Lake are stronger. It was noted that significant spatial variation existed in the strength of the winds on Nitinat Lake, and the two sets of data are unfortunately from different locations. Thus, the higher velocity winds noted in November could simply be the result of measuring wind at a different location on the lake, or it could be that the average wind strength is indeed higher.

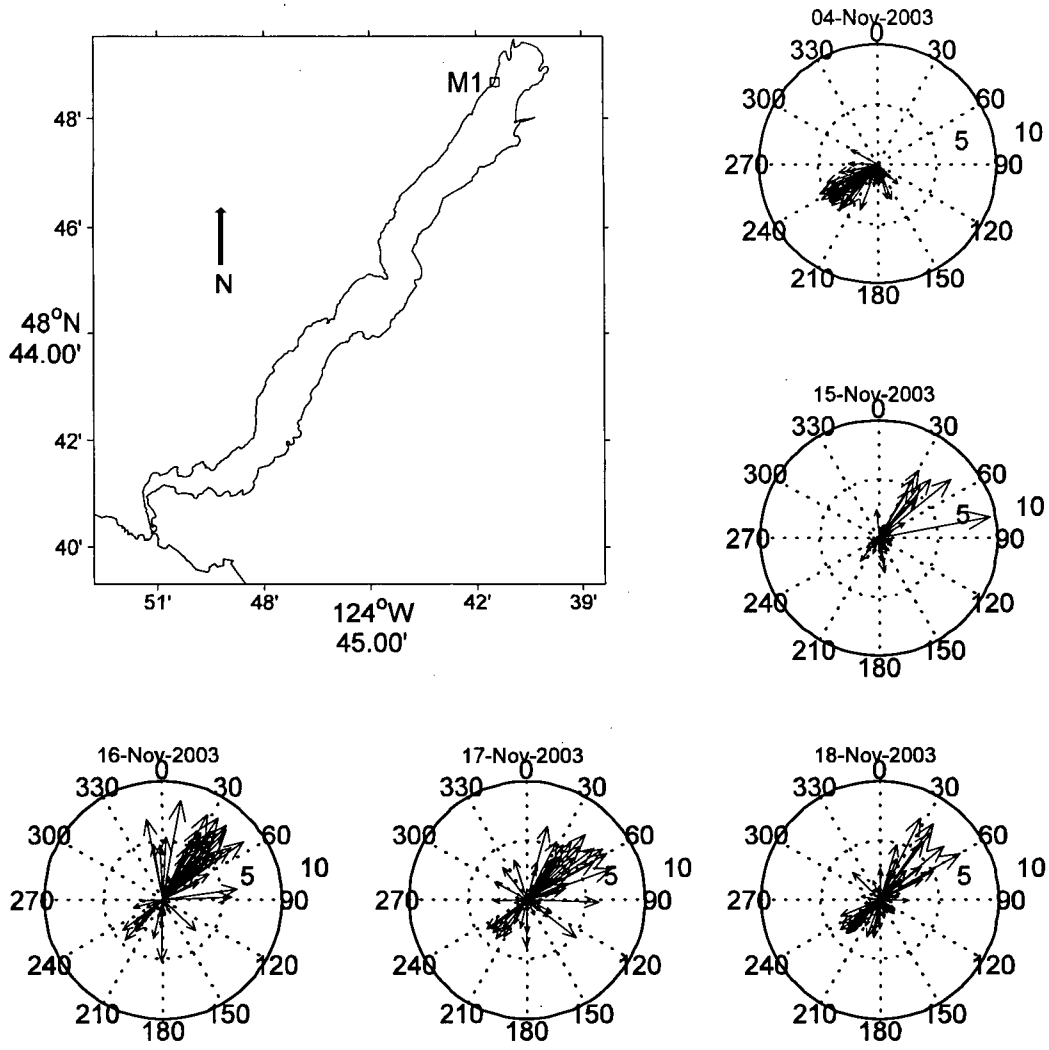

Figure 3.9.4 – Compass plots of daily wind data for M1. Inner ring represents a scale of 5 m/s, while the outer ring represents a scale of 10 m/s wind speed. (Note: 0 degrees equals true north. Thus, an arrow pointing towards 0 degrees represents a wind blowing towards north from the south. An arrow pointing towards 90 represents a wind blowing to the east from the west.

4.0 Discussion

Nitinat Lake is a unique body of water, with unusual characteristics. The anoxic bottom water, the shallow nature of the surface layer, and previous history of upwelling events (Section 1.8) are causes of concern during Fish Hatchery operations on the lake. Limnological studies in the past (Carmack et. al, 1986; Monismith, 1985; Stevens & Imberger, 1996) have investigated response of stratified lakes to wind forcing and presented models of the initial steady state response and interface tilting. The ability to predict an upwelling event in Nitinat Lake requires an ability to predict the density stratification within the lake, and the response of this stratification to predicted wind events. This chapter first examines the link between precipitation and stratification in Nitinat Lake (Section 4.1), and then compares linear theory, for predicting the response of the halocline to wind induced shear of the lake surface, with observations (Section 4.2).

4.1 Relationship Between Precipitation and Stratification

This section examines the seasonal precipitation patterns at Nitinat Lake and compares 2003 rainfall patterns to seasonal variations to the density gradient within the surface layer of the lake. An estimate is made of the residence time of the surface layer, which includes an estimate of stream flow runoff from the Nitinat Lake watershed.

Total precipitation levels show significant variations on a yearly basis (Table 4.1.1), and on a seasonal basis (Table 4.1.2). Most rainfall occurs in the fall and winter months while the spring and summer have low levels of rainfall. An examination of the 10 year record for rainfall at the Nitinat Hatchery (Figure 4.1.1) reveals that summer months often have accumulations of less than 100mm, and on occasion much less. For example, a mere 9.6mm precipitation was recorded during the entire month of August, 2003. The summers (July-September) of 1997, 2000 and 2001 (Table 4.1.2) are exceptions that were notably wetter than average. By contrast, it is not unusual for fall and winter months (October-December) to receive in excess of 300mm of total rainfall, and on occasion much more. November of 1995 was the wettest month on record during the past 10 years, with

1196mm of rainfall recorded. November of 1998 and October of 2003 also received notably high levels of precipitation.

Table 4.1.1 – Annual total precipitation at Nitinat Hatchery for years 1994 through 2003.

Year	*1994*	*1995*	*1996*	*1997*	*1998*	*1999*	*2000*	*2001*	*2002*	*2003*	*Average*
Precipitation (mm)	3942	3910	3563	4999	4170	4304	2925	3055	3491	4024	3926

Table 4.1.2 – Quarterly total precipitation at Nitinat Hatchery for years 1994 through 2003.

Season	**Year**	*1994*	*1995*	*1996*	*1997*	*1998*	*1999*	*2000*	*2001*	*2002*	*2003*	*Median**
Winter	**Jan-Mar**	1632	1317	1288	1714	1513	2087	934	744	1368	1484	1426
Spring	**Apr-Jun**	482	306	717	872	216	279	566	550	541	348	511
Summer	**Jul-Sep**	207	227	248	705	137	227	404	489	199	208	227
Fall	**Oct-Dec**	1621	2060	1311	1708	2303	1711	1021	1271	1382	1984	1664

* Median values are calculated due to the small sample size, and large variations in the range of the data.

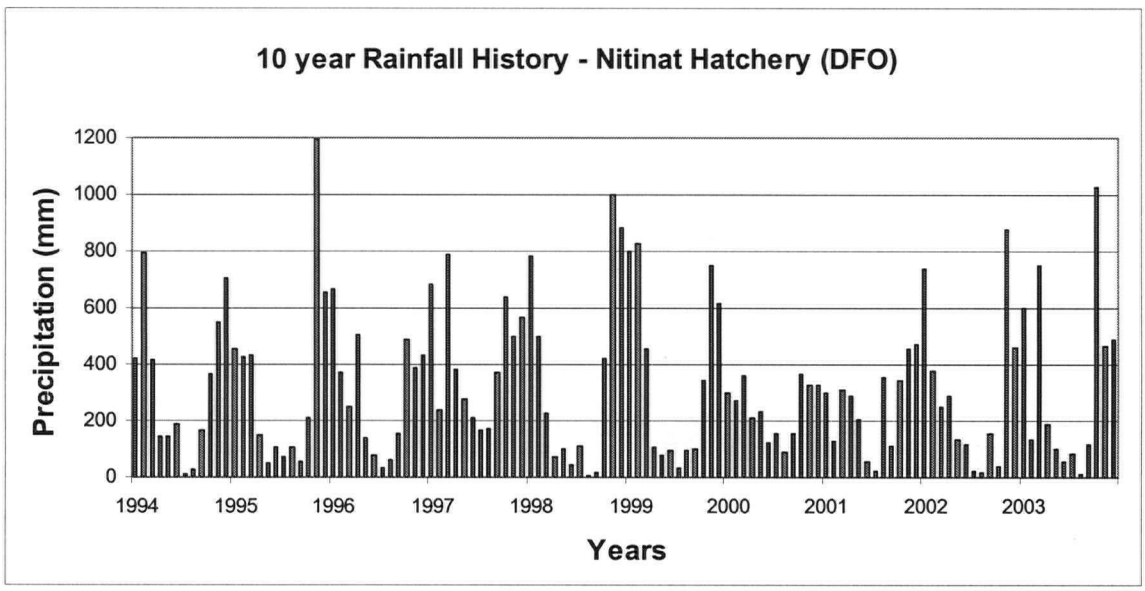

Figure 4.1.1 – Bar graph showing monthly total precipitation from 1994 to 2004, recorded at the Nitinat Hatchery. (Data courtesy Environment Canada and DFO)

The precipitation record reveals distinct seasonal variation in the Nitinat Lake watershed. This seasonal variability in turn influences the lake properties, with the surface layer observed to increase in salinity (and thus, density) during the late summer months following a period of low precipitation. Surface layer salinity in Nitinat Lake is, at any given time, a balance between seawater entering the lake across the sill and fresh water entering the lake through river runoff. The tidal prism (Section 3.8) varies in magnitude with the monthly and seasonal tidal cycles, and the river runoff varies depending upon

the rate of precipitation in the area. As in any estuary, the exchange of water between the inlet and the ocean on every tidal cycle works to increase the salinity levels, while river inputs decrease them.

There are two assumptions that will be made in the remainder of this paper. First, precipitation data are being used as a proxy for river flow; and second, river flow is the primary mechanism controlling surface layer salinity in Nitinat Lake. Daily precipitation records have been maintained at the Nitinat River Hatchery, while no seasonal stream flow measurements have been made of the primary tributaries feeding into Nitinat Lake. For this reason, it has been necessary to infer a direct relationship between stream flow rates and daily precipitation. Section 4.1.1 examines more closely the link between precipitation and stream flow and the rational for assuming that precipitation is a valid indicator of river flow. The second assumption is made due to the fact that the salinity level in the lake is seen to change slowly with time, and that relatively speaking the tidal prism is fairly constant over time. By comparison, the river runoff rate into Nitinat Lake changes significantly with over time, and high river runoff rates can fairly quickly add a significant volume of fresh water to the lake. Section 4.1.2 presents evidence of the relationship between river flow and surface layer salinities, and hence the density stratification (see Section 3.4).

4.1.1 Estimated of Surface Layer Residence Time

Residence time is the time required for 100% of the water to be exchanged in a body of water. In order to estimate the surface layer residence time, it is necessary to know the rate at which river runoff and precipitation is entering the lake. It is assumed that the net flow of water into the lake is equal to the net flow of water out of the lake, as the lake is generally at steady state with respect to volume. (This is not always the case. On rare occasions, the net inflow exceeds the net outflow, and the lake surface level rises, as occurred on October 16-21, 2003 – see Section 3.8.) However, no stream gage data are available from the study period, thus the estimation of residence time is more difficult and relies upon assumptions made from the precipitation record.

The net river runoff (volume of water) entering into the surface layer of the lake can be estimated by multiplying the area of the watershed by the precipitation. The size of the Nitinat Lake watershed was estimated to be 1050 km2. This estimate was obtained by scanning topographical maps into a graphics program and tracing the watershed boundaries to determine their area. Using the 1994 to 2004 rainfall data (Figure 4.1.1), the average annual total rainfall is found to be 3839mm. Assuming a uniform precipitation distribution over the catchment, this works out to an average rainfall rate of 10.516 mm/day. Assuming storage and evapotranspiration are negligible then a maximum theoretical average runoff for the entire catchment is 128 m^3/s. This very simple analysis assumes 100% of the precipitation eventually makes its way into the streams. This is not reasonable. Topography, soil type, land use, vegetation cover, and time of year all affect the percentage of runoff from precipitation. Precipitation-runoff and streamflow-routing models are very complex, and no such study has been attempted here. Without doubt, some percentage of precipitation is taken up by vegetation, evaporation, or ground water aquifers. That said, the west coast of Vancouver Island is classified as a temperate rain forest, and it is probably safe to assume that surface runoff is relatively high in this region compared with other areas of North America, especially during the wet winter months when vegetation is in a dormant growth phase and soils are highly saturated.

Although no stream flow data are available in the Nitinat watershed, data are available for the Sarita River which runs near Bamfield just to the north of the Nitinat watershed. This river, with a drainage area of 162 km^2, had a mean annual discharge rate of 19.7 m^3/s for the period between 1949 and 2001 (Environment Canada). The drainage area is approximately 6.5 times smaller than the Nitinat drainage. Thus, another method of determining the annual average runoff rate for the Nitinat drainage is to multiply the Sarita value by 6.5. Interestingly, this yields a value of 128 m^3/s, which is the exact same value as determined above using the Nitinat Hatchery precipitation data. It is thus reasonable to conclude that Nitinat Hatchery precipitation data can be used to obtain rough estimates of stream flow rates into Nitinat Lake for different time periods.

4.1.2 Density and Precipitation in 2003

The discharge rate based upon monthly precipitation data was calculated for 2003 (Table 4.1.3). To determine residence time, the total volume of a lake is typically divided by the river discharge rate. However, given that the bottom waters of Nitinat Lake are permanently anoxic, it is safe to assume that river discharge remains in the surface layer, and that the bottom layer is not routinely exchanged. Thus, residence time is directly calculated based on surface layer volume and river runoff rates. Results are shown in Table 4.1.3. Surface layer depth (h_1) was determined using CTD data obtained at Nitinat Lake (Further discussion of the method used to determine h_1 is given in section 4.2.2.2).

Table 4.1.3 – Monthly precipitation and average discharge rates for 2003, during months when lake properties were measured.

	Total Monthly precipitation (mm)	Average runoff rate (m^3/s)	h_1 (surface layer depth, m)	Surface Layer Residence Time estimate
Feb	134.7	58	10.8	54 days
Jul	81.7	32	6.4	57 days
Sep	116.7	47	8.4	52 days
Nov	467.7	189	8.6	13 days

Based upon these estimates, surface layer residence time is seen to vary between 13 and 57 days in 2003, with the longer residence time during July, and the shortest residence time during November. It should be noted that the h_1 estimate is significant, as the deeper h_1 in February leads to a longer residence time than in September despite the fact that average runoff in September is less than in February. If h_1 was constant throughout the year, then residence time would be directly proportional to runoff.

Somewhat complicating the estimation of residence time is the fact that variations in ocean tidal ranges will increase or decrease the exchange of water between Nitinat Lake and the ocean, and also that it is not entirely clear if river discharge water fully occupies the surface layer. It is possible that the fresh river water 'slides' along the surface of the entire lake in the absence of strong winds, and exits across the sill on an outgoing tide, with varying degrees of mixing at the interface. That said, there would still be lots of mixing of seawater and river water across the sill, which is advecting into the lake on a rising tide. There may be several distinct bodies of water residing in the 'surface layer' at any given time such as a fresh water cap, and a lower layer of incoming ocean water that

has entrained some of the fresh surface cap. The dynamic is very complex, and further study is required to answer these questions and further refine the estimate of residence time. Nevertheless, the surface layer residence time offers a rough approximation, while the residence time of the bottom water is assumed to be measured in years instead of days or weeks.

The purpose of examining residence time is to determine a time frame over which the precipitation record will be relevant for predicting the density stratification of the lake. Based upon the results of Table 4.1.3, it is suggested that the record should be considered for a time frame of several months during the dry season, while during the rainy winter months when the discharge rate is high the record of only a few weeks may be sufficient for providing an estimate.

Figure 4.1.2 gives the monthly rainfall history for 2002 and 2003 at the Nitinat Hatchery in bar form. Also included in the figure are the values for the modified acceleration due to gravity (g') shown as diamonds, based upon measured density stratification within the lake. The higher the value of g', the greater the difference between the surface layer and bottom layer density, and the lower the susceptibility of the lake to upwelling.

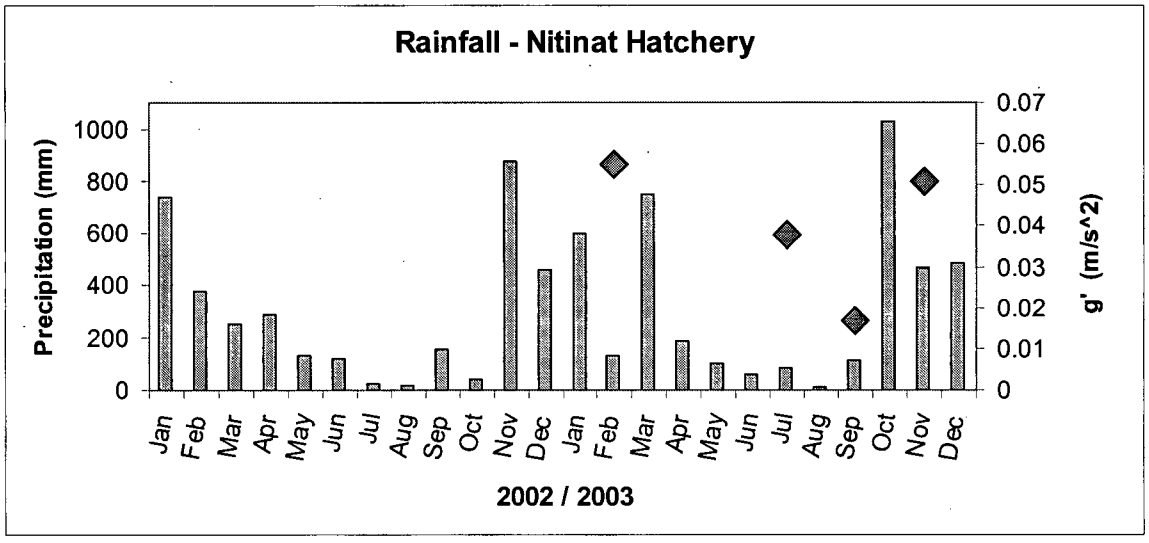

Figure 4.1.2 – Monthly precipitation for 2002 and 2003, recorded at the Nitinat Hatchery (Data courtesy Environment Canada and DFO). Also shown as diamonds is the modified acceleration due to gravity ($g' = g [(\rho_2 - \rho_1)/\rho_2]$) as determined from CTD surveys of the lake. The modified acceleration gives an indication of the relative differences between surface layer and bottom density in the lake. The lower the value, the less stably stratified the lake is.

Figure 4.1.2 shows a clear trend in g' in relation to the precipitation record. In February of 2003, the value of g' is seen to be high following three months of high precipitation. In July, following three months of low precipitation, the g' value is seen to have moved downwards, and in September, following an extremely low precipitation month the value of g' has dropped significantly. By November the value is seen to have moved upwards following a single month of heavy precipitation. Most likely, the g' value was even higher in late October, immediately following the large precipitation event that lead to a flood (section 3.8). Assuming that the surface layer (top meter of lake) salinities were zero immediately following the flood, and that the bottom layer salinity remained constant between September and November, then it is probable that g' was greater than 0.10 ms^{-2}, and maybe as high as 0.14 ms^{-2}, in late October. Thus, the value of g' most likely reached a minimum in early October, while the yearly maximum value of g' occurred during the flooding event in mid-October.

The relatively low precipitation in February does not appear to be sufficient to drop the value of g' towards the level observed in September, despite the fact that February and September had similar levels of precipitation. Conversely, just three weeks of heavy rain at the end of October and beginning on November caused the g' value to move significantly upwards. This would suggest that decreases of g' are a longer term process requiring several months of dry weather, while increases of g' happen relatively rapidly following significant rain events.

4.2 Lake Response to Wind Forcing

Internal lake response to wind forcing depends on the magnitude of the surface stress, depth of the water, and density structure of the water column. If there is a density gradient between the surface layer and the deeper water, it is possible for a strong wind to induce a downwind motion of the surface layer with a discernable shear at the pycnocline. In this case, the entire surface layer begins moving downwind as a slab above a relatively stationary bottom layer. This phenomenon is commonly referred to as "slippery water" (Thompson, 1981) In open ocean conditions, the surface layer will generally continue to move in the direction of travel until a counteracting force, such as a

wind event in another direction, is present. In a lake, the moving surface layer will encounter the downwind shoreline of the lake and begin to 'pile up'. This results in a slight elevation of the free surface, and a downward deflection of the pycnocline at the downwind end of the lake (Figure 4.2.1).

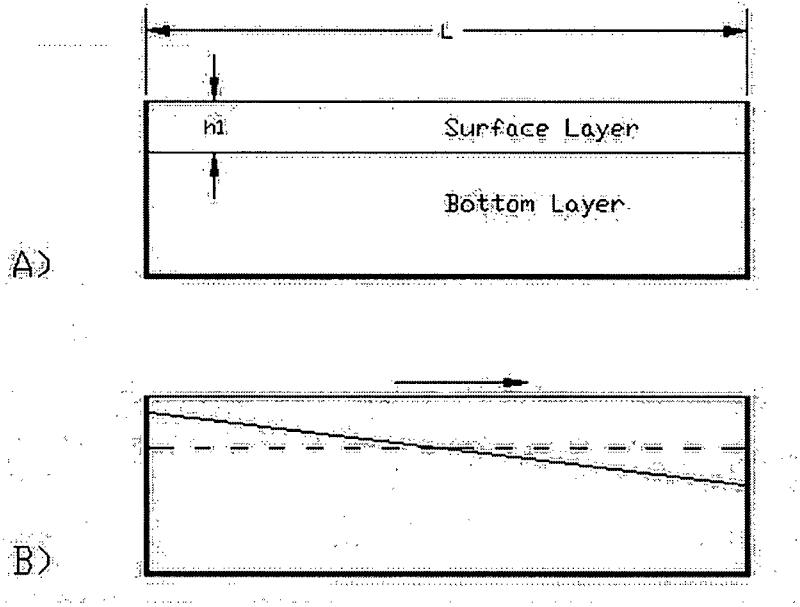

Figure 4.2.1 – Schematic diagram of idealized lake. (a) The state of the lake with no surface stress. (b) The halocline deflection due to surface stress.

In order to predict the internal response to wind forcing, it is first necessary to understand the nature of the wind shear on the surface of the lake. Section 4.2.1 examines the nature of the surface stress produced by wind on Nitinat Lake. Section 4.2.2 presents a linear analysis of internal lake response to surface stress, while section 4.2.3 compares the predicted internal response with actual measurements made in the lake using CTD and temperature sensor mooring instrumentation. Finally, section 4.2.4 reviews the assumptions and sources of error in both the prediction and lake measurements.

4.2.1 Wind Forcing On Nitinat Lake

Wind blowing over the surface of a body of water imparts energy, producing surface waves and inducing currents. The magnitude of the effect from the wind depends upon several primary factors: wind velocity, fetch, and the length of time (duration) that the wind is present. These factors in concert determine the magnitude of the waves and

currents that form within a body of water. For example, a strong blast of wind that is of very short duration (minutes) will have less effect in establishing a large internal standing wave than medium winds that are present for many hours. Likewise, a strong wind that blows across a short fetch will have less impact than a weaker wind that is fully developed along a very long fetch. Thus, when examining wind forcing, it is necessary to take into account the velocity, direction (as it relates to fetch), and duration of the wind.

4.2.1.1 – Wind Direction, Fetch, and Topography

Nitinat Lake is long, narrow, and deep, and is located within a valley that greatly influences local wind patterns. Winds aligned with the long axis of the lake have the greatest fetch, and are not restricted by local topography. In contrast, winds that are perpendicular to the long axis of the lake have a very short fetch, and are also obstructed by the local mountains and ridges that run parallel to the lake. Surface winds in these conditions are often characterized as "swirling and gusty" by local fishermen (discussions with Philip Edgar, Ditidaht First Nations, 2003). Thus the local topography, in addition to the direction, magnitude, and duration of the wind, all affect the response of the surface layer to wind forcing.

4.2.1.2 – Observations of Wind on Nitinat Lake, 2003

Observations made at the lake in 2003 indicated significant temporal variations in wind speed over the length of the lake. Wind data were collected during visits to Nitinat Lake using a hand held anemometer and compass, as well as by automated meteorological stations. Unfortunately, a significant amount of meteorological data was lost from the data logger near station S06 during the October flooding event. In general it was found that a strong sea-breeze developed on warm sunny days during summer months when inland valley temperatures were greater than coastal temperatures, while winds during the fall and winter were much less predictable and dependant upon coastal weather systems.

On summer days it was not uncommon to find fog and light winds near the mouth of the lake, while 18 km away at the head of the lake there would be blue skies and strong winds. Wind data presented in Table 4.2.1 is indicative of this summer wind pattern.

Discussions with windsurfers who were sailing near S07 (Figure 2.1) on July 7 confirmed that the winds in this location were steady during the afternoon. S07, at the northeast end of the lake, was found to have the highest wind speeds of the day as generated by the summer sea-breeze. This is most likely the result of the interaction of the local topography and the temperature gradient between the coast and inland regions.

Table 4.2.1 – Afternoon winds on July 7 showing spatial variation along length of lake.

Location	S00	S01	S02	S03	S04	S05	S06	S07
Time	13:12	13:56	14:19	14:40	14:58	15:15	15:33	15:52
U_{10} (m/s) [1]	3.7	5.5	5.6	6.4	5.6	6.2	8.4	10.1

1) Winds recorded at z=3m, corrected to z=10m. (Amorocho & DeVries, 1980)

Wind strength tends to increase with elevation above the water due to boundary layer development along the lake surface. It is generally assumed that the wind velocity profile with height is logarithmic, assuming conditions of neutral thermal stability. Formulae used to determine surface shear stress are typically based on wind speed measured 10m above the surface. However, it is not always possible to obtain wind velocity data at 10m elevation, and this was the case at Nitinat Lake. The meteorological stations were only equipped with 5m high poles for mounting equipment, while wind measurements taken on the water were done using hand held anemometers at a height of 2m to 3m above the surface. To correct for this discrepancy, formula developed by Amorocho and DeVries (1980) were used to correct the wind velocity to U_{10} values, and all wind velocity data presented in this paper is for U_{10} unless otherwise stated.

By examining wind velocity along the length of the lake, lake-wide mean wind speed on the lake was estimated to be 65% of the maximum wind speed recorded at S07 (i.e., $U_{avg} = 0.65\ U_{max}$; Table 4.2.1). Furthermore, it was found that maximum afternoon winds at location M2 (Figure 2.3.1) were on average one-third the strength of winds recorded at S07, and one half the lake-wide mean wind speed, during the month of July.

No discernable along-lake wind speed gradient was evident from the data collection in November of 2003. Winds on the lake were generally lighter during this time, with no developing whitecaps observed. Discussions with First Nations band members indicate that passing weather fronts generate the strongest winds during this time of year.

4.2.2 Linear Analysis

The simplest model of a stratified water body is a two-layered fluid. In a lake, with confining end walls, wind shear forces the surface-layer fluid towards the downwind end of the lake and creates a longitudinal pressure gradient. As a result, the free surface is displaced upwards at the downwind end of the lake, while the density interface is displaced downwards at the downwind end of the lake (Figure 4.2.1). The internal density difference is typically approximately one thousand times weaker than at the air-water interface, and as a result the vertical displacement of the internal interface is much greater than that of the free surface.

A number of experiments have been performed to examine the initial response of a stratified water body to wind forcing. Monismith (1986) presented the Wedderburn number, a dimensionless parameter, which gives an indication of the likelihood of upwelling occurring assuming a linear tilting of the interface.

4.2.2.1 Wedderburn Number

Approximating the lake as a rectangular box with two layers of constant density, and that the lake response is linear, the following equation gives the deflection of the free surface of a lake subjected to a steady wind (Spigel & Imberger, 1980)

$$\frac{dH}{dx} \approx \frac{\tau_0}{\rho_1 g h_1} \qquad (4\text{-}1)$$

where H is the elevation of the free surface above the bottom of the lake, ρ_1 is the density of the surface layer, h_1 is the depth of the surface layer, and g is acceleration due to gravity. τ_0 is the shear stress on the surface due to the wind and may be determined empirically by:

$$\tau_0 \approx C_D \rho_A U_{10}^2 \qquad (4\text{-}2)$$

where $\mathbf{C_D}$ is the drag coefficient (here taken to be 1.3×10^{-3} Imberger and Patterson, 1990), ρ_A is the density of air, and $\mathbf{U_{10}}$ is the wind speed at a height of 10 meters above the surface of the water.

Assuming a linear internal response, the slope of the interface between the surface layer and the bottom layer is given by:

$$\frac{d\zeta_1}{dx} \approx \frac{\tau_0}{\rho_1 g' h_1} \qquad (4\text{-}3)$$

Where g' is the modified acceleration due to gravity ($g' = g\,[(\rho_2 - \rho_1)/\rho_2]$) and ζ is the displacement from equilibrium depth, h_1, of the surface layer. In this case, the interface is considered to remain linear at all times, and pivots about the midpoint of the lake (i.e., $x = L/2$).

By this theory, should $d\zeta_1$ exceed h_1 upwelling will occur. The Wedderburn Number (W) is a dimensionless parameter that predicts upwelling in lakes, using the above linear and bathymetric approximations, and is defined as:

$$W \approx \frac{g' h_1^2}{u_*^2 L} \qquad (4\text{-}4)$$

$$u_* = \left(\tau_O / \rho_O\right)^{1/2} \qquad (4\text{-}5)$$

Where u_* is the shear velocity. If W is much greater than unity, then the interface will not surface, while if W is much less than unity, the interface will surface resulting in upwelling. If W is close to unity, then it suggests that the possibility of upwelling exists and other factors need to be examined.

4.2.2.2 Methodology for Determining h_1 and ρ_1

To calculate Wedderburn numbers for Nitinat Lake, it was first necessary to 'idealize' the lake as a rectangular box (Figure 4.2.2). The length of the lake was chosen to correspond

to the fetch along the thalweg as measured using GPS, which corresponded to 18.8 km. Choosing a depth scale was more difficult. The bathymetry of the lake varies, with a significant step in the bottom profile occurring near the midpoint of the lake where the average depth changes from near 130m to 190m. For the linear analysis, the depth is an important variable in determining the internal wave speed, and hence the internal response time of the lake to wind forcing. Given the length of the lake, and an average width of 1.2km, the depth of 146m was chosen such that the volume of the lake would be similar to the total lake volume as estimated based upon bathymetry ($\approx$ 3.1 x10^9 m^3, Northcote et. al., 1964).

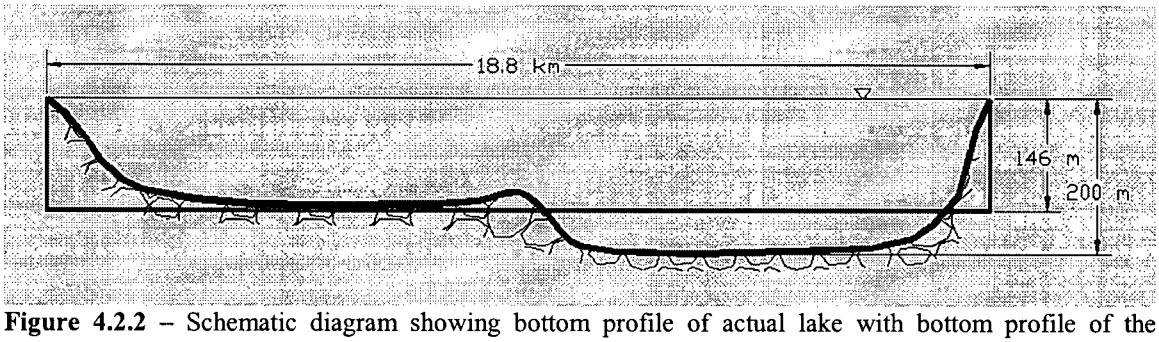

Figure 4.2.2 – Schematic diagram showing bottom profile of actual lake with bottom profile of the idealized lake (rectangular box) superimposed. Note that the length scale is different than the depth scale in this representation.

The density and depth of the two layers is determined from CTD data obtained during the 2003 field studies (Table 4.2.2). To determine the depth of the surface layer, density profiles for each station were used, and the rate of change of density with respect to depth was computed. In the deep water, the density was relatively constant and the rate of change was near zero. In the surface layer the rate of change of density with depth was highest. The interface between the surface layer and bottom layer was chosen to correspond with the average depth at which the rate of change of density with depth increased above 0.25 kg/m^3/m. This value was found by inspection to correspond well to the point at which density began to decrease rapidly in the surface waters, and was sufficiently higher than the rates of change observed in the deep water. The density of the surface layer was then computed as the average of the CTD densities determined above this depth for all stations in the lake. A similar procedure was used to calculate bottom layer density.

Table 4.2.2 – 2003 Nitinat Lake density data, base upon CTD casts. All samples listed obtained in low wind conditions.

Date	*Time*	h_1 *(m)*	ρ_1 *(kg/m^3)*	ρ_2 *(kg/m^3)*	*g' (m/s^2)*	*Ti (hrs)*
Feb 16, 2003	15:14	10.8	1017.9	1023.8	0.055	14.0
Jul 25, 2003	9:30	6.4	1020.0	1023.9	0.038	21.6
Sep 17, 2003	11:30	8.4	1022.1	1023.9	0.017	27.9
Nov 20, 2003	9:30	8.6	1018.6	1024.0	0.051	16.1

It is important to remember that W is a steady state parameter, and the response is characterized by an internal standing wave. Studies of various lakes and their responses have found that the minimum time required for the wind to blow in order to fully develop the condition identified by W as the maximum interface deflection is Ti/4 (Stevens & Lawrence, 1997). Ti is the period of the fundamental internal wave, and is determined from the internal wave speed Ti (4-5).

$$Ti = 2L/c_I \qquad \text{(Internal wave period)} \qquad (4\text{-}6)$$

$$c_I = \sqrt{\frac{g' \cdot h_1 \cdot h_2}{h_1 + h_2}} \qquad \text{(Internal wave speed)} \qquad (4\text{-}7)$$

Thus, the U_{10} values given in Figure 4.2.1 and 4.2.2 represent the time averaged U_{10} for a period equal to Ti/4.

Using data from Table 4.2.2 and equation 4-3, the theoretical deflections of the interface were determined for a range of wind speeds and are plotted in Figure 4.2.3. As seen in this figure, the interface is least stable in September and most stable in November. Not surprisingly, as the density gradients are weakest in September, and strongest in November. An examination of the h_1 values in Table 4.2.2 reveals that upwelling is predicted to occur for sustained winds of approximately 12.5 m/s in February, 7.5m/s in July, and 6.5 m/s in September as shown in Figure 4.2.1. Not shown in this figure is the depth of the surface layer. It is assumed here that wind direction is parallel to the long axis of the lake.

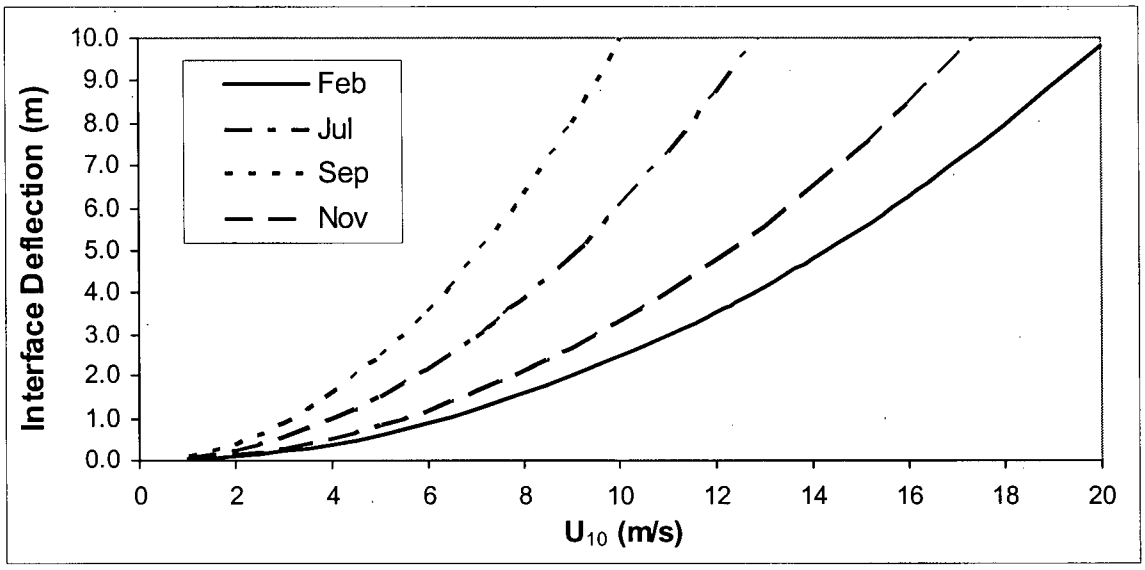

Figure 4.2.3 – Theoretical Interface Deflection (m) at end of lake as a function of wind speed, based upon a two-layer box model (H=165m) of lake system using Nitinat Lake data from 2003 as presented in table 4.2.2.

Figure 4.2.4 shows Wedderburn Number calculated for a range of wind speed for stratification observed at different times of the year. These data show that upwelling is most likely for a given wind speed during September, followed by July. It also shows that upwelling is far less likely, according to linear theory, during the winter months when the density gradient is stronger. This makes sense, as a stronger density gradient will require more forcing to overcome the different relative weights of the water, and to lift the heavier bottom water up and displace the lighter surface water.

Linear theory for deflection of the interface is directly related to the strength and depth of the density gradient. An examination of the depth and strength of the change in density with depth, as recorded by CTD casts, highlights the same trend found in the Wedderburn analysis (Figure 4.2.5). In September, the maximum value for $\delta\rho/\delta z$ is seen to be less than 2 $kg/m^3/m$ while in November the value is greater than 7 $kg/m^3/m$. Thus it is observed that the strength of the density gradient is inversely related to the likelihood of upwelling due to wind shear of the surface layer.

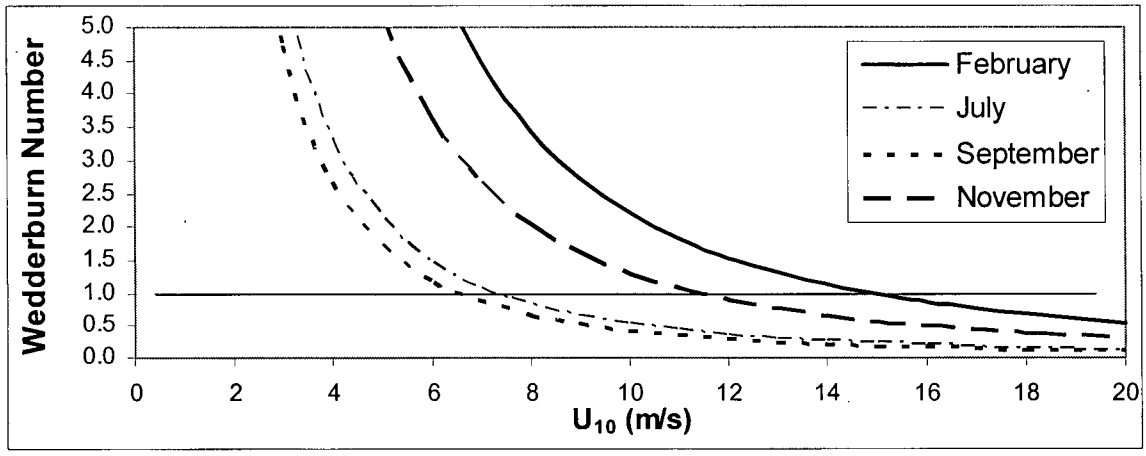

Figure 4.2.4 – Wedderburn Number as a function of wind speed, based upon a two-layer box model (H=165m) of lake system using Nitinat Lake data from 2003 as presented in table 4.2.2.

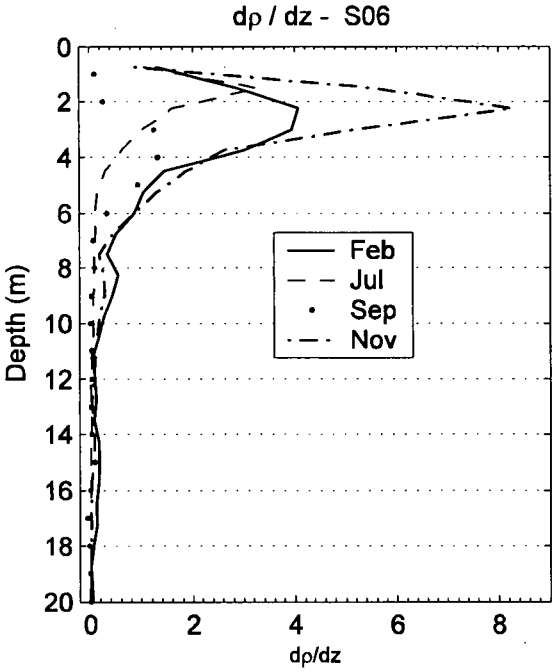

Figure 4.2.5 – Change in density as a function of depth. Data from CTD casts at station S06.

4.2.3 Observed interface Deflections – July 2003

Movements of the surface layer were readily observed from both CTD and Temperature Sensor Mooring data, and can be used to verify the accuracy of the Wedderburn predictions.

4.2.3.1 July Data

On July 10, 2003, a series of three CTD casts were made at the same location at different times of the day (09:00, 13:30, 20:00) to measure the effect of wind forcing. On this day a strong sea-breeze developed during the afternoon with peak winds of 9m/s recorded at 15:00 on shore near S07, and moderate winds present until sunset. The wind recorded during this day by hand at S07 is shown in Table 4.2.3:

Table 4.2.3 – Winds on July 10 at/near S07 recorded with hand held anemometer

Time	09:00	13:30	15:00 [2]	20:00
U_{10} (m/s) [1]	0	8.1	10.4	6.2

1) Winds recorded at z=3m, corrected to z=10m. (Amorocho & DeVries, 1980)
2) Winds recorded on shoreline near S07

Wind speed was also recorded on this day by a meteorological station located at the ocean end of the lake, and is shown in Figure 4.2.6 below. The dashed line represents measured wind speed, while the solid line represents a moving average with a time scale of Ti/4. In the early morning hours the wind is seen to fluctuate in strength between zero and 1 m/s followed by an increase in wind strength between 7:30 and 9:00 in the morning before dropping again to below 1 m/s. Just after 10:00 in the morning the wind again increases and, with several fluctuations, continues to increase towards a daily maximum near noon. Over the next three hours the wind continues to fluctuate near its daily maximum before dropping in the late afternoon after 15:00. After 18:00 there is no significant wind recorded at this station for the remainder of the day.

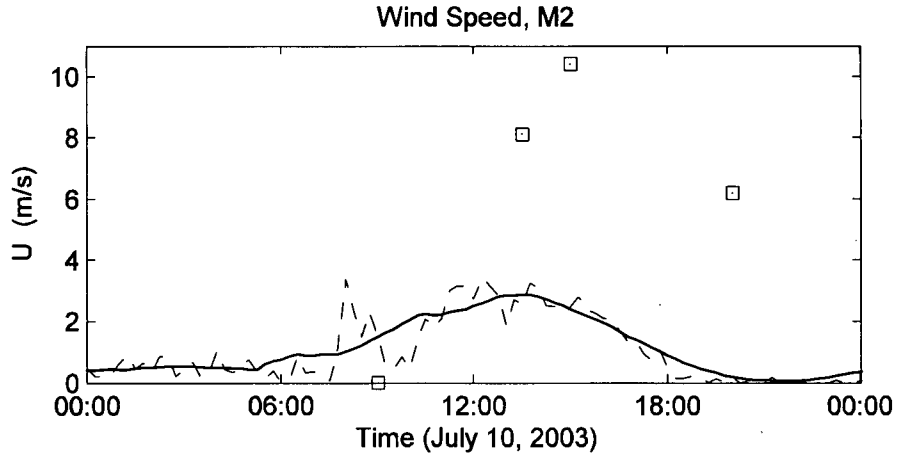

Figure 4.2.6 – Wind velocity recorded at station M2 on July 10. (Data are not available for M1). Dashed line represents raw wind speed recorded at height of 5m. Solid line represents wind speed corrected to U_{10}

and smoothed with a moving average equal to Ti/4 (≈ 5.25 hrs). Boxes represent handheld anemometer data from station S07, as shown in Table 4.2.3.

The wind pattern at the south end of the lake (Figure 4.2.6) is similar to but not exactly the same as the wind pattern at the north end of the lake (Table 4.2.3). One difference is that the peak winds at the north end of the lake occurred later in the day near 15:00 as compared with 12:00 at the south end, while the magnitude of the peak winds were significantly higher (approx. 3x) at the north end than the south end. However, the general trend of a strong sea-breeze is present throughout both sets of observations. In the absence of further spatial wind data for the lake on this day it is impossible to determine the mean wind speed over the lake, but it is reasonable to suggest that the mean is some value in the range between the two sets of data, and that an estimate of the average of the two values would not be too far off. Thus, a reasonable estimate of average U_{10} for the lake on this day would be approximately 6 m/s based upon the available data. Returning to Figure 4.2.3, the linear theory for this wind speed predicts a deflection of 2m of the interface.

Figure 4.2.7 shows CTD casts of temperature against pressure recorded at station S07 on July 10. The temperature gradients at S07 are seen to change significantly during the day with significantly warmer water becoming present at greater depths in the upper 10m. At 9:00 PDT, only the top 2.5m of water is warmer than 17 °C, while at 20:00 PDT the top 8m of water is warmer than 17 °C. Below 12m in depth, there is no notable change in temperature. The vertical density gradient is also seen to shift downwards during the day in a similar manner to the temperature profiles. The vertical movement of the density profile is approximately 6m on this day. This 6m change in depth of the pycnocline observed in Figure 4.2.7 is more than the 3m change predicted for the estimated 6m/s mean over-lake wind speed on this day by equation 4-3 (and Figure 4.2.3).

It is important to remember that after commencement of the surface stress, it takes ¼ of the internal wave period for the condition identified by equation 4-3 to occur and that, in the absence of friction, "the response overshoots and peaks at a slope twice that of Ri^{-1} at a time of ½ Ti" (Stevens & Imberger, 1996). In Nitinat Lake the friction between the surface layer and the bottom layer may be low due to the strength of the vertical density

gradient, and thus promote this overshoot at time ½ Ti. On July 10, the surface stress began around 10:00 PDT, and the final measurement of the interface occurred at 20:00 PDT, which is close to the time of ½ Ti (≈ 10.8 hours – Table 4.2.2). The observed 6m deflection corresponds very well with the estimated overshoot of the response in the absence of friction, and suggests that linear theory provides an adequate estimate of the lake response to surface stress.

It must be noted that July 8 and 9, 2003 also experienced strong afternoon sea-breeze on the lake. Given that Ti (natural period of lake) is close to 24 hours at this time of year, and that the wind forcing events are occurring once every 24 hours, it is possible that the amplitude of the interface deflections is greater than predicted due to resonance between the wind forcing the internal response of the lake. Thus the thermocline may be shallower in the early morning as a response to the previous days forcing, and would not represent an 'unforced' state of the lake. This could be another reason why the Wedderburn prediction of deflection is less than the actual deflection observed.

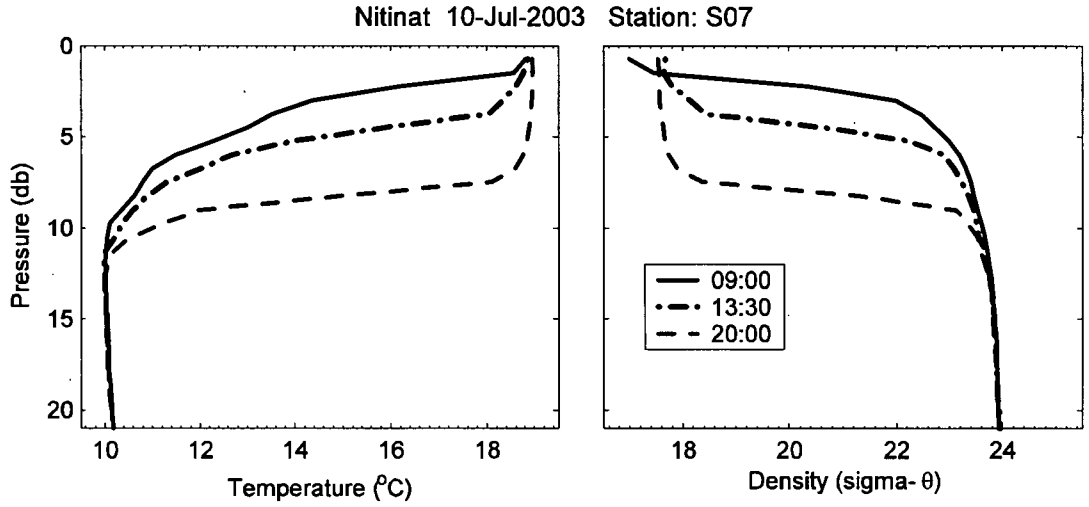

Figure 4.2.7 – Temperature and density profiles from CTD data obtained at S07 during three different times of the day. A strong sea-breeze mixed the surface layer on this day, beginning at 10:00am and continuing until 19:00 PDT in the evening.

On July 21 and 22 2003, two thermistor chains were deployed in Nitinat Lake. These sensors were able to record movements of the thermocline due to wind forcing. Unfortunately, wind data from the north end of the lake (M1) is not available for this time period, but wind data are available from M2 at the south end of the lake until July 25.

Figure 4.2.8 shows lake response at two separate locations on the lake over a two-day time period in late July of 2003. A strong sea-breeze was prevalent on these days, with strong afternoon winds observed at the inland end of the lake and lighter winds observed at the ocean end. Continuous wind data recorded at M2 during this period records the onshore afternoon winds that were typical of the sea-breeze. Winds at M2 were generally weaker than over the rest of the lake, due both to the wind gradient present in the valley, and that M2 is located at the upwind end of the fetch where the lake turns before heading across the narrow sill to the ocean. Figure 4.2.8(b) shows the 12 °C temperature contour at TC1 located in the north basin near S06, while Figure 4.2.8(c) shows the 12 °C temperature contour in the south basin, near station S03. It should be noted that TC2 is located closer to the midpoint of the lake than TC1. The response to wind forcing is clearly evident in both sets of data, and is as expected. In the north basin (downwind end of lake) the temperature contour is seen to drop significantly in the early afternoon and remain down until near midnight. At TC2, the opposite is seen with cooler water being drawn up towards the surface during the afternoon time period.

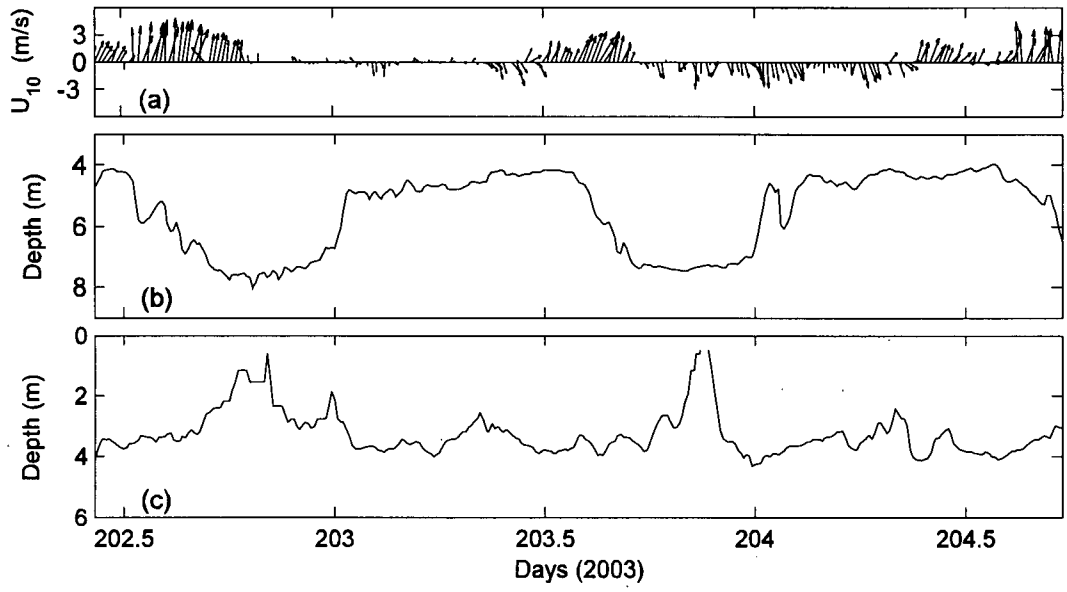

Figure 4.2.8 – Wind data from MC2 (a) at ocean end of lake. Up arrows represent wind from the west, while down arrows represent winds from the east. TC1 (b) and TC2 (c) temperature contours at 12 °C show lake response to daily wind forcing. Time period is from 10:30 July 22 to 17:30 July 24.

The shape of the two temperature contours from TC1 and TC2 are not mirror images of each other, suggesting that the lake response is not entirely linear. On day 203 (July 23,

2003) the temperature contour at TC1 is observed to begin responding to the wind forcing in the early afternoon (at approximately 14:00) and reaches a maximum displacement three hours later. It then remains at this maximum displacement until shortly before midnight. However, TC2 is not observed to respond to the wind forcing until much later in the day (approximately 19:00) and the response occurs for a significantly shorter time period. If the lake response were truly linear, then each basin would respond on the same time scale, thus the response to wind forcing, as shown by changes in temperature data, is not perfectly linear.

It must be noted here that the movements of the isotherms do not correspond in a one-to-one manner with movement of the isopycnals, due to the discrepancy between temperature and density stratification. From previous data, it is more likely that in July the response at TC1 is closely related to movements of the pycnocline (Figure 4.2.7) while at TC2 it is less likely that changes in temperature directly correlate with variations in density. Thus, while the data from the thermistor chains clearly shows a response to wind forcing, the movement of the pycnocline can not be completely known from the temperature sensor data set, but can only be estimated from CTD comparisons of temperature and density. Unfortunately, no multiple CTD casts were made on these days to track temporal changes in both temperature and density near TC2 to provide further insight.

4.2.3.2 November Data

November data are more scattered with no strong correlation between wind and isotherm movement. Figure 4.2.9 shows wind data recorded at MC1 (post flood – new met station), calculated Wedderburn number, and deflection of the 11.2 isotherm beginning on October 30 (Day 302) and continuing until November 19, 2003 (Day 322). During this period of time a number of wind events were recorded, but the correlation between wind events and isotherm movements is not clear.

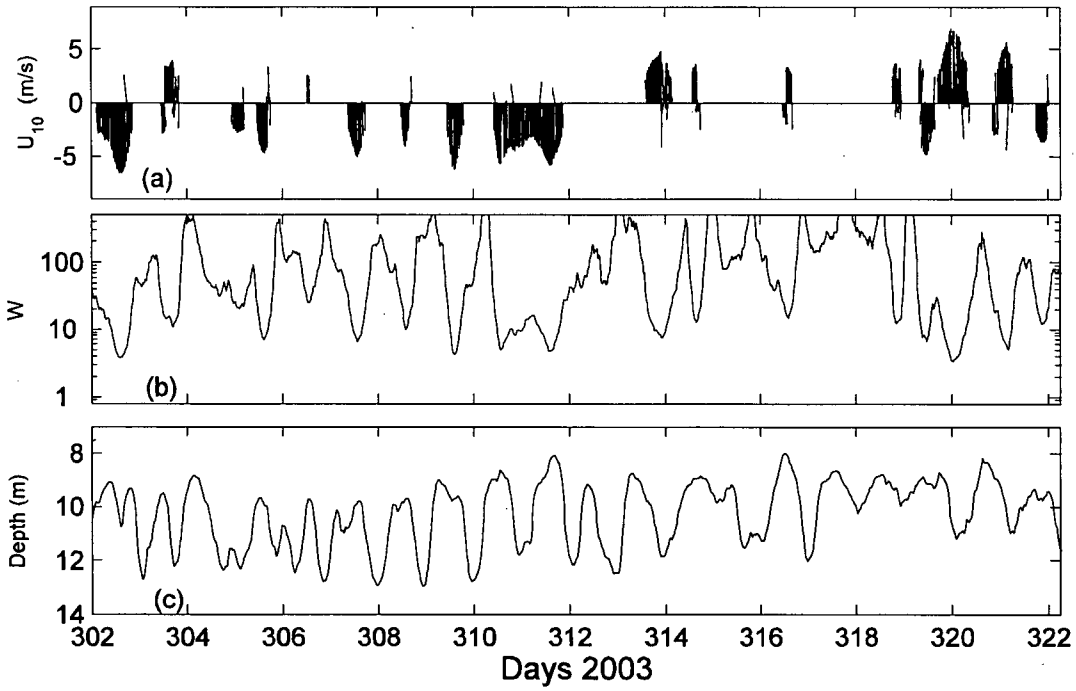

Figure 4.2.9 – (a) U_{10} wind data from location M1. Vectors pointed straight up represent wind coming from the southwest and going to the northeast. The long-axis of Nitinat Lake is oriented on a SW-NE angle. Wind data have been low pass filtered at $T_1/4$. **(b)** Wedderburn numbers (W) are plotted using wind data from M1. Square marks indicate minimum W during northeast winds, while circles indicate minimums associated with southwest winds. **(c)** Depth of the 11.3 °C isotherm at TC1.

Between days 307 and 312 (Nov 4-9) there were several strong wind events from the northeast. This would correspond to outflow winds, and it would be expected that the isotherms at TC1 would be drawn upwards by such events. Indeed, there are strong daily peaks at this time culminating with the highest on day 311. However, on day 316 a small wind was recorded from the SW, representing an in-flow wind from the ocean, but the isotherm is response is similar to that on day 311 when the winds were from the opposite direction. Thus, there is no discernable response correlation from wind forcing.

The error is most likely due to the nature of the temperature stratification at TC1 during the fall. An examination of Figure 4.2.10 shows a CTD profile of temperature near TC1 on day 322 (Nov 19, 2003). This plot shows that a temperature maximum occurs near a depth of 8m, with temperature decreasing below this. Figure 4.2.11 and 4.2.12 show temperature data from sensors on the two moorings in the lake during the end of October and first week of November when lake surface temperatures decreased below the bottom

water temperatures forming an inversion. Figure 4.2.10 also shows the location of the three working temperature sensors, and the depths that they were located at, for TC1. The top sensor on the mooring (5m depth) had stopped recording by October, and thus no data are available above 7.5m depth for this time. As a result, the top working sensor of the thermistor chain was located near the peak temperature, and any deviation in temperature could indicate either an upwards or downwards motion of the isotherm. It is thus not possible to attempt to infer the lake response to wind forcing from these temperature data with any reliability.

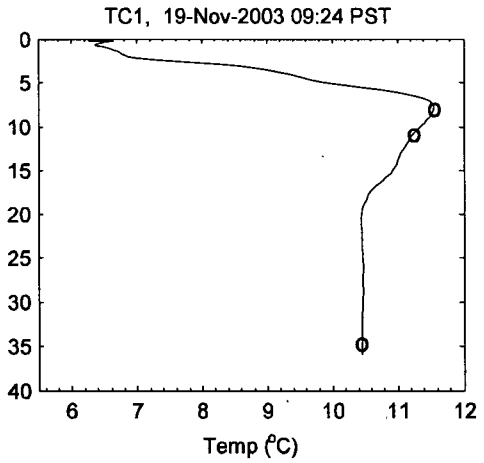

Figure 4.2.10 – Temperature depth profile taken using a CTD on November 19, 2003. Circles represent depths of temperature sensors located at TC1.

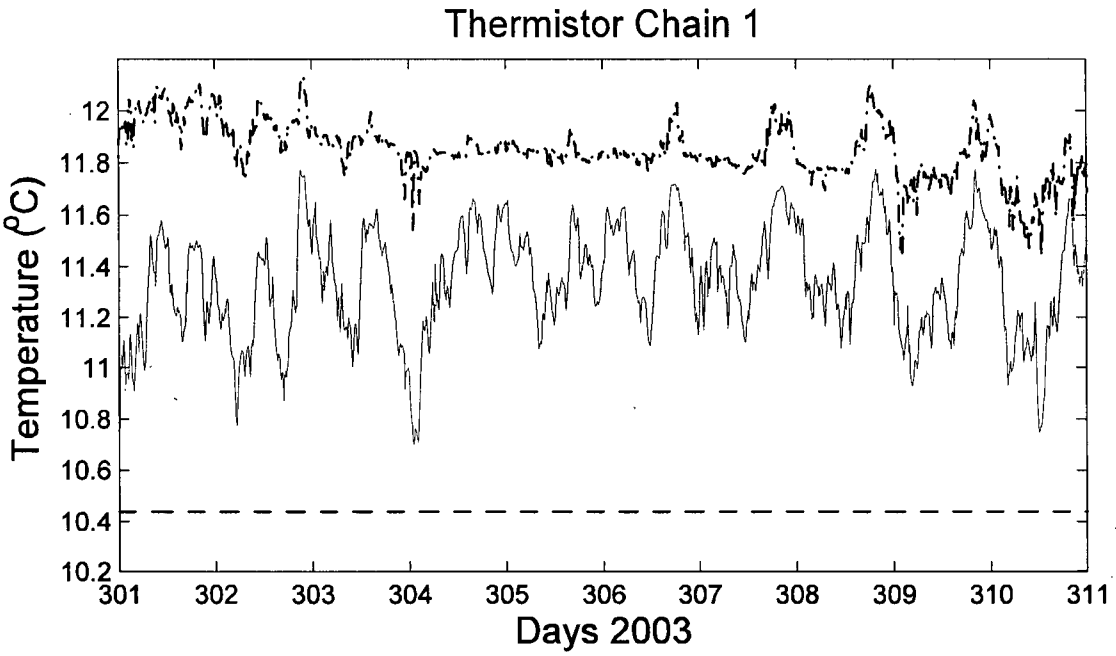

Figure 4.2.11 – Temperature plots from sensors at TC1 mooring in 2003 (October 28 – Nov 7). Dash-dot line is temperature at depth of 8 m, solid line is temperature at depth of 11m, and dashed line is temperature at depth of 35m. (Uppermost sensor on mooring at depth of 4m was not working during this time period.)

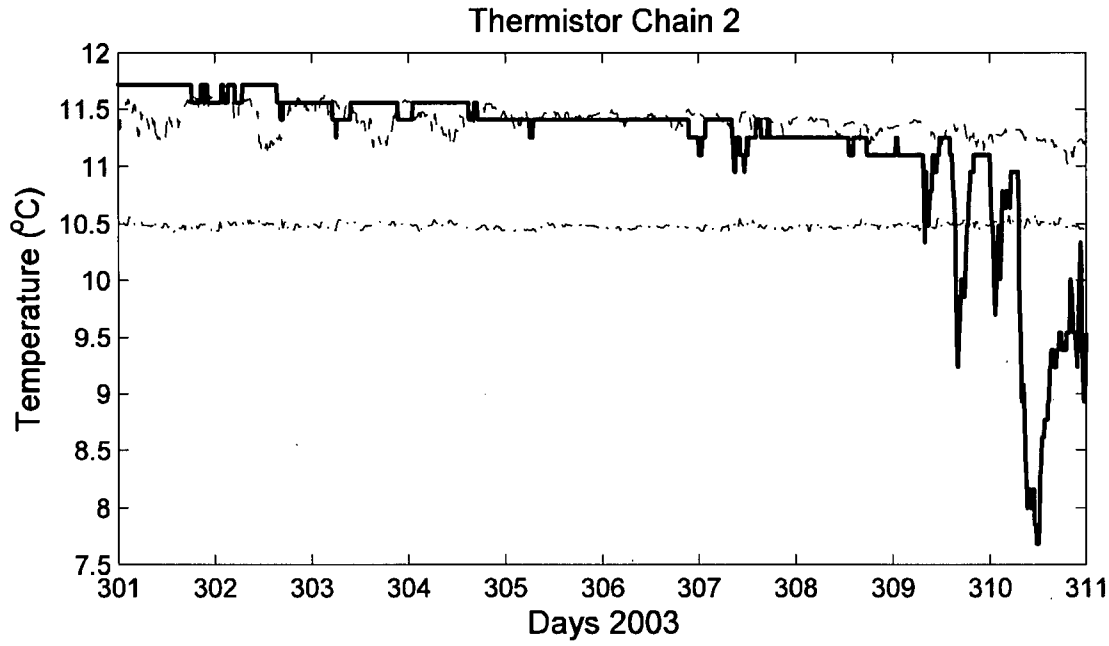

Figure 4.2.12 – Temperature plots from sensors at TC2 mooring in 2003 (October 28 – Nov 7). Solid line is temperature at depth of 4m, and dashed line is temperature at depth of 9m, and dash-dot line is temperature at depth of 23m. Data shows formation of surface layer temperature inversion during this time period.

4.2.4 Observed complications

Despite good overall agreement between predicted maximum initial interface deflections (Stevens & Imberger, 1996) and the measured deflections in Nitinat Lake, there are several points regarding assumptions and complexities in the actual lake that should be noted. A three dimensional lake is much more complicated in reality that the two dimensional analysis allows for, and Section 4.2.4.1 discusses some of the assumptions made in linear theory and adjustments made to the analysis to minimize these possible sources of error. Section 4.2.4.2 looks at the differences between salinity and temperature with respect to the vertical density gradient in Nitinat Lake, and how vertical changes to the temperature gradient may not reflect vertical changes to density at certain times of the year. As a result, it is seen that movements of the vertical temperature gradient are not always a good proxy for movements of the pycnocline.

4.2.4.1 Beyond Linear Theory

Based upon observations of Nitinat Lake, it is clear that there are several physical factors that complicate the actual lake dynamics in comparison to theory. These factors include both spatial and temporal variations in the wind strength, non-rectangular bathymetry, strong density gradients in the surface layer, a non-linear lake response, and a thermocline and oxycline that do not mirror the pycnocline.

As stated above, wind was frequently observed to vary spatially over the length of the lake, especially as wind strength increased. To improve the prediction given by the Wedderburn Analysis, a determination of the wind velocity averaged over the entire length of the lake is used. However, spatial variations in the wind stress may induce variations in the velocity and direction of the surface currents, complicating the true response. The wind velocity was rarely observed to remain constant for more than a few hours, while the Wedderburn number is based upon steady wind stress. To correct for this discrepancy, wind speed was first adjusted to reflect the average lake U_{10} wind speed, and then filtered using a moving average based on a time frame of Ti/4.

Bathymetric and topographic irregularities in the actual lake will also lead to error in the Wedderburn prediction, as the actual lake response will differ from the predicted response. Nitinat Lake is a very long and narrow lake with two distinct basins, and the abrupt change in depth between the two basins, coupled with a promontory that extends from the north side of the lake at the midpoint, complicates the propagation of internal waves within the lake at this region. The promontory at the midpoint of the lake also disrupts the wind flow along the length of the lake. This reality is significantly different from the idealized flat bottomed, rectangular lake assumed by the analysis.

The Wedderburn model also assumes a two layer water body, with a strong pycnocline separation. In this model, each layer is assumed to be of constant density. In reality, Nitinat Lake does have a very homogenous deep water layer with a very small density gradient. However, in the absence of wind mixing the surface layer was often found to be highly stratified, as compared to the homogenous surface layer depicted in the model. As a result, the determination of h_1 and ρ_1 is somewhat subjective, and small changes in these values can have a large impact on the final W prediction.

The small ratio of surface layer depth to lake depth coupled with the strength of the density stratification suggests that the internal response to wind forcing might be non-linear. The depth of the pycnocline was observed to vary between 5 and 11 m depth in a lake that is 18km in length while observed deflections of the surface layer due to wind shear were between 2 and 7 m. The surface layer is thus a very shallow body of water with respect to the length, and the response of the surface layer to wind forcing will not necessarily be linear, especially when the wind forcing varies spatially across the surface of the lake. Furthermore, the observed pycnocline deflections (Figure 4.2.7) are a significant proportion of the surface layer depth, while linearity requires that deflections remain small (Stevens & Imberger, 1996). Once wind forcing is removed, the subsequent propagation of internal waves is most likely in the form of an undular bore, and this was indeed observed in the Nitinat temperature mooring data (Figure 4.2.8).

Finally, the thermocline response to wind forcing that is observable using thermistor chain moorings do not necessarily correspond to the response of the pycnocline or

oxycline. Thus, changes in density measured at a given location are not necessarily linearly correlated with changes in temperature or oxygen. As discussed in the following section, the temperature structure in the lake varies spatially, and the shape of temperature contours is not always similar of the density contours.

4.2.4.2 Comparison of Density and Temperature contours

Since long term monitoring of the lake was done using temperature probes, it is important to assess the relationship between temperature and density profiles in the lake. As seen in Figure 4.2.13 below, the temperature distribution does not always correlate with the density structure within the lake. Vertical density variation remains constant across the length of the lake. The only minor deviation is seen at the surface in the north basin, and can be attributed to the inflow of river waters into the lake.

In contrast, the temperature profiles in the lake are seen to have significant vertical and horizontal deviations. At the surface there is slightly warmer water present at the north end of the lake, with strong temperature gradients seen in the top 6 meters (Figure 4.2.13). Below that depth, spatial variations are more pronounced. In the south basin, the 11 °C contour is seen to drop to roughly 25m depth at stations S01 and S02, while in the north basin the temperature drops below 11 °C at a depth 7.5m. Following a depth of 10m along the thalweg of the lake, the temperature is seen to change from 12 °C at S01 to 11 °C at S04 to below 10.25 °C at S06 and S07. At this depth, the warmest waters are near the ocean sill, and the coldest waters are at the inland end of the lake, which is the opposite of the trend observed at the surface.

Near S03, at 9m depth the temperature is changing at a rate of -0.4 °C/m (decreasing temperature with depth) while at S06 at 9m depth the rate of change is -0.1 °C/m. At the same time, the rate of change of density with depth at S03 is 0.06 $kg/m^3/m$, while at S06 the rate of change is 0.05 $kg/m^3/m$ (Figure 4.2.14).

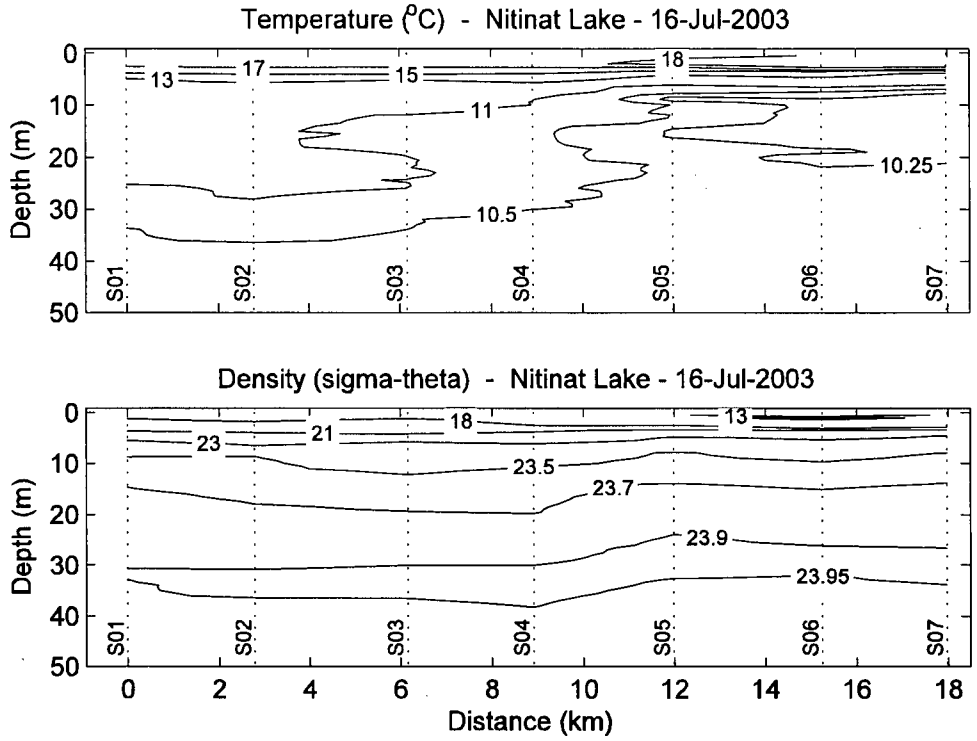

Figure 4.2.13 – Comparison of temperature and density contours in Nitinat Lake on July 16, 03.

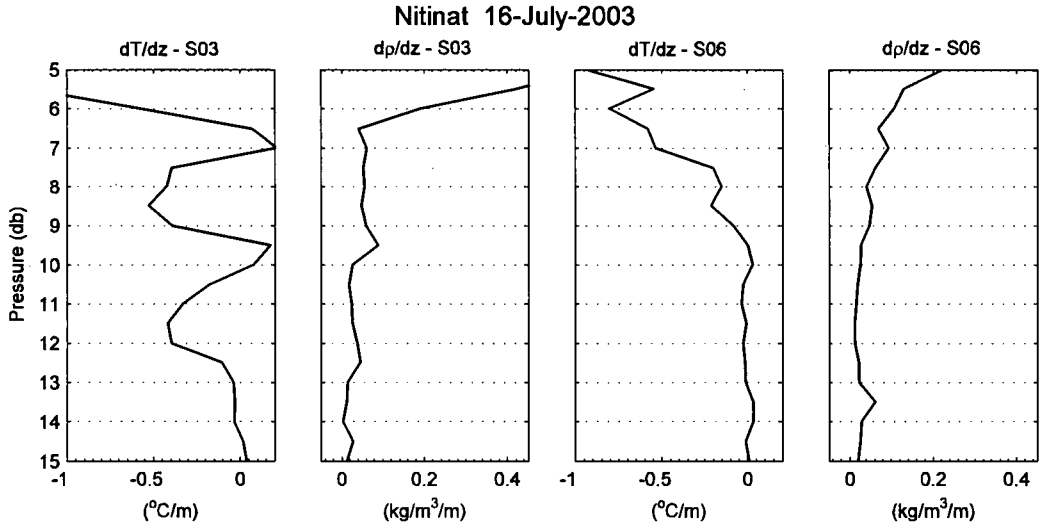

Figure 4.2.14 – Comparison of rates of change of temperature and density with depth at two different stations in Nitinat Lake on July 16, 03. Note that the rates of change with depth are location specific and are not the same. Specifically, temperature was seen to vary in a random pattern with depth in the south basin, making it difficult to infer deflections of the pycnocline based upon changes in temperature.

Thus, temperature is not always a good indicator of pycnocline movement within the lake. Temperatures change seasonally within the surface layer, and unless the relationship

between temperature and density is well known, it is not possible to determine pycnocline deflections based solely upon temperature data. This is particularly relevant during the fall and spring months when surface temperature gradients are undergoing significant changes while density gradient changes are less pronounced.

5.0 Conclusions

5.1 Lake Characteristics

Nitinat Lake is an unusual body of water. It is a salt stratified 'fjord-lake' with a brackish surface layer whose salinity changes with seasonal variations in precipitation and river runoff. The strong salinity-induced density stratification in the surface layer ensures that the lake remains meromictic, causing permanent anoxia in the deep waters of the lake. Density is primarily controlled by salinity, while temperature does not significantly affect density in the surface layer. Temperature variations do become more important in the deep waters where salinity variation is less.

By comparison with previous studies done of the lake, it appears that conditions in the lake are not changing significantly with time. The range of temperatures and salinities observed in 2003 were in the same range as those observed in the 1960's and '70's. The only notable long-term trend observed was a very slight increase in average deep water (below 60m) temperatures in the lake, although this is difficult to establish with precision due to the different instrumentation used in the early studies of the lake.

5.2 Relationship between Precipitation and Density

There is a direct correlation between precipitation in the Nitinat watershed and density stratification in the lake. At any given moment the properties of the surface layer represent a balance between river inputs and ocean exchanges across the sill.

Data collected during 2003 showed that during dry summer months, the salinity of the surface layer increased and the relative difference in densities between the surface and bottom layer (as measured by g') decreased. Conversely, heavy rains in the fall were able to completely reverse the conditions created during the summer, decreasing the salinity of the surface layer and increasing the relative differences in density.

The rate at which these changes occur is of interest, but difficult to establish without weekly or even monthly data for the entire year. What is clear is that extreme levels of precipitation, either very low or very high, can quickly change conditions within the lake.

The month of August had very little rain, and the surface salinity saw a marked increase between the end of July and mid-September. At the same time, the last half of October had very high levels of rain, and the surface layer salinity decreased significantly.

It would appear that the actual rate of change of salinity in the surface layer is also dependant upon the initial conditions. For example, if salinity is very low, then a month of low precipitation (100mm total rainfall or less) will lead to an increase in surface salinity. However, if surface salinity is already high after a very dry month, then even a month of relatively little rainfall may cause the opposite effect, and decrease the surface salinity. Furthermore, the rate at which fresh water enters the lake is much more variable than the rate at which salt water enters the lake. As salt water can only enter from tidal pumping across the sill, the maximum rate at which salinity is introduced to the surface layer is less than the maximum rate at which fresh water can enter the lake during heavy rains. This would suggest that only a few days of heavy rain could compensate for several weeks of very dry weather. To more fully understand these relationships, exchange across the sill and the mixing of ocean water with lake water must be studied further.

5.3 Interface Response to Wind Forcing

Nitinat Lake has a very shallow surface layer, relative to its length and depth. As a result, it is not likely that the interface responds in a linear fashion to forcing. Indeed, moored temperature sensor data suggests that internal waves propagate as undular bores within the lake. However, linear theory does offer a very simple model with which to examine initial interface response to wind forcing, and was used for this purpose.

At first glance, linear theory reasonable predicts the initial interface response to wind forcing. On July 10 of 2003, maximum sustained winds of 9.3 m/s were observed at the lake, and deflections of 5-6 m were observed. Linear theory predicted a deflection of 4.9m for a 9m/s wind speed given July lake conditions. Moored temperature sensor data from July 22-23 are also in agreement with predictions made by linear theory.

There are several things that should be pointed out with respect to the linear analysis of lake response to wind forcing and this study. First, linear theory assumes a constant wind

stress across the entire lake, and this was never observed to be the case when doing field studies at the lake. Further study of wind stress on the lake is required. Second, density is primarily controlled through salinity while temperature plays a very minor role. Thus, moored temperature sensors do not necessarily provide a good indication of isopycnal response to wind forcing. Third, if the density gradient is very strong between the surface layer and bottom layer, strong wind forcing may lead to the entire surface layer moving downwind as a 'slab' of water. This condition is often referred to as 'slippery water' (Thomson, 1981). In Nitinat Lake, this moving slab of surface water would be constrained at the downwind end of the lake, displacing some of the bottom water towards the other end of the lake and causing a tilt in the interface (as predicted by linear theory.) But the actual shape of the interface between surface layer and bottom water better resembles a bulge at the downwind end than a linear tilt. Also observed during windy days at the downwind end of the lake were surface currents near the shorelines flowing in the opposite direction of the wind, suggesting that the true lake response is complex and three-dimensional.

5.4 Prediction of Anoxic Upwelling

Of interest in Nitinat Lake is the ability to accurately predict an upwelling of anoxic water. This is not possible given the current knowledge of the lake, and the limited ability to accurately forecast surface winds in this region. What is possible is the ability to determine when the lake is more or less susceptible to upwelling. It appears that a limited program of lake monitoring with a CTD, in conjunction with precipitation data, can provide an accurate prediction of lake conditions. From this, it should be possible to determine when there is a low, medium, or high risk of upwelling occurring given a strong wind event.

Based upon previous studies and information presented in this paper, it is possible to draw some conclusions about the time of year when upwelling is most likely. If the oxycline were at a constant depth within the lake, then upwelling would be most likely to occur in the late summer and early fall when surface layer salinity reached its annual maximum. This would be due to the fact that the density gradient would be weakest at

this time of year and the pycnocline would be most susceptible to surface stress. However, the oxycline is not at a constant depth, and the anoxic interface is 1.5 to 2 times deeper at the south end of the lake than the north. As a result, a significantly greater surface stress is required to promote upwelling at the south end of the lake than the north, and for this reason upwelling events during strong southwesterly winds are rare (Table 1.8.1). Thus, Nitinat Lake is more likely to experience upwelling during very strong winds blowing from the northeast to the southwest along the thalweg of the lake, and is most likely to experience upwelling when very strong north easterly winds occur during the late summer or early fall when the density gradient is weakest.

It should be asked of what usefulness a prediction of upwelling would be. In actual fact, there are only limited times during the year when it is of great interest to know if an upwelling event is imminent. These times coincide with fish hatchery operations on the lake that involve capturing and releasing operations, and times when fish are held in lake pens. Having knowledge that the lake is very susceptible to upwelling, and that there is a forecast of strong winds, may be of use to Hatchery personnel when planning lake operations. Ditidaht residents and recreational users would also be interested in knowing if the lake was at an increased risk of turnover, although it is not entirely clear what impact this knowledge would have on their daily activities.

5.5 Future Studies

There are several areas that deserve further study in order to better understand Nitinat Lake. These include quantification of the spatial variation in wind stress along the surface of the lake during different seasons, a precipitation-runoff study of the watershed, analysis of ocean-lake exchanges across the sill, multi-year tracking of lake characteristics during different seasons, and study of the propagation of internal waves within the lake.

As observed during the 2003 field study work, there is significant spatial and temporal variation in wind along the length of Nitinat Lake. There are very few locations along the shore of the lake that are suitable for collecting wind data due to the steep terrain and heavy vegetation, but despite this challenge it would be instructive to simultaneously

collect data from several locations on the lake. A good understanding of wind behaviour on the lake could be obtained from three stations operating simultaneously, with a station located at each of the lake and one near the middle, and should be considered for future studies if possible.

Precipitation runoff is not well defined for the Nitinat Lake watershed, and stream gage data for the Nitinat, Caycuse, and Hobiton rivers would be very useful towards defining the actual percentage of precipitation that reaches the lake during different times of the year. DFO personnel currently record precipitation data at the Nitinat River Hatchery. It would be instructive to obtain comparative data at several other locations within the watershed. A second location could be at the Ditidaht village, as it would be easy for land and resource officers to establish a monitoring program in conjunction with the school science program. With stream gage data and precipitation data, a good precipitation-runoff model should be possible for the watershed.

While precipitation runoff accounts for the fresh water input into the surface layer, exchange across the sill accounts for the salt water input and must be better understood in the same manner. Exchange across the sill between ocean water and lake water is fairly complex, and warrants a study of its own. Ultimately, to properly model the surface layer properties requires knowledge of the rate at which tidal pumping of sea-water into the surface layer occurs on an incoming tide, and the rate at which fresh water is removed on an outgoing tide, given an initial set up conditions in the lake and a specified tide. This is not a trivial investigation.

Obtaining multiple years of lake property data would give a much better understanding of lake response to precipitation levels, and long term trends in lake data. Of course, the more information the better, but a reasonable understanding of the lake could probably be obtained from a single CTD transect of the lake performed 6 times a year at regular intervals. These surveys could be performed by Hatchery personnel in cooperation with UBC, and would only need to be of the top 60m. Once a year, a detailed CTD survey of the entire lake depth should be done to track long-term changes in the deep water. If such

a program were to be carried out for a period of two or three years, a good understanding of the response of lake properties to environmental inputs could be obtained.

Finally, further study of the response of the interface to wind forcing, and the propagation of internal waves would be of use to refining the prediction of upwelling based upon wind forcing for a given lake state. Temperature is a poor indicator of isopycnal movement, especially during late fall or early spring when density stratifications remain but temperature profiles experience a turnover. Sensors that monitor salinity would give a much better indication of density movements. Of ultimate interest is movement of the oxycline, and efforts should be made to monitor the response of the oxycline to wind forcing at various locations in the lake.

References

Amorocho, J. & J.J. Devries. 1980. A new evaluation of the wind stress coefficient over water surfaces, *Journal of Geophysical Research, Vol 85 (C1): 433-442.*

Broenkow, W.W. 1969. The distribution of non-conservative solutes to the decomposition of organic material in anoxic marine basins. *Ph.D. Thesis*. University of Washington, Seattle.

Carmack, E.C., R.C. Wiegand, R.J. Daley, C.B. Gray, S. Jasper, and C.H. Pharo. 1986. Mechanisms influencing the circulation and distribution of water mass in a medium residence-time lake. *Limnology and Oceanography, Vol 31 (2): 249-265.*

Farmer, D.M. 1978. Observatiosn of Long Nonlinear Internal Waves in a Lake. *Journal of Physical Oceanography, Vol 8: 63-73.*

Fedorenko, A.Y., F.J. Fraser, and D.T. Lightly. 1979. A Limnological and salmonoid resource study of Nitinat Lake: 1975-1977. *Fisheries and Marine Service technical report No. 839: 86p.*

Gilmartin, M. 1962. Annual cyclic changes in the physical oceanography of a British Columbia Fjord. *J. Fish. Res. Board Can. v19(5): 921-974.*

Imberger, J. 1985. The diurnal mixed layer. *Limnology and Oceanography, Vol 30 (4): 737-770.*

Nitinat River Hatchery. 2003. Background Information from website. Fisheries and Oceans Canada. (Available from http://www-heb.pac.dfo-mpo.gc.ca/facilities/Nitinat/background_e.htm; INTERNET)

Northcote, T.G, M.S. Wilson, and D.R. Hurn, 1964. Some characteristics of Nitinat Lake, an inlet on Vancouver Island, British Columbia. *J. Fish. Res. Board Can. Vol 21: 1069-1081.*

Monismith, S.G. 1985. Wind-forced motions in stratified lakes and their effect on mixed layer shear. *Limnology and Oceanography, Vol 30 (4): 771-783.*

Ozretich, R.J. 1975, Mechanisms for deep water renewal in Lake Nitinat, a permanently anoxic fjord. *Estuarine and Coastal Marine Science, Vol 3:189-200.*

Segar, D.A. 1997. *Introduction to Ocean Sciences*. Wadsworth Publishing Company.

Seapoint Sensors Inc., Seapoint Turbidity Meter Datasheet, 2000. *Seapoint Sensors Inc. 87 North Road, Kingston, NH, 03848-3056, USA.*

Shortreed, K., J. Stockner, and E. MacIssac, 1987. Report on a November 7, 1987 survey of Nitinat Lake. (Fraser Lakes and Lake Enrichment Program, DFO, unpublished. Copy cited with permission from Nitinat River Hatchery, Fisheries and Oceans Canada.)

Spigel, R.H., and J. Imberger, 1980. The classification of mixed-layer dynamics in lakes of small to medium sizes. *Journal of Physical Oceanography, Vol 10: 1104-1121.*

Stevens, C.L. and J. Imberger, 1996. The initial response of a stratified lake to a surface shear stress. *Journal of Fluid Mechanics, Vol 312: 39-66.*

Stevens, C.L. and G.A. Lawrence, 1997. Estimation of wind-forced internal seiche amplitudes in lakes and reservoirs, with data from British Columbia, Canada. *Aquatic Sciences, Vol59: 115-134.*

Thomson, R.E. 1981. *Oceanography of the British Columbia Coast.* Canadian Special Publication of Fisheries and Aquatic Sciences 56, Department of Fisheries and Oceans, Canada.

WET Labs Inc., WET Labs Wetstar User Guide, Revision K, 2003. *Wet Labs Inc. 620 Applegate St. Philomath, OR 97370, USA.*

WET Labs Inc., WET Labs C-Star User's Guide, Revision K, 2003. *Wet Labs Inc. 620 Applegate St. Philomath, OR 97370, USA.*

Wheless, G.H., and A. Valle-Levinson, 1996. A modeling study of tidally driven estuarine exchange through a narrow inlet onto a sloping shelf. *Journal of Geophysical Research, Vol 101, no. C11: 25,675-25,687.*